Handover Characteristics and Handover Performance in Digital Mobile Systems

Dohun Kwon

Thesis submitted for the degree of

Doctor of Philosophy

The University of Adelaide

Adelaide, South Australia, 5005

Department of Electrical and Electronic Engineering

Faculty of Engineering, Computer and Mathematical Sciences

September 1999

Contents

Summary

In wireless communication systems having unpredictable radio propagation environments, it is most important from the user's point of view to maintain an adequate level of service quality during call conversation and a low probability of call drop. Moreover, for future wireless systems in which small radius cells and heavy user demands are being considered, fast handover request processing is becoming a more noteworthy factor. The handover request processing time itself and the delay caused by heavy signalling traffic, can have an effect on call quality and/or the probability of call conversation disconnection during handover procedures.

A well known reason for call drop is a lack of free radio channel resources at the new base station. The other reason is low call quality, i.e. the received signal strength for the current base station falling below the threshold of reception. This low call quality makes the user's conversation quality poor and may result in the conversation being disconnected, even if the base station can provide a new radio channel to the user. To provide a better quality of call service where the radio link quality is poor, handover algorithms, which monitor the radio link of the Base Station, are used. If the handover algorithm can support a very accurate handover decision, while the handover request processing delay is too long, this accurate handover decision would not be processed properly. The received signal strength of the current base station during the handover request processing time will fall below the receive threshold, that is the radio link between the Mobile System and the Base Station becomes poor. On the other hand, if the system can provide fast handover request processing, while the handover decision is not accurate, then extra unnecessary handovers can occur or the call may be disconnected due to low call quality. Therefore an accurate handover decision and a fast handover request response time are needed to provide high quality of call conversation and low

Declaration

This work contains no material which has been accepted for the award of any other degree or diploma in any university or other tertiary institution and, to the best of my knowledge and belief, contains no material previously published or written by another person, except where due reference has been made in the text.

I give consent to this copy of my thesis, when deposited in the University Library, being available for loan and photocopying.

SIGNED: DATE: 98. AUG. 13

Acknowledgements

I would like to thank my supervisors, Dr. Kenneth Walter Sarkies and Professor Reginald Coutts, for informative and helpful discussions, and for assistance and support.

My thanks also to: Dr. David Everitt and Mr. Gamini Senarath at the University of Melbourne, Australia for useful discussions and suggestions concerning handover algorithm and power control analyses; and Dr. Derek Rogers and staff at the Center for Telecommunications Information Networking at Adelaide, Australia, for helpful discussions and support.

This work was supported by the Special Overseas Postgraduate Fund from Commonwealth Government Scholarship Section, Australia, and a Scholarship from the University of Adelaide, Australia. This work is also partially supported by Samsung Electronics Telecommunication Laboratory, Seoul, South Korea.

My thanks also to my colleagues Ted and Fujio. Finally, special thanks to my parents, Young Jun Kwon and Young Hee Lee, my parents in law, Shin Ha Kang and Ok Yoon Kim, and my brothers and my sister for assistance and support. In particular I thank my lovely wife, Min Jung Kang, and my daughter, Bo Young Kwon, for the support and understanding that helped me through the difficult times since 1992.

Chapter 1

Introduction

Since the first generation mobile system, Advanced Mobile Phone Service (AMPS), was introduced in the 1970's, user demands have increased dramatically and will continue to do so in the future. The forecast is that 20% of communication terminals will be mobile by the year 2000 increasing to 50% in the 21st century [1]. In the European Community, for example, recent data [2] shows mobile and personal user penetration per 1,000 of population increased from 23 to 33, an increase of approximately 2.3 million users during the period between Nov. 1993 and Oct. 1994. It is estimated that the number of users will be about 50 million users at the end of century and 100 million by 2005 in Europe. Both forecasts show how fast the number of users in personal and mobile communications is growing.

In order to provide for the increasing user demand, a concept using a small radius of cell with channel reuse has been proposed. This is more efficient in cellular mobile systems [3] as it provides more channels within the limitations of the available frequency allocations. Unfortunately the cell radius reduction gives rise to new problems in system design and operation. One of these is related to handovers. Two major aspects of the handover issue are firstly that an accurate handover decision is required for all mobile radio propagation environments, and secondly that fast handover processing is needed.

From the user service point of view, it is very important to achieve accurate handover decisions to ensure high quality of call conversation and low probability of call disconnection. The handover decision can only be made through knowledge of some system

- **Hysteresis window**

In an ideal case, the number of handover requests per boundary crossing is unity. In reality however it is usually greater than one because of the effects discussed above. Only one of the multiple handover requests is necessary, all the remainder are called *unnecessary* handover requests, which only serve to load the handover processor to no purpose. To reduce the number of these unnecessary handover requests, a hysteresis effect (HYS) is introduced which raises the received signal strength threshold at which a boundary crossing is detected. As HYS increases the number of handover requests decreases until it eventually becomes unity [10, 11]. However there is a disadvantage: the resulting handover request generation is delayed away from the boundary as HYS increases. Vijayan *et al.* [11] demonstrated this characteristic. This can give rise to a situation in which the call quality is degraded, even if only one necessary handover request occurs. The studies which we have already mentioned did not examine this issue. Therefore it is important to check the call quality for handover algorithms having various HYS values. In our studies [12, 13], we found that when HYS increased the number of handover requests was reduced down to unity, but the call degradation rate (that is, the probability that the received signal strength at the MS, of the current BS, falls below the receiver's signal detection level) was increased. Even if the cells are covered well by the BS signals, an unnecessarily high HYS generates significantly higher call degradation rates than low and medium HYS.

- **Signal Averaging**

We also found [14] that the handover request characteristics such as number of handover requests, call degradation, delay of handover occurrence and zone selection rate, are strongly affected by the parameters of the handover algorithms. One of these is the time over which signals are averaged, called the *signal average interval.* Lee [15] showed how the signal average interval affects the accuracy of the estimated log-normal fading mean. If the signal average interval is too short, the averaged signal value will be affected by the rapid Rayleigh fading. However if it is too long, then deep fades in which a handover may be needed, may be smoothed over if they are shorter than the signal averaging interval. For such a situation, we can say that the handover request characteristics measured and averaged with inappropriate signal intervals will not provide reliable results. In our

Not only is an accurate handover decision required, but also fast handover processing is essential for achieving an acceptable handover performance for the user. Fast handover processing will become even more important in future systems. The investigation of Bye [20] showed that, under the same circumstances, there are on average 50% more handover requests generated for a small radius cell (100m radius) than for a medium radius cell (1km radius). Because other signalling traffic such as call requests and mobility requests will also increase in future, providing fast handover request processing is not an issue of handover itself. It is a signalling traffic issue of the mobile system. It is difficult to obtain an understanding of how this signalling traffic will affect handover performance, in particular call drop and quality of service, if we use a complex, comprehensive signalling traffic model of a mobile system. However, with a simple signalling traffic model in which only handover request traffic is of concern, the analysis of the effect of handover delay on call drop can provide valuable results which reveal the reasons behind call drop at the system level.

Because avoiding call drop is more important than avoiding new call blocking, many studies have been carried out seeking to improve the call dropout rate. In particular, Gudmundson [9] presented results for the performance of handover algorithms with a simple layout consisting of two BS and one MS. His analytical model gives the call dropout condition, handover blocking condition, and expected number of handover requests. Hong *et al.* [21] showed that giving a higher priority to handovers in the call processors produces a better system performance than a non-priority scheme. Different approaches for improving system performance, in particular call dropout rate and new call blocking probability, were studied by Posner *et al.* [22] and Guérin [23] using analytical models. Their studies were concerned with reduction of call dropout rate while at the same time minimised call blocking probability. However none of the above considered a realistic mobile environment.

Recently Kuek *et al.* [24] investigated system performance using a mobile propagation model in highway microcell systems. They used a load-sharing scheme to improve the system performance. This reduced the handover request blocking probability but the call dropout rate was not improved. The average number of unnecessary handover requests was reduced, but the blocking of the necessary handover requests which are directly

- Fourthly, to construct and examine the soft handoff algorithm in CDMA systems, a simple power control algorithm is developed and its handover characteristics are investigated by combining with soft handoff algorithms. We show that to achieve the same handover request characteristics as the hard handoff algorithm, care must be taken in development of the power control algorithms for the soft handoff algorithm. Otherwise soft handoff with power control achieves worse performance than soft handoff algorithms without power control or the hard handoff algorithms.

- Fifthly, to enhance the call dropout rate, the call drop conditions are examined. In particular, we focus on the behavior of the handover server to reduce the delay call drop. We do this via "Handover Rejection Schemes". These schemes include two algorithms. One is the classification of the handover request into normal and enforced handover conditions with the latter having higher priority. The other is the load sharing of handover requests between BS or BSC. These schemes provide much better call dropout rate when the system is suffering from a long handover request delay.

1.1 Contributions of This Thesis

The author of this thesis recognises the importance of handover in mobile and personal communication systems. The author has also noted an increasing interest in this field during the last five years. There are difficulties in attempting to develop a precise handover model and to obtain accurate data for analysis of handover algorithms, because of the random nature of the radio environment and user behavior. The work reported in this thesis tackles both of those issues by contributing to an understanding of fundamental characteristics of the handover algorithm from the user service and system performance point of view. In particular, the handover algorithm in this thesis uses the rectangular (block) window, which has not been extensively investigated, rather than the sliding window for averaging the received signal strength. The rectangular window scheme has the advantage that it generates a smaller number of handover requests compared to the rectangular sliding window or the exponential sliding scheme [25].

Two measures of handover performance are developed here: call degradation and modi-

1.2 Outline of Thesis

We will present the basic elements of our study in Chapter 3. First of all we will discuss the mobile radio propagation environment in which a mobile station can communicate with other mobile stations or fixed network subscribers by maintaining radio links between the MS and BS. Because highly fluctuating and randomly fluctuating radio signals make an accurate handover decision difficult, we will first focus on the path loss and fading to understand the nature of the radio propagation channel. At that point we will introduce and explain our simulation radio channel model. Soft and hard handoff will be discussed to introduce the basic differences between handover algorithms.

We then discuss in Chapter 3 a modified handover algorithm called the enforced and normal (EN) handover algorithm which attempts to force a handover when link quality becomes critical. Also in Chapter 3, we will present a simulation model and an analytical model of the handover algorithms. We start with a simple cell layout consisting of two base stations having 2km radius, and one mobile station. An analytical model using the assumption that the received signals at the receiver are Gausian distributed will be derived from the signal difference function between the two BSs and the signal coverage determination function [26]. Various handover request performance measures such as the mean number of handover requests, mean number of call degradations, handover area (or handover point when the number of handover requests is equal to one) and call degradation point will be evaluated in the simulation model. These measures will also be studied for the enforced and normal (EN) handover algorithm in this chapter. Finally comparisons between the simulation model and an analytical model, with both basic and EN handover algorithms, will be given.

In Chapter 4, various handover request performance measures for the case where neigbouring BSs have different transmit powers are studied. In addition another scenario with a worst case MS movement model is studied. Since we have already examined the two handover algorithms in Chapter 3, the same performance measures will be used to study these particular environmental scenarios. The study of the worst case MS movement scenario, that is, where the MS travels around the cell boundary all the time, is investigated for both equal and unequal transmit power models. We investigate the com-

Chapter 2

Background for Cellular Mobile Radio Systems

2.1 Mobile Radio Propagation Environment

Radio signals linking a mobile station and base station are affected by the topography of terrain and man-made structures which give rise to multipath pheonomena. The heights and types of the antennae can also affect the amount and nature of the signals arriving at the receivers in these stations. To analyse the received signal at the receiver antenna we consider the following three major influences: path loss; short term fading; and long term fading.

The path loss between the receiver and the transmitter antennae decreases the power of the transmit signal as a result of direct line of sight absorption in the air, or reflection losses where the signals are received indirectly. Fluctuations of signal strength over short and long term periods of time are caused by multipath phenomena due to terrain reflections. Where the signal variations occur over a few wavelengths, the fluctuiations are called *short term fading.* The term *long term fading* is used where these signal variations occur over macroscopic distances. In this thesis, in common with other studies [27, 28, 29], short term fading is modelled by a Rayleigh distribution, while long term fading is modelled by a log-normal distribution. We now examine the details of these three major parameters: path loss; Rayleigh fading; and log-normal fading in the mobile

Table 2.1: Lists of Terms

terms	name	unit
h_b	height of BS antenna	[m]
h_m	height of MS antenna	[m]
f_c	carrier frequency	[MHz]
P_t	transmitting power	[dB or watts]
P_r	receiving power	[dB or watts]
P'_t	transmit power of dipole antenna	[dB or watts]
d	distance between transmitter and receiver	[km]

the receiver. The simple form is as follows:

$$L_p = K_1 + K_2 log_{10}(d) \tag{2.1}$$

where K_1 and K_2 are functions of the frequency and antenna heights of the MS and BS.

Since we use Hata's empirical formula for the path loss in this thesis, we provide his derivation as follows. The path loss L_p, the power difference between the transmitter and the receiver, is given in dB by:

$$L_p = P_t - P_r \qquad \text{[dB]} \tag{2.2}$$

The first term, P_t, in equation 2.2 is based on Okumura's prediction curves derived for a dipole antenna. By adding the absolute power gain of a dipole antenna, 2.2dB, to the transmit power of a dipole antenna P'_t, we get the power gain between isotropic antennae:

$$P_t = P'_t + 2.2 \qquad \text{[dB]} \tag{2.3}$$

The second term P_r in equation 2.2 is obtained by adding the absorption cross section of an isotropic antenna A_{eff}, to the received power density P_u:

For a typical urban area the Hata model is obtained by determining K_1 and K_2 with the slope of the field strength curve. The basic characteristics of both constants are that K_1 is a function of h_b and f_c. Thus K_1 is given by:

$$K_1 = \alpha - 13.82log_{10}(h_b) - a(h_m) \tag{2.10}$$

where α is given by:

$$\alpha = 69.55 + 26.16log_{10}(f_c) \tag{2.11}$$

K_2 which is independent of f_c and h_b is given by:

$$K_2 = 44.9 - 6.55log_{10}(h_b) \tag{2.12}$$

Thus the path loss L_p becomes:

$$\begin{aligned} L_p(dB) &= 69.55 + 26.16log_{10}(f_c) - 13.82log_{10}(h_b) - a(h_m) \\ &\quad +(44.9 - 6.55log_{10}(h_b))log_{10}(d) \end{aligned} \tag{2.13}$$

where

- f_c : 150 - 1500 MHz,
- h_b : 30 - 200 m,
- h_m : 1.5 - 10m,
- d : 1 - 20Km,
- $a(h_m)$ is the correction factor of h_m.

The correction factor $a(h_m)$ for a medium-small city is

$$a(h_m) = (1.1log_{10}(f_c) - 0.7)h_m - (1.56log_{10}(f_c) - 0.8) \tag{2.14}$$

$$E[x^2] = \sigma^2 \tag{2.18}$$

- **Long Term Fading**

The investigation by Egli [32] showed that the signal strength variation is log-normally distributed over a small area, that is, distance of the order of tens of meters. The experiments of Okumura *et al.* [36] also showed that the received median signal value varies when the MS moves from place to place. This is caused by terrain contour and local topography. The experiment of Reudink [38] showed that the standard deviation of the median signal strength was more strongly affected by the local environment than by the range from the transmitter [39]. This variation is known as "shadow fading" or "slow fading", which is the antilogarithm of a normal distribution, that is, the long term signal envelope variation is normally distributed when represented in decibel form.

The studies of slow fading by Reudink [38] and Black and Reudink [40] found that if fast fading was smoothed out by averaging the received signal, then the variation of the received signal mean empirically is very close to the log-normal distribution function. The probability density function of the log-normal random variable x is:

$$p_{LN}(x;\mu,\sigma) = \frac{1}{x\mu\sqrt{2\pi}} \exp\{-\frac{1}{2}\left(\frac{\ln x - \mu}{\sigma}\right)^2\}, \quad x, \sigma \geq 0 \quad \text{and} \quad -\infty \leq \mu \leq \infty \tag{2.19}$$

where μ is the mean and σ is the standard deviation. The log-normal distribution function is:

$$P_{LN}(x;\mu,\sigma) = \frac{1}{\mu\sqrt{2\pi}} \int_0^x \frac{1}{x} \exp\{-\frac{1}{2}\left(\frac{\ln x - \mu}{\sigma}\right)^2\}\, dx \tag{2.20}$$

E_0 of the electric component E_z is Rayleigh distributed and the phase is rectangularly distributed through 0 to 2π [41, 37, 44], unless there is also a direct arriving wave of significant magnitude from the transmitter.

Experimental data [44] showed that if there are significant direct waves at the receiver from the transmitter, then the envelope is no longer Rayleigh distributed. If the power of the significant direct wave is much greater than that of the combined scattered waves, then the phase and the envelope are approximately Gaussian distributed. The former is assumed to be the case for non line-of-sight (NLOS) and the latter is assumed to be the case for line-of-sight (LOS).

In this thesis, we use the approach of Aranguren and Langseth [45]. This is based on a model of Jakes [26] who introduced a simulator which generates a Rayleigh fading waveform includes multipath propagation. This model has as an assumption that the number of arriving waves is large enough that the Rayleigh distribution is approximately valid. The three components of the received field follow a complex Gaussian process and the direct wave is not significant. This Rayleigh fading simulator uses a discrete approximation to the power spectrum as described in section A.1 of Appendix A. The log-normal fading is also derived by delaying the quadrature component of the simulator output (see section A.2 of Appendix A). Carter and Turkmani [46] also used this method.

2.3 Received Signal Strength

In this thesis we have studied the radio propagation environment by means of the radio channel simulator to understand the basic characteristics of the received signal strength (RSS) which will be used for the handover decision criterion in the handover algorithm analysis. A reliable channel model is very important for the design of effective handover algorithms. The technique for measurement of received signal strength is also used for mobility updates in current mobile systems.

Figure 2.1 shows the block diagram of the radio system that we study. The transmitted signals from the transmitter (Block1) are modified by path loss, and fast and slow fading in the channel (Block2). To cope with a wide range of received signals, logarithmic

loss, and compares these with those from other BSs to determine the stronger signal. Thus from the system operation point of view, the system should know the averaged RSS between the MS and the current BS and between the MS and neighbouring BSs. The threshold is set for a minimum level of received signal strength. For a minimum quality of communication usually it is greater than -130dBm.

The process by which the system analyses the signal strength and allocates a new channel to the MS is called the "Handover Algorithm". We discuss this in the next section.

2.4 Handover Algorithms

2.4.1 Why Handover?

In the cellular mobile radio concept, each cell is given a set of frequency channels and provides these channels to the MSs to communicate with other fixed subscribers or other MSs. When the MS crosses a cell boundary into a cell which is controlled by a neighbouring BS, the MS cannot retain the same frequency channel which was allocated to it by the current BS, because the received signal strength (RSS) of the MS approaches the minimum receive threshold level or falls to a value less than that of the neighbouring BS. Thus the system provides a new channel to the MS to ensure that the conversation is maintained. These procedures are called handover procedures. They are processed by the system with the assistance of the MS.

The basic trigger for a handover algorithm based on the received signal strength is:

$$RSS(N_1) \leq RSS(N_k) \tag{2.25}$$

where N_1 is the ID of the current BS and N_k is the ID of a neighbouring BS which carries the strongest RSS to the MS ($k \neq 1$). It is very difficult to develop a good handover algorithm which gives a satisfactory performance by providing a very accurate single handover request per boundary crossing.

In GSM [19], the handover decision process is managed by the Base Station Center (BSC) or the Mobile Switching Center (MSC) with RSS data measured by the MS using

always access the BS with the best (strongest) signal, even if the number of handover requests occurring is quite significant. There is a quite low probability that an MS would connect to a BS with a weak signal which may cause the signal connection to be dropped or result in a low quality of user service. From a system point of view, the system needs an accurate and efficient handover algorithm and also a fast handover request processor which can complete the processing of handover requests before the RSS at the MS and BS falls below the minimum RSS threshold at which point the user can experience poor call quality or call drop. Many researchers have been involved in analysing handover algorithms and evaluating their performance. Some have proposed the modified handover algorithm of equation 2.25 using hysteresis windows to reduce the number of handover requests per boundary crossing. We look at this algorithm and its performance in the next section.

2.4.2 Hysteresis Windows

To reduce the number of handover requests per boundary crossing, the concept of hysteresis windows was introduced and analysed in a number of other studies [43, 11, 9]. The concept is that a handover request is not generated until the difference between the RSS of a neighbouring BS, and that of the current BS, is greater than the hysteresis window (HYS) threshold. The major role of hysteresis windows in the handover algorithm is to reduce the number of handover requests. In fact as HYS increases, the number of handover requests per boundary crossing approaches unity.

We investigate here the trade off between HYS and the number of handover requests. The handover algorithm with hysteresis window, referred to as the *basic* handover algorithm in this thesis, is modified from equation 2.25 to give:

$$RSS(N_1) + HYS \leq RSS(N_k) \tag{2.26}$$

where N_1 is the ID of the current BS, N_k, $k \neq 1$, is the ID of a neighbouring BS which carries the strongest RSS to the MS, HYS is the hysteresis window level in dB. When HYS is equal to 0dB in equation 2.26, the result is the same as equation 2.25.

2.4.3 Signal Average for Discrete Samples

There are several methods which can be used to average the received signal strength.

1. **Exponential Sliding Window** [11, 24, 48, 25] The signal average is given by:

$$\begin{aligned} S(k) &= \alpha S(k-1) + (1-\alpha)s(k) \\ &= (1-\alpha)\sum_{j=0}^{n-1} \alpha^j s(k-j) \end{aligned} \tag{2.27}$$

   where α is a constant that determines the rate of signal decay ($|\alpha| < 1$). $S(k)$ is the output of the algorithm, and $s(k)$ is the current signal sample. The handover decision is made every signal sample.

2. **Rectangular Sliding Window** [9, 49, 25] The signal average is given by:

$$S(k) = \frac{1}{n}\sum_{j=0}^{n-1} s(k-j) \tag{2.28}$$

   where n is the width in signal samples of the window. The handover decision is made every signal sample.

3. **Rectangular (Block) Window** [43, 13, 14]. The signal average of n samples is shown in figure 2.4, and is given by:

$$S(k) = \frac{1}{n}\sum_{j=1}^{n} s((k-1)\times n + j) \tag{2.29}$$

The exponential sliding window can track the signal variations more accurately than can the rectangular sliding window as Corazza *et al.*[25] showed. On the other hand, while the rectangular sliding window produces a smaller number of unnecessary handover requests, the first handover occurrence points are delayed further than those for the exponential sliding windows. From the number of handover requests point of view, the rectangular sliding window method is more attractive than the exponential sliding window.

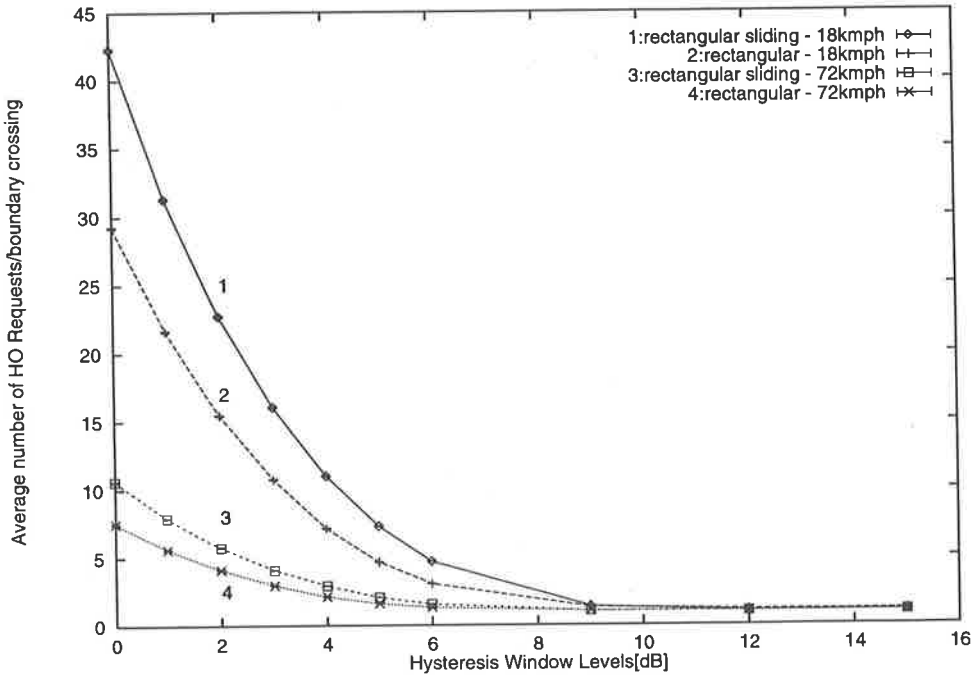

Figure 2.5: Average number of handover request per boundary crossing against HYS for different averaging window algorithms

more precise but is moving further away from the true boundary as HYS increases.

Therefore the study of handover algorithms using the rectangular (block) window is expected to provide very useful and valuable results. In particular this study will be useful for handover algorithm development and handover performance improvement.

We now consider in more detail the length of the sampling time T_s and the averaging time T_{av} of the block window. It is not reasonable to fix these quantities for every kind of mobile environment or for all speeds and direction of motion of the MS. If T_{av} is too short and the received signal is affected by Rayleigh fading, then the averaged signal will be fluctuating significantly up to 40dB depth or more [33, 50]. Thus this measured signal value may not be reliable. In contrast if T_{av} is too long then even though the Rayleigh fading is smoothed out, the system may pass the point at which the MS needs a new channel. Thus the MS may experience a poor quality of signal or it may be disconnected. In our study [14] we compared call quality for both very long and for relatively short signal averaging intervals (averaging distances about 60λ). We showed that the measured received signal strength is dependent on the length of the signal average interval.

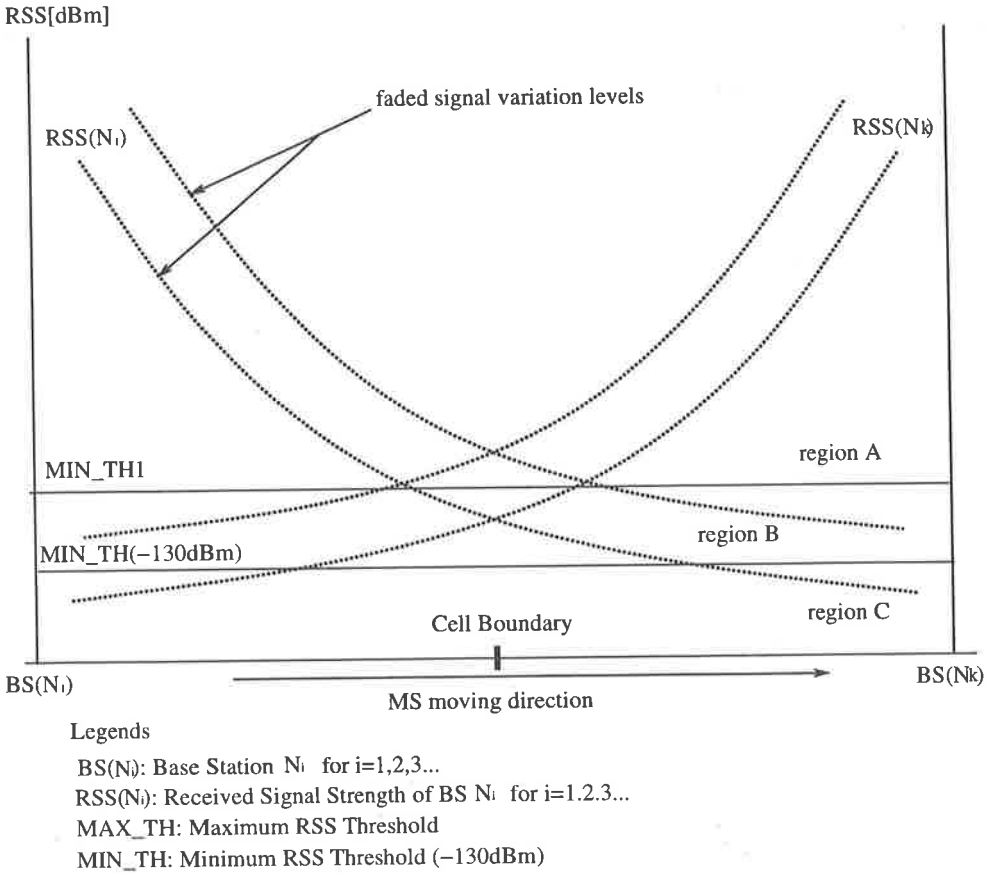

Figure 2.8: Illustration of Enforced and Normal handover algorithms

We now introduce the handover algorithms and show how their performance differs between the algorithms.

2.4.4 Enforced and Normal (EN) Handover Algorithms

The EN algorithm, which is based on the basic handover algorithm given by equation 2.26 and a 'two-handoff-level' algorithm [33], has two advantages. One is that the handover request occurrence is based on the signal strengths of relative BSs. This is not used in the 'two-handoff-level' algorithm which uses only absolute power levels. The other is that the handover request is classified into two types which can be processed with different priorities at the system level, and which are the major advantages of the 'two-handoff-level' algorithm.

In EN handover algorithms, two absolute levels: MIN_TH and MAX_TH (also referred

for the same k as in equation 2.6, regardless of whether the normal handover request condition is satisfied or not. Here MIN_TH and MAX_TH are RSS threshold band limits:

- MIN_TH is a minimum RSS level: -130dBm is used for acceptable service quality,
- MAX_TH is a maximum RSS threshold for the enforced handover request $MAX\_TH \geq MIN\_TH$

The performance of the EN handover algorithm is based on the threshold MAX_TH. Generally speaking, if the NHR cannot be processed (for example due to processor overloads), it may not necessarily cause call quality to drop or call conversation to disconnect. However if an EHR cannot be processed, there will be a higher probability that the call quality will degrade or the call conversation will disconnect. If MAX_TH is reduced until it approaches MIN_TH, the EHR becomes more important than the NHR from the call degradation or call disconnection point of view. An enforced handover can also occur if, due to a high HYS, the RSS of base station N_1 falls within the threshold band before the normal handover condition occurs. It could also occur if a NHR is generated but suffers from excessive handover processor delay.

The EN handover algorithm, which does not distinguish between the handover request and the call degradation characteristics, is as follows:

1. The Normal Handover Request (NHR) condition is:

$$RSS(N_1) + HYS \leq RSS(N_k) \quad \text{and} \quad RSS(N_1), RSS(N_k) \geq MIN\_TH \tag{2.32}$$

2. The Enforced Handover Request (EHR) condition is:

$$RSS(N_1) \leq MIN\_TH \quad \text{and} \quad RSS(N_k) \geq MIN\_TH \tag{2.33}$$

In equation 2.32 the NHR only occurs when the RSS of a neighbouring BS is greater than or equal to MIN_TH. Otherwise if the RSS of the neighbouring BS is less than

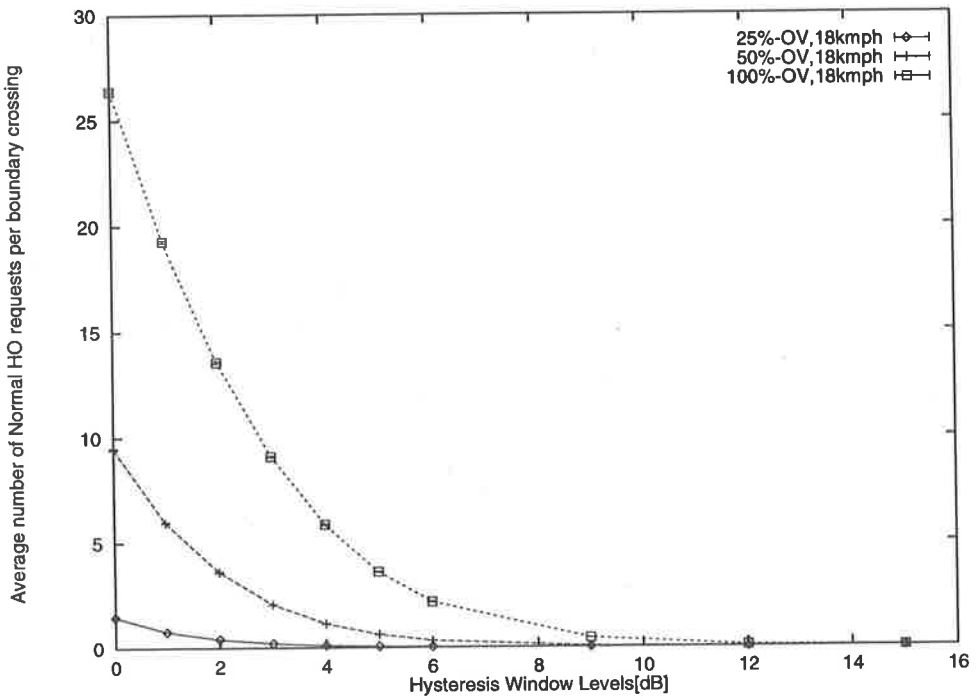

Figure 2.9: Average number of NHR per boundary crossing against HYS

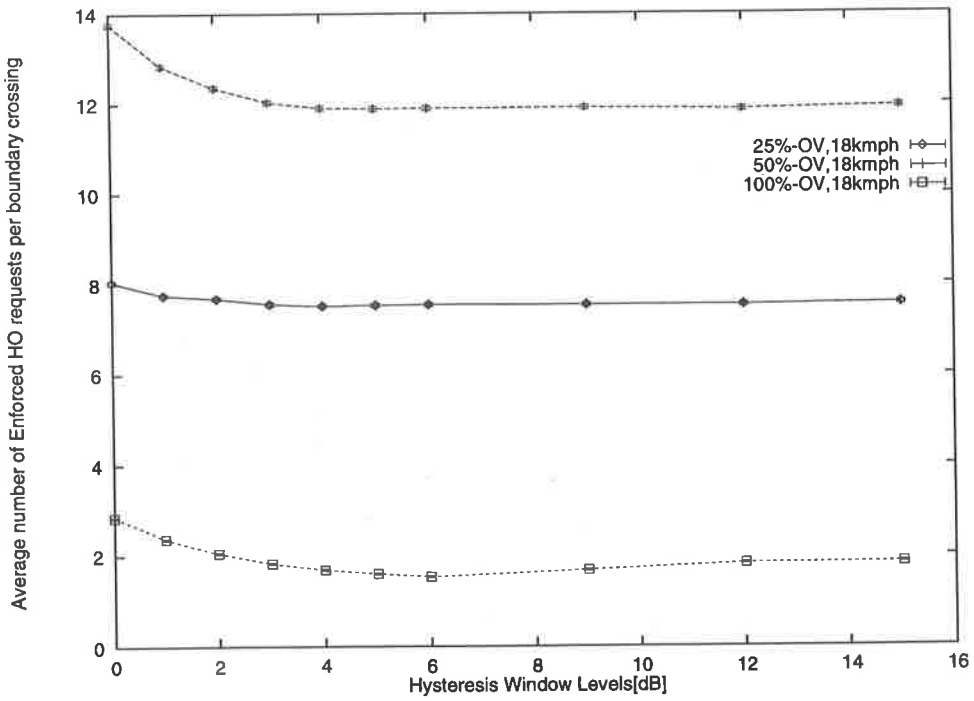

Figure 2.10: Average number of EHR per boundary crossing against HYS

dividually by each BS. Thus after the handover decision at time t_2, the soft handoff algorithm allows the MS to choose one of the links with negligible handover processing time, while in hard handoff the MS must spend significant time to choose a new radio link. This difference becomes a major parameter in the hard and soft handoff algorithm analysis. However from the point of view of system capacity, soft handoff has the disadvantage that multiple channels must be provided to each MS, thus reducing capacity for the system operator. In this thesis we are concerned with the question of handover algorithms rather than system capacity issues.

As Viterbi [52] has stated, the handover algorithm of Vijayan *et al.* [11] assumes that the handover processing time is very short. Most previous handover algorithm analyses [10, 9, 7, 24, 43, 16, 14] have also assumed that the handover decision time t_{h_dec} and the handover request process time t_{h_pro} are equal to zero, that is they are ignored even for hard handoff. This is not realistic for real mobile environments. If $t_{h\_dec} + t_{h\_pro}$ is not negligible, the link quality in the hard handoff algorithms may be affected. Previous analyses should be reconsidered by including the handover decision and process time periods. We have shown [12, 13] that the handover request processing time does indeed affect the system performance. As the handover processing interval increases, the system performance decreases for a single handover server model under heavy load.

We will analyse the hard and soft handoff algorithms with the assumptions that a hard handoff needs processing time to be considered, while soft handoff has a negligibly small handover processing time. Handover algorithm comparisons between hard and soft handoff should focus on the handover request processing time, as this is an important contributor to the system performance. Thus we investigate this parameter from the call quality and system performance point of view. These analyses will be done with a model consisting of one MS and two BSs.

The handover algorithm will be investigated using simulation and analytical models in the next chapter, for a variety of parameters affecting the call quality and/or system performance. The analytical model will be developed using a rectangular window for signal averaging.

Chapter 3

Statistics of The Handover Algorithms

3.1 Introduction

In the previous chapter we argued that handover algorithms are affected by the mobile radio propagation environment, the mobile system configurations such as the height of BS and MS antennae, the carrier frequency and parameters of the handover algorithm. These are studied through the number of handover requests in the handover algorithm performance analysis described earlier.

As well as the number of handover requests, other important characteristics such as call degradations and their occurrence points and handover area are analysed for the basic and EN handover algorithms.

In particular, call degradation, in which the current and the strongest neighbouring BS's RSS both fall below the minimum RSS threshold MIN_TH during call conversation, is studied in this chapter. Call degradation is an important consideration for handover algorithm development to achieve more reliable performance analyses of various handover algorithms whose handover decision criteria is based on the RSS.

In this chapter, we build both an analytical and a simulation model of two different handover algorithms, which include various handover request characteristics with various

tions are introduced for the simulation and analytical model. Simulation results for the basic and EN handover algorithm are displayed and evaluated with zero fading autocorrelation in section 3. In the fourth section, a mathematical analysis of both handover algorithms is derived. In the fifth section we compare the analytical and simulation results, again for zero autocorrelation. Finally the effects of autocorrelation in the simulation and analytical models is compared in section 6.

3.2 Simulation Model

To study the basic characteristics of the handover algorithm, we firstly choose a simple mobile system model consisting of two BSs and one MS. The MS starts travelling in a straight line from one BS to the other. This sort of model has been used in other studies because it is simple to implement and it shows well what are the characteristics of the handover algorithm. In particular we combine this model with a mobile radio propagation model to make a realistic mobile environment and to achieve a more realistic behavior of the handover algorithm. However note that we do not consider co-channel interference in this case. That aspect is considered in the chapter 6 where we model a number of mobile and base stations.

3.2.1 Radio Channel Model

In this thesis, we consider both uncorrelated and correlated slow fading models. As we have already mentioned in section A.1 of Appendix A, the standard deviation of simulated log-normal component is derived by delaying the quadrature component of the Rayleigh fading. The baseband component of the slow fading is given by:

$$X_s(t') = kX_s(t') = 2k \sum_{n=1}^{N_0} \sin(\beta_n) \cos(\omega'_n t') \tag{3.1}$$

where k is a constant, t' is a time delay function managing the auto-correlation property of slow fading, $\omega'_n = \omega_{ds} \cos(\frac{2\pi n}{N})$, $\omega_{ds} = \frac{\omega_m}{B}$ is the slow fading rate, ω_m is the fast fading rate and B is a constant which can be as large as 400 [56].

[9, 7, 11, 24, 58] of handover issues made use of this model.

The exponentional autocorrelation function is given by:

$$\begin{aligned} Rxx(jd_s) &= E\{x_i x_{i+jd_s}\} \\ &= \delta_s^2 \varepsilon_D^{jd_s/D} \end{aligned} \tag{3.2}$$

where δ_s^2 is the variance of the slow fading, D is the mean distance at which correlation rate decays to ε_D, d_s is the sampling distance and j is number of samples $j = 1, 2, ...$

This has been expressed in another way by Vijayan *et al.* [11] as follows:

$$\begin{aligned} R_{xx}(jd_s) &= E\{x_i x_{i+jd_s}\} \\ &= \delta_s^2 e^{-\frac{jd_s}{dec_0}} \end{aligned} \tag{3.3}$$

where dec_0 determines how fast the correlation decays with distance. The relation between dec_0 and D is given by:

$$e^{-\frac{D}{dec_0}} = \varepsilon_D \qquad \text{and} \qquad dec_0 = -\frac{D}{ln(\varepsilon_D)} \tag{3.4}$$

The signal sampling distance d_s is an important parameter which affects the amount of correlation between samples. Its proper determination, however, is difficult as the parameters dec_0 and D change with different mobile radio environments.

The four parameters; dec_0 and D for the correlation model and d_s and d_{av} for the signal sampling and averaging model, are considered in detail to investigate the performance of the handover algorithm in the correlation model. The results of the handover performance analysis for the model is compared with those for uncorrelated model.

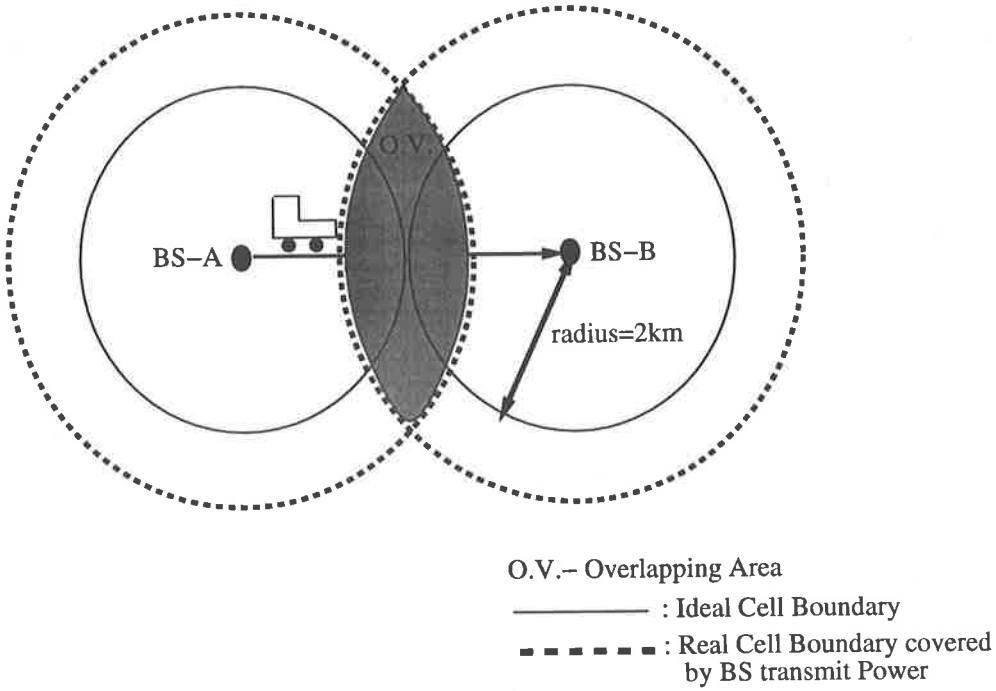

Figure 3.1: Diagram of Cell Layout

3.2.4 Overlapping Conditions (OV)

One of the important parameters in mobile systems is the transmitting power at the BS and the MS. The transmitting power levels are determined by adding the mean path loss L_p measured at the cell boundary, to the minimum received signal strength (MIN_TH)=-130dBm. Therefore as the cell radius is varied the transmitting power also varies.

For example, to achieve a 25% overlap in a 2km cell radius, the transmit power is set by adding the L_p measured at a point 2.5km away from the BS to the minimum RSS of -130dBm. This is given by:

$$P_t = L_p + MIN\_TH \tag{3.5}$$

where $L_p = K_1 + K_2 log_{10}(2.5)$ and $MIN\_TH = -130dBm$

As the transmitting power increases, the overlapping area between two cells in which the RSS is adequate for reception by either BS, increases. However this results in increased

neighbouring BS can provide better quality of service than the current BS. One of main reasons causing this condition is that the handover algorithm decision based on the RSS criterion may not predict the best BS for future communication in a randomly fluctuating radio signal environment. In other words, the signal fade makes the RSS based handover decision difficult. However we assume that the sudden call degradation rate would be small in an effective handover algorithm.

The handover algorithm is analysed in terms of these two call degradation conditions, by determining their occurrence points.

3.3 Results of Simulation Study

In this section, the results of the simulation model are compared for various HYS levels, overlapping conditions, and speed of MS. Two handover algorithms are investigated. The first one is the basic handover algorithm which has been used in analyses by other researchers. A major difference in this thesis is that we investigate the two call degradation conditions and their occurrence points with various overlapping conditions. The second algorithm is the enforced and normal (EN) handover algorithm having RSS level isolation between the handover request condition and the call degradation condition. For simplicity of the EN handover algorithm analysis, we use a value of -124dBm for the upper RSS threshold MAX_TH.

The average number of handover requests, sudden and no-signal call degradations, mean handover area (the region between the first handover request and the last handover request) and the mean of the sudden and no-signal call degradation occurrence points are measured as handover request characteristics.

To determine the simulation accuracy, we will assume that the distribution of measurements $\bar{X}$ of μ is approximately Gaussian distributed and independent. This allows us to establish confidence intervals for the estimates of the mean μ when the simulation time n is sufficiently large. The confidence interval $\pm z_{\alpha/2}$ is given by:

$$P(-z_{\alpha/2} < Z < z_{\alpha/2}) = 1 - \alpha \tag{3.9}$$

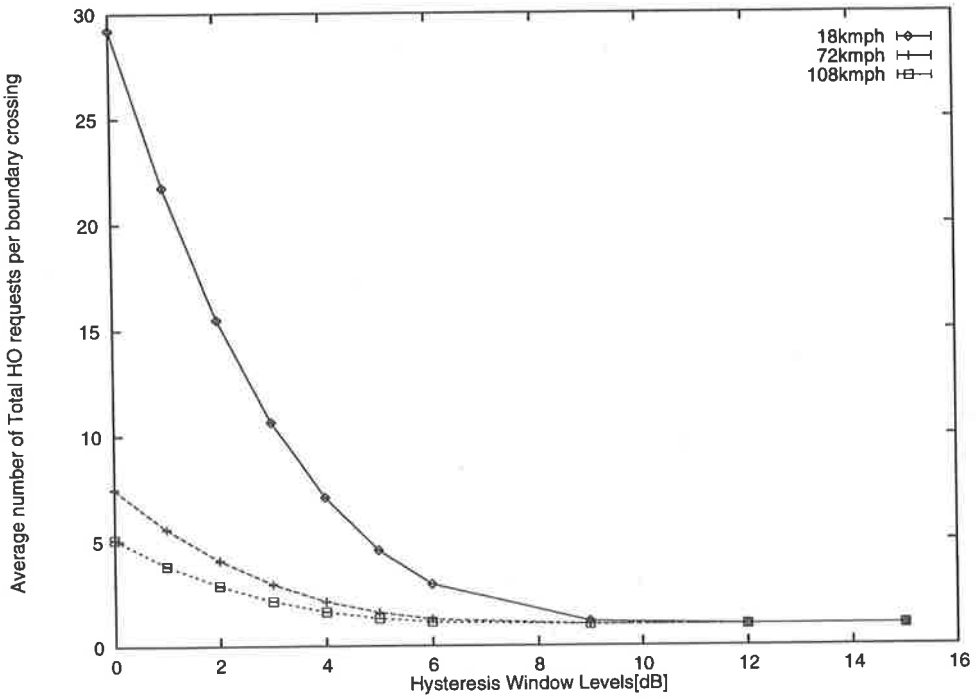

Figure 3.2: Average Number of HO Requests of Basic Algorithm for 50% overlap

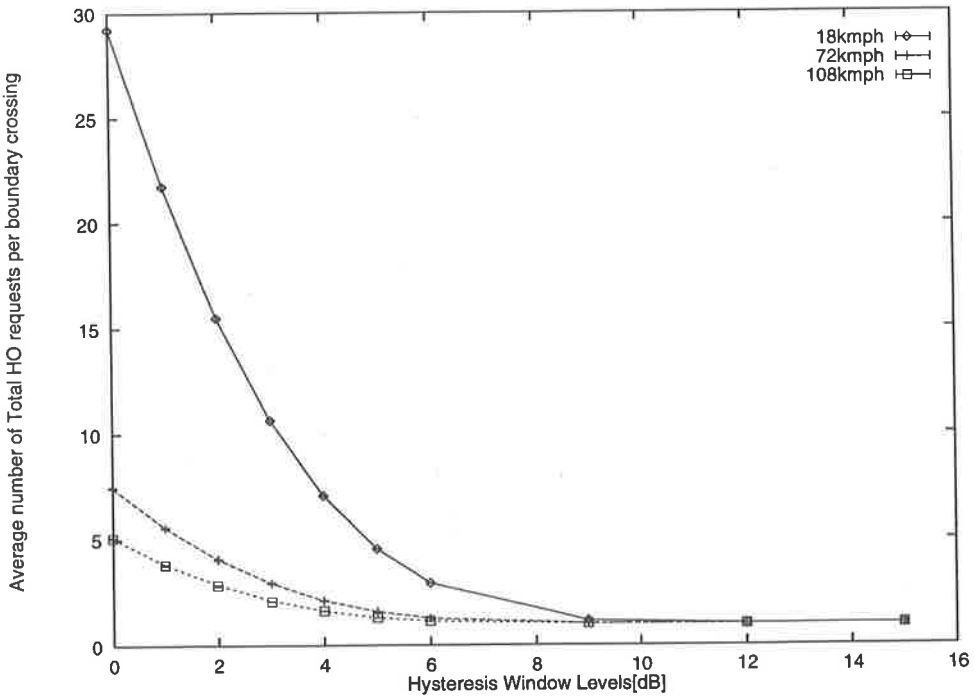

Figure 3.3: Average Number of HO Requests of Basic Algorithm with 100% overlap

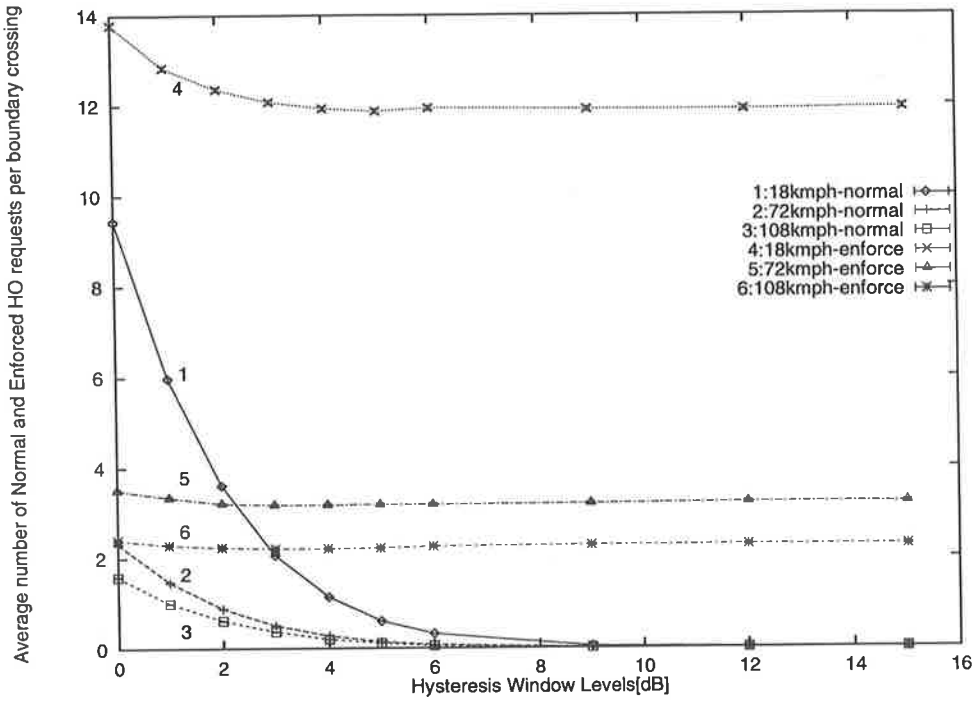

Figure 3.5: Average Number of Normal and Enforced HO Requests of EN Algorithm with 50% overlap, MAX_TH=-124dBm

handover algorithm follows the basic handover request characteristics, that is, as HYS increases the mean number of handover requests decreases. Therefore the handover request characteristics of the EN handover algorithm with shown in figure 3.6) appear very similar to those of the basic handover algorithm with shown in figure 3.2) for 100% OV.

The basic handover algorithm analysis however does not tell us anything about call degradation. Even if the mobile system were well designed, in a randomly fluctuating radio propagation environment we cannot say if the probability of the MS experiencing the RSS of its current BS falling below MIN_TH, is small. Thus we need to use two call degradation conditions, measured independently of the handover request conditions in the basic and the EN handover algorithms. We can gain a clearer understanding of the handover algorithm analysis by combining the number of call degradations with the number of handover requests.

3.3.2 Average Number of Call Degradations

We consider further the two types of call degradations classified earlier. In our simulation runs, the call degradations are counted and summed every signal averaging interval, and averaged over all simulation runs. Thus we represent the call degradation with a single mean value, even if we consider it as a parameter measuring the call quality in RSS based handover algorithms. The mean number of total call degradations is the sum of the mean number of the no-signal and the sudden call degradation.

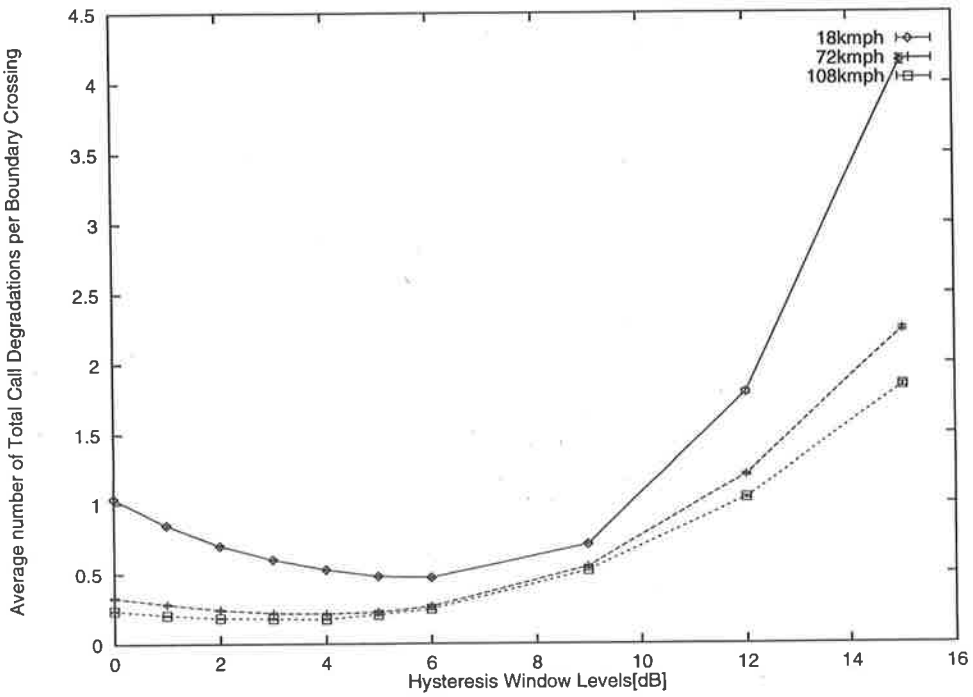

Figure 3.8: Total Call Degradation of Basic Algorithm with 50% overlap

- **Basic Handover Algorithm**

In figure 3.8, the total call degradation is shown for an overlapping condition of 50% and for MS speeds between 18kmph and 108kmph. The mean number of total call degradations increases for HYS levels from 6dB and above, while it decreases for HYS levels between 0db to 6dB. This characteristic remains the same for different speeds. This means that high HYS provides rather poor call quality to users compared to low HYS. For example, the mean number of total call degradations at 15dB HYS is about four times greater than at 0dB HYS, or about eight times greater than at 6dB HYS. Thus the call drop probability will be very high in particular when HYS is high, if call

see that sudden call degradation is affected by variations of HYS and the MS speed, but no-signal degradation is affected by the MS speeds only.

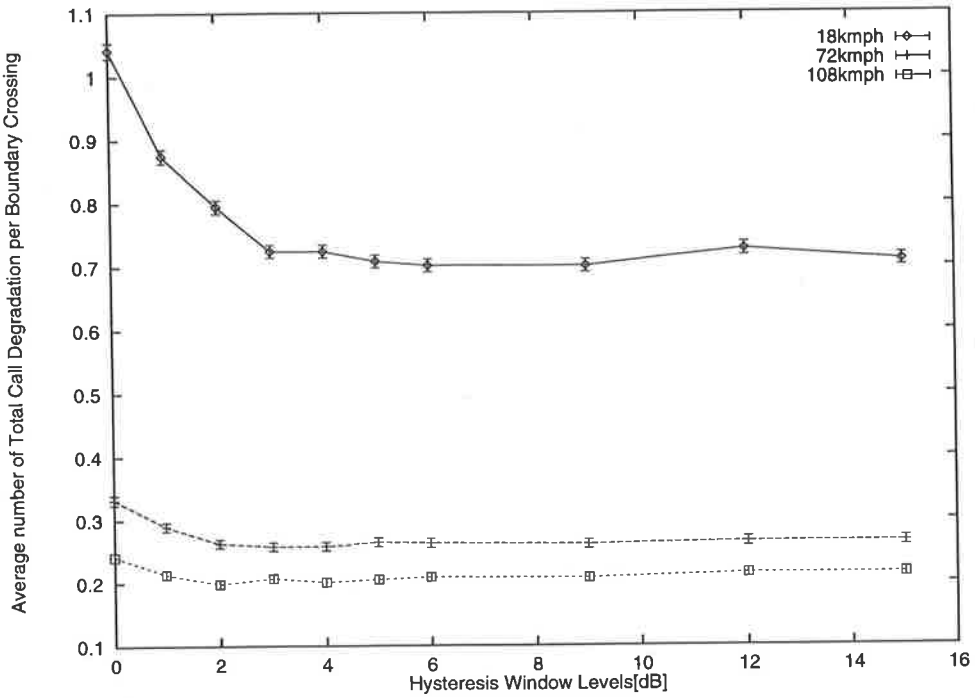

Figure 3.10: Average Number of Total Call Degradation of EN Algorithm with 50% overlap, MAX_TH=-124dBm

3.3.3 Handover Area (Point)

We now turn our interest to the actual occurrence points of the handover request and the call degradation to investigate the amount of delay of these points from the cell boundary. It is known that high HYS reduces the average number of handover requests per boundary crossing to unity in the basic handover algorithm. When the signalling traffic load is heavy, high HYS in handover algorithms is a better solution because only a small number of handover requests occur. However we need to extend investigations of other characteristics which are important for call quality. One of these is *handover area.* This is the region between the first and last handover request at a cell boundary crossing. We shall use this term even if only one handover request occurs.

As HYS increases, the handover area is delayed from the cell boundary [11, 13]. There is therefore a trade-off between the number of handover requests and the handover area

of call degradations. An unnecessarily high HYS on the other hand results in a small number of handover requests which are delayed excessively from the boundary with the destination BS, resulting in a large number of call degradations.

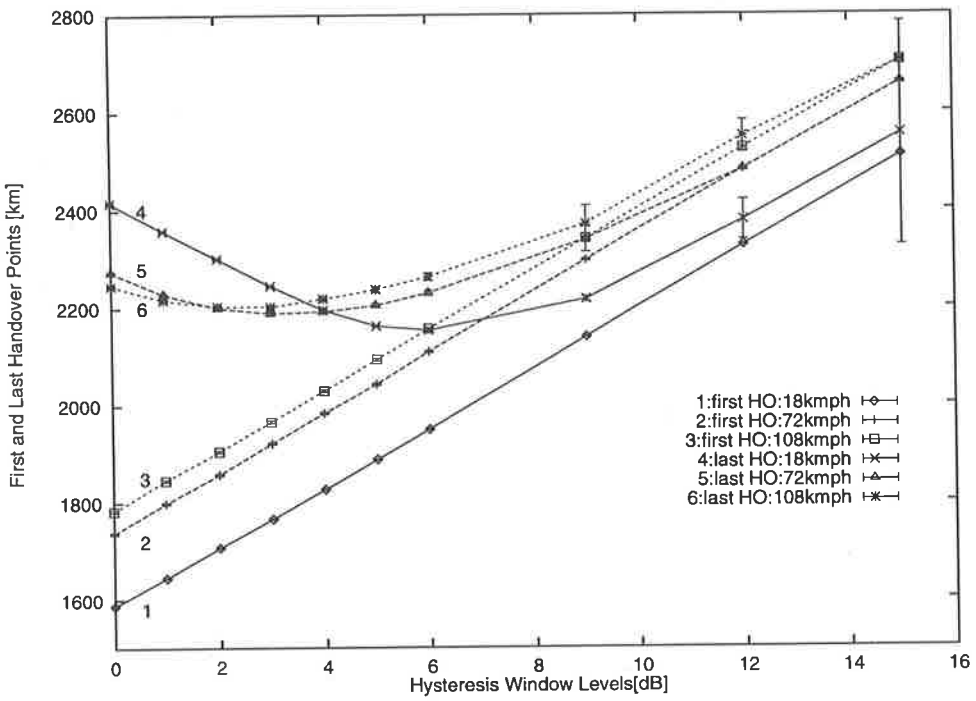

Figure 3.12: Handover Area (Point) of Basic Algorithm with 50% overlap, call boundary at 2km

- **Enforced and Normal (EN) Algorithm**

This algorithm provides significantly different results in terms of handover area as shown in figure 3.13, compared to that of the basic handover algorithm. The handover area is not significantly delayed and is wide over the whole range of HYS levels. Figure 3.5, curves 4,5 and 6, and figure 3.7, curves 3 and 4, show that the mean number of enforced handover requests does not change much as HYS increases. The handover point of the enforced handover request also does not change significantly as HYS increases as shown in figure 3.13. The EN handover algorithm has the feature that multiple enforced handover requests occur relatively close to the cell boundary with a small amount of call degradation at high HYS, while the basic handover algorithm generates one handover request quite far from the cell boundary but with a large number of call degradations. The handover requests occur within the overlapped area for the EN algorithm, while for the basic handover algorithm they generally occur outside the overlapped area. Since

the MS continuing to communicate with the original BS even as it moves further into the cell covered by the second BS. Thus the probability that the signal level of the current BS falls below MIN_TH will increase. The delay of the sudden call degradation point follows that of the handover area. As the MS speed increases from 18kmph to 108kmph, the handover area is delayed further from the cell boundary, and the sudden call degradation point is delayed by about 10% of the cell radius at 15dB HYS.

On the other hand, the mean point of no-signal call degradation has a significantly different behavior from that of the sudden call degradation. In figure 3.15, it can be seen that the no-signal call degradation point occurs near the cell boundary over the whole range of HYS levels, and for various MS speeds.

It can be seen in figures 3.12 and 3.14 that the sudden call degradation points located within the handover area are affected by the overall HYS, while the no-signal call degradation points (figure 3.15) seem to be unaffected by HYS. To understand the reason for this we note that the no-signal call degradation condition (equation 3.7) contains reference to absolute power measurements of the current and the destination BS, but not to HYS. However the condition of sudden call degradation uses the relative measurement of the received signal strength of the BSs. This is dependent on HYS as shown in figure 3.14 and so causes the handover characteristics to vary with HYS. The mean number of sudden or no-signal call degradations show similar dependence or independence on HYS as do their respective occurrence points.

- **Enforced and Normal (EN) Handover Algorithm**

The call degradation point for this algorithm has similar behavior to that of the basic handover algorithm. The behavior of the total call degradation point is the same as that of the sudden call degradation point because the latter dominates the total call degradation. The behavior of the total call degradation point as a function of HYS is similar to that of the handover area, as we have already seen for the basic handover algorithm. In contrast to the basic handover algorithm however (figure 3.14), under 50% overlapping conditions the total call degradation point for the EN handover algorithm does not change significantly with HYS level (see figure 3.16).

The sudden and no-signal call degradation conditions in the EN handover algorithm

shows similar characteristics of the call degradation point as does the basic handover algorithm. Unlike the sudden call degradation condition (equation 3.8) in the basic handover algorithm, the sudden call degradation condition in the EN algorithm is not affected by HYS, as the basic handover algorithm condition uses relative measurements (equation 2.26) while the EN handover condition (equations 2.30 and 2.31) uses a mixture of relative and absolute measurements. The sudden call degradation condition is not affected by HYS in the latter case, as shown in figures 3.16 and 3.17.

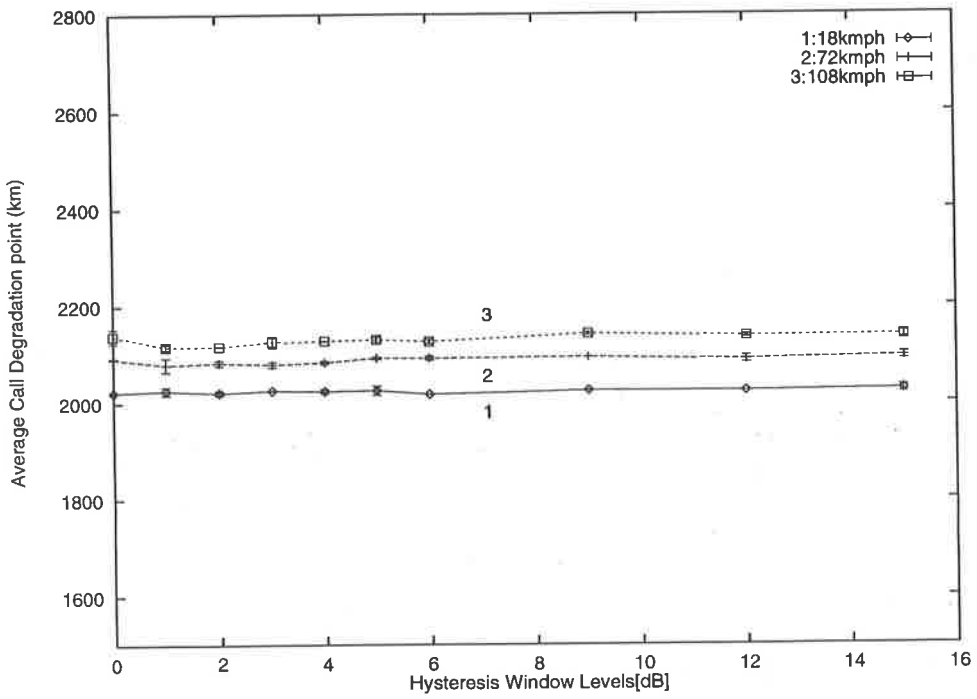

Figure 3.16: Total Call Degradation Point of Enforced and Normal (EN) HO with 50% overlap, MAX_TH=-124dBm

3.3.5 Conclusions

In section 3.2 we investigated two different handover algorithms, the basic and the EN handover algorithm, for the case where the autocorrelation of low fading is negligibly small. Those handover algorithms were studied using measures such as the number of handover requests, the number of call degradations, handover area and the occurrence point of call degradations. We considered only certain important system parameters such as HYS, MS speed and overlapping conditions.

that is, a large number of call degradations per cell boundary crossing. Therefore call degradation plays a very useful role in the basic handover algorithm analysis.

In the EN handover algorithm analysis the enforced handover request condition generates handover requests independently of HYS as shown in figure 3.7. This handover algorithm provides a small number of call degradations at high HYS compared to the basic handover algorithm. The number of handover requests (most of them are enforced handover requests) is about 8 times greater than that of the basic handover algorithm. This EN handover algorithm also result in smaller delay of the handover area and the sudden call degradation points than the basic handover algorithm.

The trade-off between the number of handover requests and the number of sudden call degradations, the mean handover area delay or the sudden call degradation point delay was obtained by comparison between different handover algorithms. In this study we found that the mean number of no-signal call degradations and its occurrence point near the cell boundary were not affected by any handover algorithm, because of the independence of the no-signal call degradation condition (equations 2.30) on MS speed and HYS.

3.4 Analytical Model

In our analytical study of handover algorithms, we use the same cell layout model and mobile system model as that of the simulation study. Before creating an analytical model of the handover algorithm, we review the mobile system model shown in figure 2.1 in Chapter 1. The transmitting signal, affected by slow and fast fading, is received every sampling interval and averaged after passing through the logarithmic circuit (transforming the log-normal distribution function to a Gaussian distribution function). Then the averaged signal is analysed at the system to provide a handover decision.

We begin by explaining the mathematical basis for the sampled and the averaged signal. Following that, a two state Markov model for the basic handover algorithm is developed using the signal difference function, and the mathematical approach for determining the number of handover requests per boundary crossing is derived. This is very similar to

$$n = \frac{T_{av}}{T_s} \tag{3.12}$$

where T_{av} is the signal averaging interval and T_s is the signal sampling interval. Because we use the n sample rectangular window signal averaging technique as described in section 2.3, the average over a block k is given by:

$$\mu_{x_k} = \frac{1}{n}\sum_{i=1}^{n} x(t_i) \tag{3.13}$$

where μ_{x_k} is the measured averageg of n samples, i represents each signal sample within the signal average block k, $i = 1, 2, 3, ..., n$ and n is the total number of samples shown in equation 3.12.

The measured average of the signal average μ_{x_k} is assumed to be an n-dimensional stationary gaussian random variable whose mean models path loss and whose variance models slow fading. Thus the second order joint moment of the n-dimensional random variables x_k needs to be considered in the signal averaging process, in other words in the handover algorithm analysis.

To examine the performance variation of handover algorithms based on this second order joint moment, we derive the analytical handover algorithm model with and without considering autocorrelation among the n-dimensional random variables. Firstly we consider uncorrelated gaussian random variables x_k for a special case where the random variables are statistically independent [60]. Secondly we consider autocorrelation of the n-dimensional random variables.

- **Uncorrelated Stationary Gaussian Random Variables**

According to the central limit theorem the weighted sum of n random variables (our sampled signals) with a weight $\{a_i\}$ is also a Gaussian random variable x_k with mean μ_{x_k} and variance $\sigma^2_{x_k}$ given by:

$$\mu_{x_k} = \sum_{i=1}^{n} a_i \mu_i \tag{3.14}$$

and

$$\sigma_{x_k}^2 = \frac{\sigma^2}{n^2(1-\rho)^2}(n - 2\rho + 2\rho^{n+1} - n\rho^2) \tag{3.19}$$

where ρ is the correlation coefficient $|\rho| < 1$ and n is the number of signal samples given by equation 3.12.

When $\rho = 0$, equation 3.19 reduces to equation 3.17.

If for all i, μ_i and σ_i are equal to $\hat{\mu}$ and $\hat{\sigma}$ respectively, then the mean and the standard deviation of the averaged signal for the uncorrelated multi random variables x_k are given by:

$$\mu_{x_k} = \hat{\mu} \quad \text{and} \quad \sigma_{x_k} = \frac{\hat{\sigma}_i}{n(1-\rho)}\sqrt{(n - 2\rho + 2\rho^{n+1} - n\rho^2)} \tag{3.20}$$

The mean and the standard deviation given in equation 3.20 are used for the analytical model of the handover algorithm. The weighted received signal for two particular BSs, namely BS-A and BS-B, may be written:

$$F_N(\mu_A, \sigma_A) \tag{3.21}$$

and

$$F_N(\mu_B, \sigma_B) \tag{3.22}$$

where μ_A is the mean of the averaged signal for BS-A, μ_B is the mean of the averaged signal for BS-B, σ_A is the standard deviation of the averaged signal for BS-A and σ_B is the standard deviation of the averaged signal for BS-B.

that, however, unequal BS transmit power between BSs will be studied in Chapter 4). Therefore the signal difference in equation 3.24 is simplified by extracting $P_t^A(d_A)$ and $P_t^B(d_B)$ as follows:

$$X(d) = (-L_p^A(d_A) + F^A(d - A)) - (-L_p^B(d_B + F^B(d_B)) \tag{3.25}$$

by manipulating, the signal difference we get:

$$X(d) = (-L_p^A(d_A) + L_p^B(d_B)) + (F^A(d - A) - F^B(d_B)) \tag{3.26}$$

Now the received signal of BS-A or BS-B has a mean μ_A or μ_B and a variance σ_A or σ_B respectively. Thus the signal difference random variable X has as mean value the difference of two means μ_A and μ_B and as variance the sum of the squares of two variances σ_A and σ_B as follows [61]:

$$\mu_X = \mu_A - \mu_B \tag{3.27}$$

and

$$\sigma_X^2 = \sigma_A^2 + \sigma_B^2 \tag{3.28}$$

We now consider the basic handover algorithm in terms of the signal difference function. The handover condition in the basic handover algorithm is:

$$RSS(m) + HYS \leq RSS(n) \tag{3.29}$$

where m and n are BS identifiers, $m \neq n$, and m is the current BS. HYS is the hysteresis window in dB.

In terms of the signal difference function the handover condition is as follows:

1. A handover from BS-A to BS-B will occur in any interval if:

$$(L_p(A) - L_p(B)) - (F(A) - F(B)) \geq HYS \tag{3.30}$$

where $P_{B/A}(k)$ given in equation 3.30 is the probability that the MS changes its current BS from BS-A to BS-B at the beginning of interval k, and $P_{A/B}(k)$ given in equation 3.31 is the probability that the MS changes its current BS from BS-B to BS-A at the beginning of interval k.

3.4.3 Calculation of Performance of the Handover Algorithm using the Signal Coverage Determination Function

The model for the handover conditions of equations 3.30 and 3.31 are based on the signal difference function which is Gaussian distributed with a mean μ_X and a standard deviation σ_X. To calculate the functions $P_{B/A}$ and $P_{A/B}$ we use the signal coverage determination function [26]. This is the probability that the received signal strength exceeds the received signal strength threshold x_0 at a distance d between the MS and the BS:

$$P_{x_0}(d) = P[x \geq x_0] = \int_{x_0}^{\infty} p(x)\, dx \tag{3.34}$$

where $p(x)$ is the Gaussian density function with mean μ_X and variance σ_X^2:

$$p(x) = \frac{1}{\sigma_X \sqrt{2\pi}} \exp\left(-\frac{(x-\mu_X)^2}{2\sigma_X^2}\right) \tag{3.35}$$

The mean and the variance of $p(x)$ is defined in equations 3.27 and 3.28. The mean μ_X is the path loss difference between BS-A and BS-B, and is obtained by substituting equation 2.1 into equation 3.27 as follows:

$$\begin{aligned} \mu_X &= \mu_A - \mu_B \\ &= (K_1(A) + K_2(A)\log(d_A)) - (K_1(B) + K_2(B)\log(d_B)) \end{aligned} \tag{3.36}$$

where d_A is the distance between the MS and BS-A in km, d_B is the distance between the MS and BS-B in km. $K_1(A)$ and $K_1(B)$ are given in equation 2.10 while and $K_2(A)$ and $K_2(B)$ are given in equation 2.12.

1. The MS is connected to BS-A at the beginning of the $k-1th$ interval and the signal difference random variable X exceeds HYS at the beginning of the kth interval (equation 3.30), or

2. The MS is connected to BS-B at the beginning of the $k-1th$ interval and X falls below $-HYS$ at the beginning of the kth interval (equation 3.31).

Therefore the probability that a handover occurs at the beginning of the kth interval is simply obtained from the two state handover model of figure 3.18 as follows:

$$\begin{aligned} P_{ho}(k) &= P_A(k-1)P_{B/A}(k) + P_B(k-1)P_{A/B}(k) \\ P_{ho}(0) &= 0 \end{aligned} \tag{3.41}$$

The average number of handover requests during the MS travelling time from BS-A to BS-B is given by:

$$E_{ho} = \sum_{k=1}^{N} P_{ho}(k) \tag{3.42}$$

where N is the total number of signal average intervals. A lower bound for E_{ho} is obtained in Appendix D.

3.4.5 Analytical Model of the Enforced and Normal (EN) Handover Algorithm

Now we derive an analytical model for the EN handover algorithm. The normal and the enforced handover request conditions are reviewed again as follows.

1. The Normal Handover request (NHR) condition:

$$RSS(m) + HYS \leq RSS(n) \quad \text{and} \quad RSS(m), RSS(n) \geq MAX\_TH \tag{3.43}$$

2. The Enforced Handover request (EHR) condition:

$$MIN\_TH \leq RSS(m) \leq MAX\_TH \quad \text{and} \quad RSS(n) \geq MAX\_TH \tag{3.44}$$

In the EN handover algorithm, there are two ways for a handover to occur at the beginning of interval k as follows:

1. The MS is connected to BS-A at the beginning of the $k-1th$ interval and experiences either a normal or enforced handover condition for BS-A, or
2. The MS is connected BS-B at the beginning of the $k-1th$ interval and experiences either a normal or enforced handover condition for BS-B.

We have noted that the normal and the enforced handover conditions are mutually exclusive. Consider the conditional probability $P_{A|B}$ where A and B are related events, and suppose that A can be decomposed into two independent events N and E representing the normal and enforced handover conditions, that is, $A = N \cup E$ and $N \cap E = \Phi$. The conditional probability can be computed as:

$$\begin{aligned} P(A|B) &= P(N \cup E|B) = \frac{P[(N \cup E) \cap B]}{P(B)} \\ &= \frac{P(N \cap B)}{P(B)} + \frac{P(E \cap B)}{P(B)} \\ &= P(N|B) + P(E|B) \end{aligned} \tag{3.46}$$

therefore we can write:

$$\begin{aligned} P^T_{B/A}(k) &= P^N_{N_1/A}(k) + P^E_{E_1/A}(k) \\ P^T_{A/B}(k) &= P^N_{N_2/B}(k) + P^E_{E_2/B}(k) \end{aligned} \tag{3.47}$$

We now derive the normal and enforced handover condition based on the conditions given in equations 3.43 and 3.44 as follows. The normal handover request condition (NHR) consists of:

1. $RSS(m) + HYS \leq RSS(n)$, that is, the RSS of the current BS plus HYS is less than the RSS of the neighbouring BS,

We also can derive the probability that the MS is connected to BS-A, $P_A^T(k)$, or BS-B, $P_B^T(k)$, at the beginning of interval k by substituting equation 3.50 into equation 3.45.

Therefore the probability that any handover (normal plus enforced) occurs at the beginning of interval k is:

$$P_{thr}(k) = P_A^T(k-1)(1 - P_{B/A}^T(k)) + P_B^T(k-1)P_{A/B}^T(k) \tag{3.51}$$

By substituting equation 3.50 into equation 3.51, we get:

$$\begin{aligned} P_{thr}(k) &= P_A^T(k-1)((P_{B/A}(k)P_{ub}(k)P_{ua}(k)) + (P_{ub}(k)P_{ua1}(k))) \\ &+ P_B^T(k-1)((P_{A/B}(k)P_{ua}(k)P_{ub}(k)) + (P_{ua}(k)P_{ub1}(k))) \end{aligned} \tag{3.52}$$

Thus the average number of handover requests (normal plus enforced handover requests) per boundary crossing is given by:

$$E_{tho} = \sum_{k=1}^{N} p_{thr}(k) \tag{3.53}$$

We obtain a lower bound of the equation 3.53 in Appendix D.

We obtain expressions for the probabilities in the above equations by using the signal coverage determination function of section 3.4.3. The condition for P_{ua} and P_{ub} is obtained from equations 3.34 and 3.35 with a mean value $\mu_A = (K_1(A) + K_2(A)\log(d_A))$ and a variance σ_A for P_{ua}, and with a mean value $\mu_B = (K_1(B) + K_2(B)\log(d_B))$ and a variance σ_B for P_{ub}. The probability that the received signal from BS-A exceeds the signal threshold MAX_TH at the beginning of kth interval is given by:

$$\begin{aligned} P_{ua}(k) &= P_{MAX\_TH}(k) \\ &= \int_{MAX\_TH}^{\infty} \frac{1}{\sigma_A\sqrt{2\pi}} \exp\left(-\frac{(x-\mu_A)^2}{2\sigma_A^2}\right) dx \end{aligned} \tag{3.54}$$

where d_A is the distance between the MS and BS-A in km. Following the same procedure, the probability that the RSS of BS-B is greater than the minimum signal threshold at the beginning of the kth interval is given by:

We obtain a lower bound for equation 3.59 in Appendix D.

- **Enforced Handover Request**

Following similar procedures to the above, we derive the probability that an enforced handover occurs at the beginning of interval k as follows:

$$P_{ehr}(k) = P_A^T(k-1)(P_{ub}(k)P_{ua1}(k)) + P_B^T(k-1)(P_{ua}(k)P_{ub1}(k)) \tag{3.60}$$

where P_{ua1} and P_{ub1} are obtained by using equations 3.56 and 3.57.

Substituting equations 3.54, 3.55, 3.45 and 3.47 into equation 3.60, gives the average number of enforced handover requests during the MS trip:

$$E_{ehr} = \sum_{k=1}^{N} P_{ehr}(k) \tag{3.61}$$

A lower bound of the equation 3.61 is derived in Appendix D.

3.4.6 Modelling of the Call Degradation Condition

As we found from the previous simulation study, the call degradation condition is very important because the received signal falling below MIN_TH may lower the call quality or cause a call disconnection. We derive an analytical model of the call degradation in this section. The two call degradation conditions are modelled as follows:

1. No-Signal call degradation condition (NDEG):

$$RSS(m) \leq MIN\_TH \quad \text{and} \quad RSS(n) \leq MIN\_TH \tag{3.62}$$

2. Sudden call degradation condition (SDEG) in which the received signal from the current BS is less than MIN_TH but that of any neighbouring BS is greater than MIN_TH:

$$RSS(m) \leq MIN\_TH \quad \text{and} \quad RSS(n) \geq MIN\_TH \tag{3.63}$$

$$E_{sdeg} = \sum_{k=1}^{N} P_{sdeg}(k) \quad (3.67)$$

$$E_{tdeg} = \sum_{k=1}^{N} (P_{ndeg}(k) + P_{sdeg}(k)) \quad (3.68)$$

- **EN handover algorithm**

We can derive the probabilities for both types of call degradation by using the two state model for the EN handover algorithm of figure 3.19. As we have already developed similar expressions for the basic handover algorithm in equations 3.64 and 3.65, we can make a simple adaptation for the EN handover algorithm by replacing $P_A(k)$ and $P_B(k)$ with $P_A^T(k)$ and $P_B^T(k)$ respectively. Thus the probability that the MS experiences a no-signal call degradation at the beginning of the interval k is given by:

$$P_{ndeg1}(k) = P_A^T(k)(1 - P_{ua}(k))(1 - P_{ub}(k)) + P_B^T(k)(1 - P_{ub}(k))(1 - P_{ua}(k)) \quad (3.69)$$

where $P_A^T(k)$ and $P_B^T(k)$ represent the probability that BS-A and BS-B respectively are connected to the MS in the EN handover algorithm, P_{ua} is the probability that the RSS of the current BS, BS-A, is greater than MIN_TH (see equation 3.54) and P_{ub} is the probability that the RSS of BS-B is greater than MIN_TH (see equation 3.55).

By following the same procedures, we can also derive the probability that the MS experiences a sudden call degradation at the beginning of interval k. This is given by:

$$P_{sdeg1}(k) = P_A^T(k)(1 - P_{ua}(k))P_{ub}(k) + P_B^T(k)(1 - P_{ub}(k))P_{ua}(k) \quad (3.70)$$

The average number of no-signal call degradations, sudden call degradations and total call degradations during the MS trip is:

$$E_{ndeg1} = \sum_{k=1}^{N} P_{ndeg1}(k) \quad (3.71)$$

$$E_{sdeg1} = \sum_{k=1}^{N} P_{sdeg1}(k) \quad (3.72)$$

$$E_{tdeg1} = \sum_{k=1}^{N} (P_{ndeg1}(k) + P_{sdeg1}(k)) \quad (3.73)$$

3.5 Comparison of Analytical and Simulation Results

Using the same system parameters as those of the simulation study, we obtain the results for the analytical model for the basic handover algorithm and the Enforced and Normal (EN) handover algorithm for various HYS levels and MS speeds. We mainly consider the mean number of handover requests for the basic handover algorithm, the mean number of normal and the enforced handover requests for the EN handover algorithm, and the mean number of no-signal and sudden call degradations for both handover algorithms.

As we have already indicated in section 3.1, we now evaluate the analytical model by comparing with the simulation model in which the slow fading autocorrelation is assumed to be negligible. The effects of autocorrelation are considered in the following section. While autocorrelation is considered to be a very important parameter for handover performance studies, we begin with the simple uncorrelated models to obtain initial verifications of our analytical results.

3.5.1 The Average number of Handover Requests

The analytical study shows that as HYS increases the mean number of handover requests decreases in the basic and EN handover algorithm while the mean number of enforced handover requests in the EN handover algorithm increases. This was demonstrated also by the simulation model.

- **Basic Handover Algorithm**

Figure 3.20 shows the analytical and simulation results for the mean number of handover requests for the basic handover algorithm. Both models show very similar results at high HYS (above about 6dB), but are very different for lower values of HYS. To clarify the reasons for these differences, we examine the radio propagation models used in the analytical and simulation models. In simulation a very long time delay t' (equation 3.1) is usually used to approximate uncorrelated slow fading. The resulting autocorrelation coefficient is about 10^{-5}, which is not negligible for very low HYS. Substitution of this value into analytical results which include the effect of autocorrelation, shows that au-

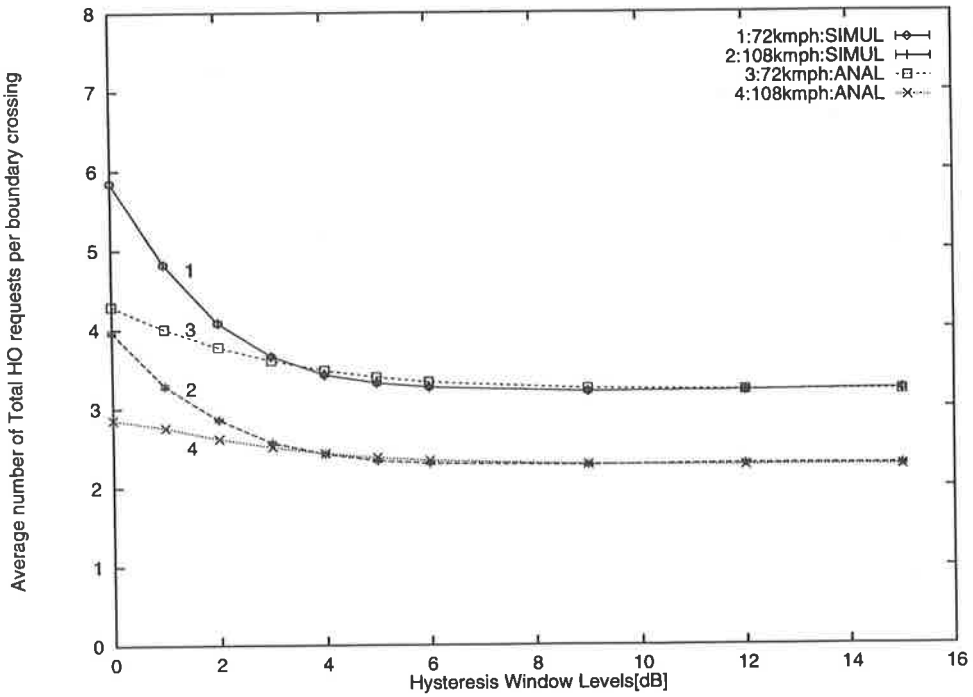

Figure 3.21: Average Number of Total HO Requests of EN Algorithm with 50% overlap

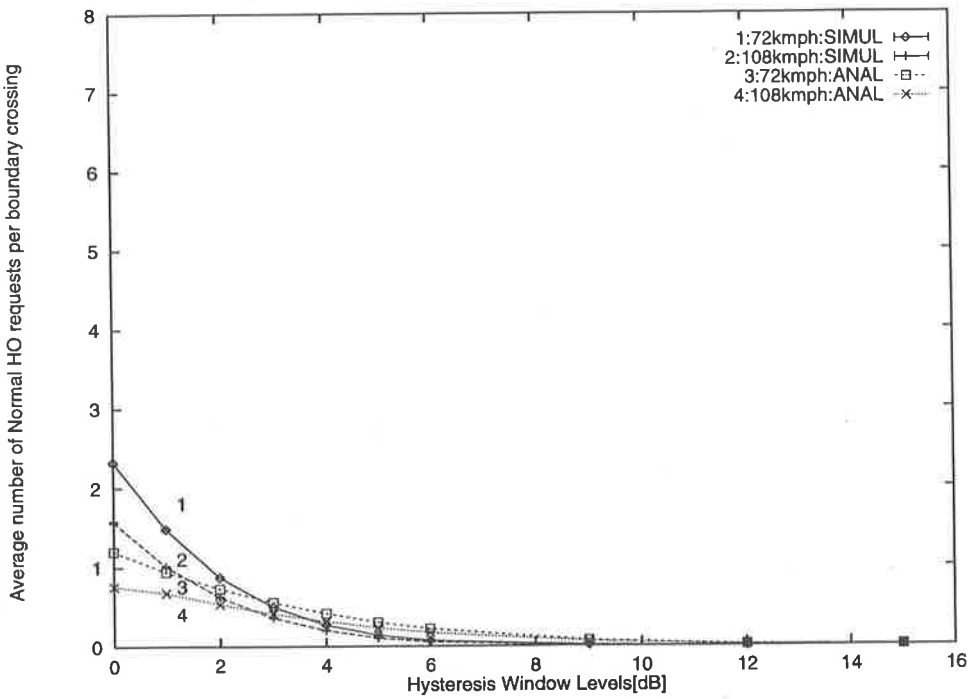

Figure 3.22: Average Number of Normal HO Requests of EN Algorithm, 50% overlap and MAX_TH=-124dBm

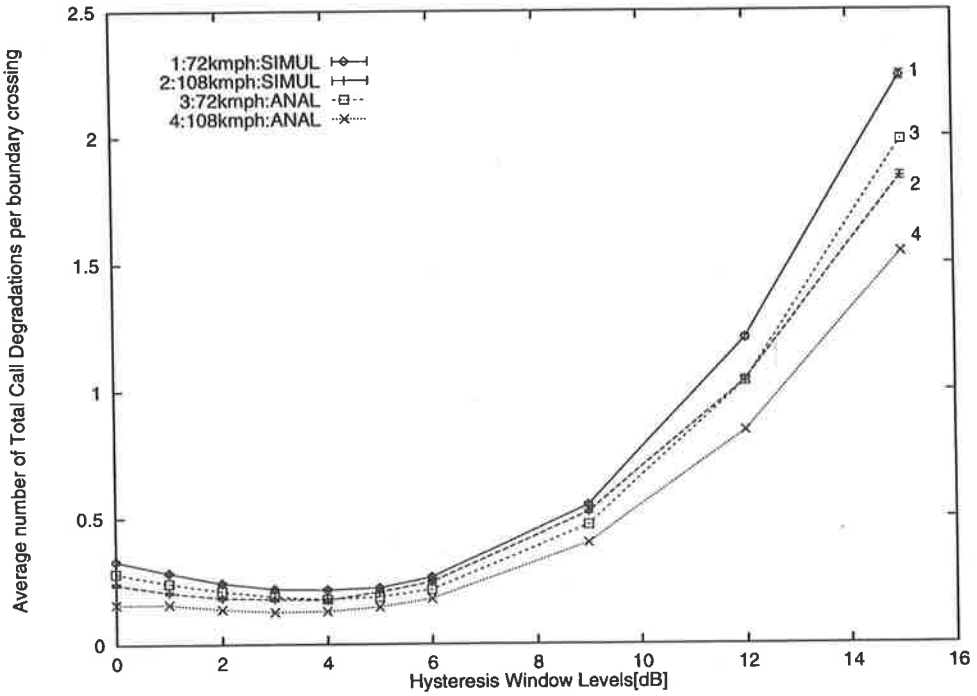

Figure 3.24: Average Number of Total Call Degradation of Basic Algorithm with 50% overlap

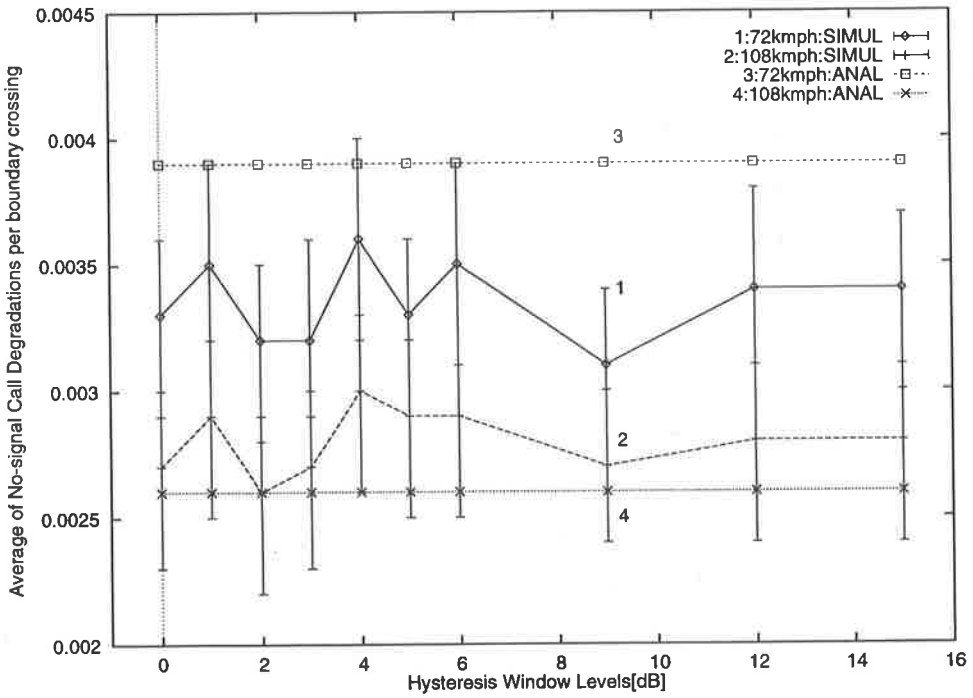

Figure 3.25: Average Number of No-Signal Call Degradation of Basic Algorithm with 50% overlap

3.6 Effects of Autocorrelation in Slow Fading

It has been found that autocorrelation in slow fading has an important effect on the performance of the handover algorithm [7, 24, 11]. We investigate here the difference in performance of the handover algorithm as a result of this autocorrelation. We use the exponential autocorrelation model [49] (see equations 3.2, 3.3 and 3.4) mentioned in section 3.2.2 consisting of two important parameters:

1. dec_0 representing how fast correlation decays with distance;
2. the mean distance D over which correlation rate decays.

Two parameters in the handover algorithm are considered to be mainly related to the autocorrelation:

1. The signal sampling distance d_s (T_s in time domain);
2. The signal averaging distance d_{av} (T_{av}).

There are four scenarios which we can use to investigate the performance of the handover algorithm in terms of the four parameters mentioned above.

1. short signal sampling and a short signal averaging: $dec_0 > d_s$ and $D > d_{av}$.
2. short signal sampling and an long signal averaging: $dec_0 > d_s$ and $D \leq d_{av}$.
3. long signal sampling and an short signal averaging: $dec_0 \leq d_s$ and $D > d_{av}$.
4. long signal sampling and a long signal averaging: $dec_0 \leq d_s$ and $D \leq d_{av}$.

Note that we assume $\epsilon_D = 0.1$ where D is the mean autocorrelation decay distance.

These discriminations allow us to investigate the autocorrelation effects from the radio propagation viewpoint, and the signal sampling and averaging methods from the signal detection viewpoint.

Based on the previous studies on the autocorrelation coefficient of Gudmundsen [9, 49], the correlation decay rate (dec_0) and the mean autocorrelation decay distance (D) are

opportunity for handover requests to occur becomes large.

Figure 3.29 compares the mean number of handover requests for scenarios 1 and 2 (see table 3.3). As the normalised autocorrelation rate increases from scenario 2 (graphs 3 and 4) to scenario 1 (graphs 1 and 2), the difference between the results from the analytical model and those of the simulation model increases. This is because the signal sampling distance (d_s) is less than the correlation decay rate (dec_0) and/or the signal averaging distance (d_{av}) is less than the mean autocorrelation decay distance (D) in scenario 1. In general if the autocorrelation coefficient becomes large, the accuracy of our analytical model compared with the simulation model will be reduced.

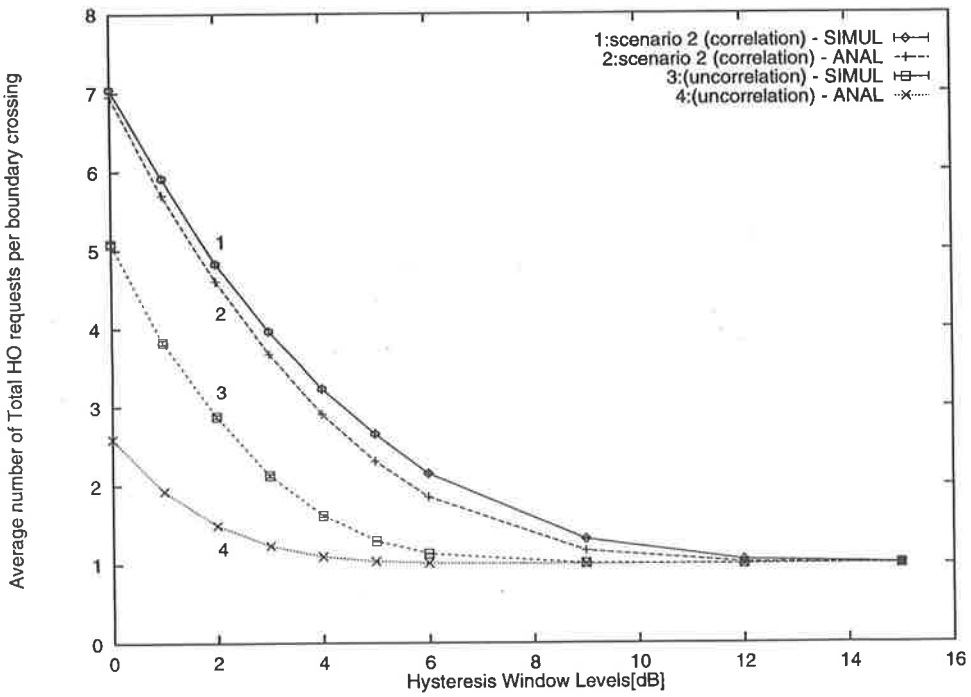

Figure 3.28: Average Number of HO Requests of Basic Algorithm with 50% overlap

3.6.2 Average Number of Call Degradations

Because of correlation effects, the mean number of total call degradations increases quite significantly over the whole range of HYS as shown in figure 3.30. The simulation and the analytical models do not compare well but both models show similar behavior against HYS. As we have mentioned in subsection 3.6.1, figure 3.31 shows that the mean number of call degradations increases and the accuracy of the analytical results decreases as the

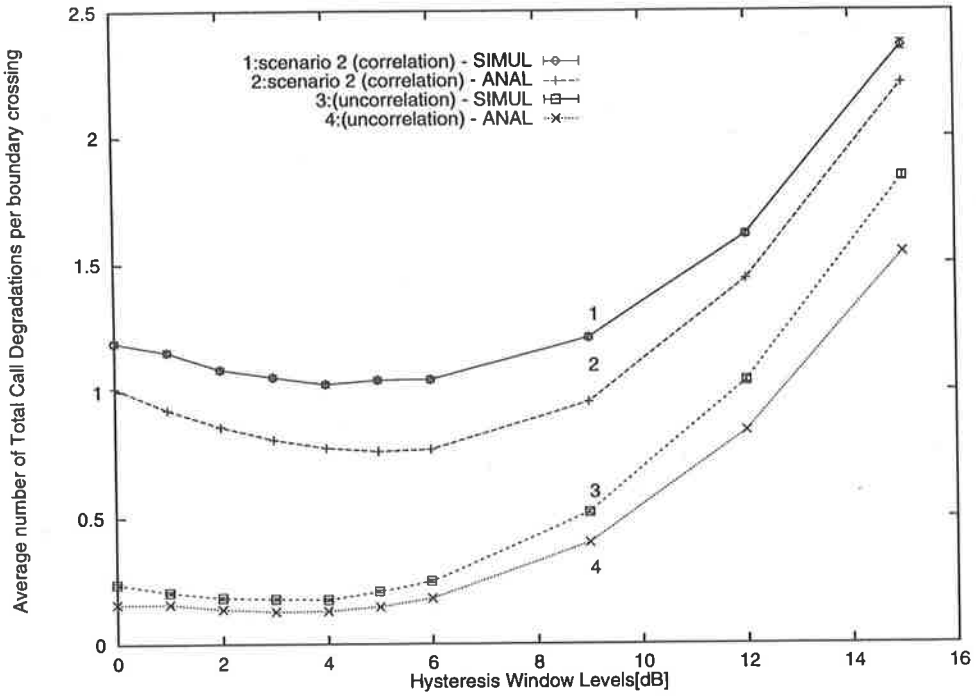

Figure 3.30: Average Number of Total Call Degradation of Basic Algorithm with 50% overlap

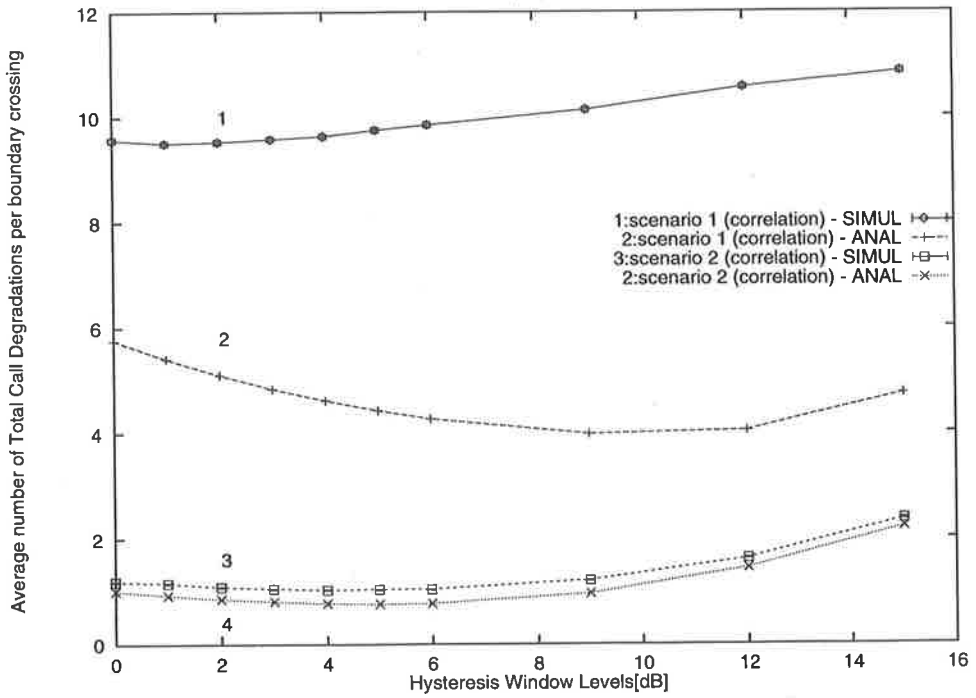

Figure 3.31: Average Number of Total Call Degradation of Basic Algorithm with 50% overlap

(b) The handover area delays as HYS increases (simulation model only).

(c) The sudden call degradation point delays as HYS increases (simulation model only).

(d) Based on the above conclusions, the choice of the HYS level to use in the handover algorithm should be made on the basis of the number of call degradations, the number of handover requests and their occurrence point rather than just the number of handover requests which is the normal case [20, 10, 43].

(e) The no-signal call degradation point occurs at the cell boundary (simulation model only)

(f) The mean number of no-signal call degradations is not dependent on HYS.

(g) The sudden call degradation is dependent on HYS.

2. In the EN handover algorithm analysis the handover request characteristic determined from the analytical and simulation models is as follows:

(a) As HYS increases the number of normal handover requests decreases but other characteristics such as the number of enforced handover requests and the number of no-signal and sudden call degradations are not strongly related to HYS.

(b) Based on 1(a) and 2(a), we understand that different handover algorithms can generate totally different results: at medium and high HYS the EN handover algorithm provides a smaller number of call degradations but a larger number of handover requests than the basic handover algorithm, while at low HYS the EM handover algorithm generates a larger number of call degradations and a smaller number of handover requests than the basic handover algorithm.

(c) Based on the above conclusion, the mean number of no-signal call degradations does not change with HYS.

3. In comparisons between the simulation and analytical models with autocorrelated slow fading, our conclusions are as follows:

When we compare the results of the analytical model to that of the simulation model, we see greater accuracy for results in which relative RSS measurements appear (such as handover request condition), compared to those in which absolute measurements occur (such as the call degradation condition and the no-signal call degradation condition).

When the handover algorithm is analysed based on the handover characteristics which we have investigated, more accurate and efficient analyses can be achieved. Moreover these analyses will further understanding of the handover algorithm and therefore assist in developing a more efficient handover algorithm.

The handover analysis model of Vijayan *et al.* is produced by including the autocorrelation of the log-normal fading. They use an exponential sliding window with very short signal averaging distance. However the performance of their model does not agree well with their simulation results when HYS is low to medium. This is because the normalized autocorrelation coefficient of fading is relatively large, with the autocorrelation length being larger than the signal sampling interval. Further investigation is required in regard to the handover algorithm model development when autocorrelation of log-normal fading is significant.

Chapter 4

Application of Handover Algorithm

4.1 Introduction

The analytical and the simulation studies for the basic handover algorithm and the Enforced and Normal (EN) handover algorithm have been discussed in Chapter 3 under the condition that the transmit powers from both base stations were equal. In this chapter, we consider unequal transmit powers between BSs in both the simulation and analytical models of the basic handover algorithms. To enable us to study the handover algorithms under worst case conditions, we introduce a new scenario in which the MS moves along the cell boundary, maintaining an equal distance from both BSs at all times. This worst case study will be done using both equal and unequal BS transmit power conditions. From these studies we can obtain further insights into the handover algorithm performance beyond those obtained from the studies reported in Chapter 3. We shall only consider the basic handover algorithm in this chapter.

A handover algorithm analysis for investigating the number of handover requests versus the signal averaging interval is also examined to show that longer signal averaging intervals can reduce the average number of handover requests [43]. We measure the number of call degradations per boundary crossing versus the signal averaging interval in order to study how the latter affects call degradation. We then introduce a new parameter which combines the *normalised average fade duration (AFD)* [62, 33] with the probability that the MS is connected to the BS during a signal averaging interval. We call this

condition is chosen for the equal BS transmit power model. We assume in this chapter that the uplink power (transmission from the MS to the BS) is equal to that of the downlink power (transmission from the BS to the MS).

We shall use the same analytical handover algorithm model developed in Chapter 3 for evaluating the simulation results of the unequal BS transmit power model.

4.2.1 Simulation Model

The unequal BS transmit power model is illustrated in diagrams (a) and (c) of figure 4.1. In that figure, the ideal cell boundary, that is, 2km distance from the BS, is shown with a plain line. The real cell boundary of the region covered by the BS transmit power is shown with a dotted line. When both BSs have equal transmit power, we assume that the overlapping area is equally divided between BSs shown in diagram (b) of figure 4.1. As the transmit power of BS-A increases and becomes greater than the power of BS-B (diagram (a) of figure 4.1), the cell coverage of BS-A expands towards BS-B. In the same way, as the transmit power of BS-B increases and becomes greater than that of BS-A, the cell coverage of BS-B expands toward BS-A as shown in diagram (c) of figure 4.1.

To analyse the autocorrelation effects in the equal and the unequal BS transmit power models we use a correlation coefficient of 0.6 in the slow fading model.

We now consider the cell layout, the transmit power initialisation (overlapping conditions), the call degradation conditions and the basic handover algorithm conditions.

- **Cell Layout**

Our model consists of two BSs having 2km radius, and one MS which travels from BS-A to BS-B with a constant speed of 72kmph. The signal averaging interval is chosen to be 2 seconds. Thus the signal averaging distance is 120λ where λ is the wavelength. There is no call blocking and the call holding time is equal to the MS travelling time. Power control is not considered. Note that the mean power consumption can vary in the unequal BS transmit power model, because of the unequal transmit power between BSs.

Table 4.1: BS transmit power based on overlapping condition

overlapping condition [%]	(y)	[watts]	[dBm]
25	0.25	21.44	43.3121
50	0.5	41.63	46.1937
75	0.75	72.93	48.6191
100	1.0	118.5430	50.7388

r is 2[km] and MIN_TH is -100[dBm]

is shown in table 4.1 in dBm.

We will use two unequal transmit power models:

1. 50% overlap for the source BS and 100% overlap for the destination BS;
2. 100% overlap for the source BS and 50% overlap for the destination BS.

The equal transmit power model, that is, 75% overlap for the source BS and 75% overlap for the destination BS, is also used.

- **Call Degradation Conditions**

The two types of call degradation conditions used in Chapter 3 are:

1. No-Signal call degradation condition:

$$RSS(\text{all BSs}) \leq MIN\_TH \tag{4.2}$$

This states that the MS cannot be served properly by any BS because the RSS of all BS's is less than MIN_TH. We assume that this condition can only be improved by increasing the transmit power level of the BSs or redesigning the cell layout to provide the necessary power to users.

2. Sudden call degradation condition:

$$RSS(\text{current BS}) \leq MIN\_TH \quad \text{and} \quad RSS(\text{neighbour BS}) \geq MIN\_TH \tag{4.3}$$

This is an interesting condition from the handover algorithm point of view, because the MS experiences poor quality of call conversation, even if the best neighbour

transmit power model.

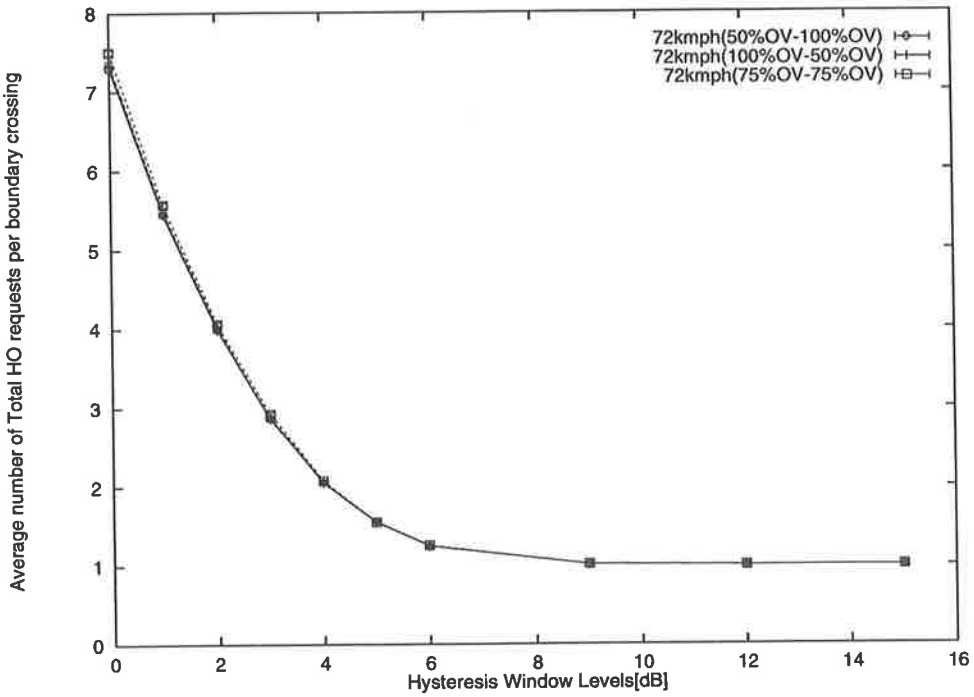

Figure 4.2: Average Number of HO Requests for the Basic HO Algorithm

connected to the weaker source BS over a greater portion of the travel. However if the source BS has a stronger transmit power than the destination BS (for the case of curve 2 in figure 4.3), then for higher HYS, the MS will remain connected for a longer time with the stronger BS.

- **Average Number of Total Call Degradations**

In contrast to the mean number of handover requests, the mean number of call degradations shown in figure 4.4 is different for the three BS transmit power models. From 0 to 6dB HYS, there is little difference between them. However as HYS increases above 6dB, the difference among the three BS transmit power models is significant. The unequal BS transmit power model with 50% overlap for BS-A and 100% overlap for BS-B, has the worst call degradation (curve 1 in figure 4.4) over the whole range of HYS. The model with 100% overlap for BS-A and 50% overlap for BS-B has the best call degradation (curve 2 in figure 4.4).

Recall that the mean number of call degradations can be improved by increasing the BS transmit power. This explains the results of figure 4.3. The stronger the BS transmit power, the lower the call degradation. From this point of view, the model with 100% overlap for BS-A and 50% overlap for BS-B provides the strongest power to the MS over the trip and therefore maintains the lowest number of call degradations out of three models, as shown in figure 4.4. On the other hand, the model with 50% overlap for BS-A and 100% overlap for BS-B exhibits a sharp increase with HYS in the mean number of call degradations compared to other models, because the mean power provided to the MS is less. All models generate the same number of call degradations at low and medium HYS. This is consistent with the observation that the mean power consumption is maintained at a similar level for all models.

The following subsection provides more insight into this observation.

- **Handover Area (Point)**

When the transmit power of the source BS is greater than that of the destination BS (curve 1 of figure 4.5), the handover area shifts further towards the destination BS compared to the equal BS power model (curve 3 of figure 4.5). However when the destination BS transmit power is greater than that of the source BS (curve 2 of figure 4.5),

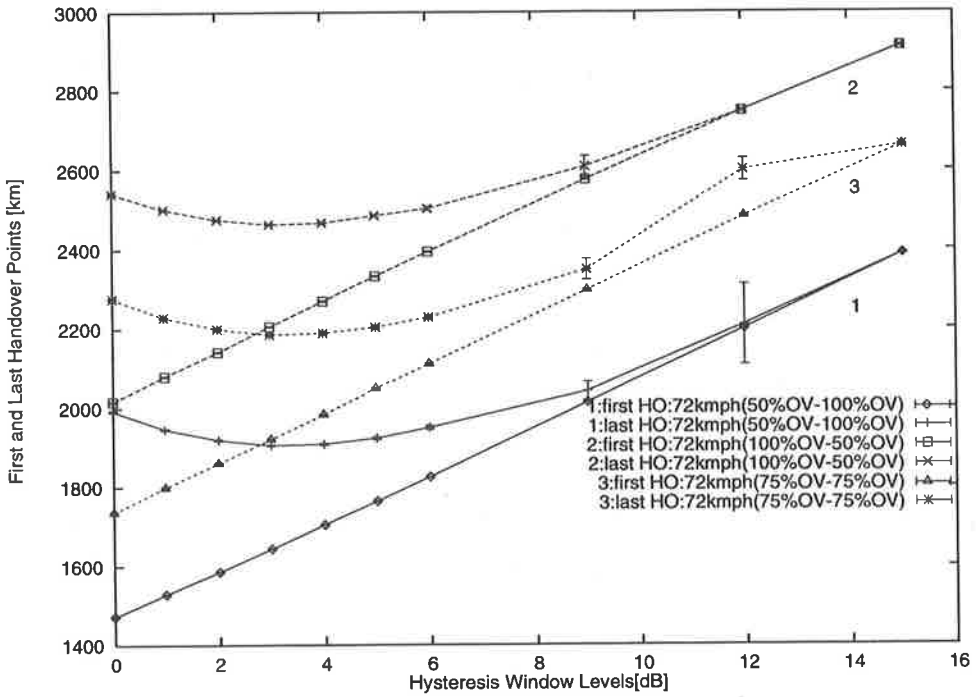

Figure 4.5: Mean Handover Area (Point) Variation Versus HYS for the Basic Handover Model

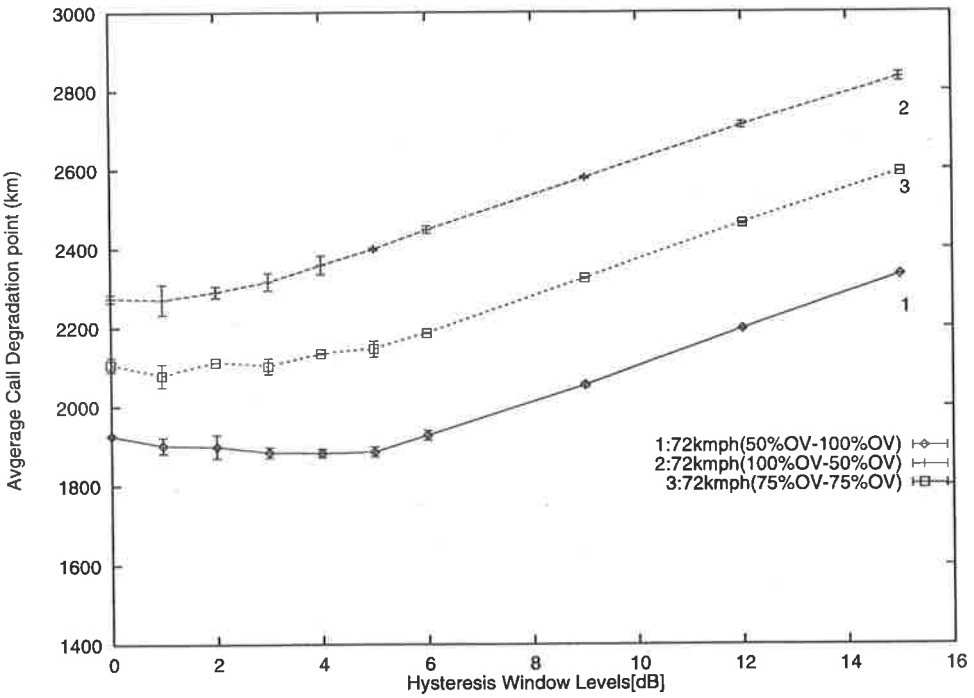

Figure 4.6: Mean Call Degradation Point Variation Versus HYS for the Basic Handover Model

In figure 4.8 when the correlation (curves 1 and 2) is high, the mean number of call degradations (curves 1 and 2) is much larger than that of the uncorrelation model (curves 3 and 4).

In the comparisons shown in figures 4.7 and 4.8, we see that when the signal averaging interval is of fixed length in the handover algorithm, the role of HYS becomes very attractive to minimise the mean number of handover requests. The mean number of call degradations can be used as an indicator for finding the best HYS level for a particular slow fading environment because it monitors the absolute level of the received signal strength of the current BS as well as that of the neighbouring BS. The bigger the autocorrelation coefficient, the lower the call quality.

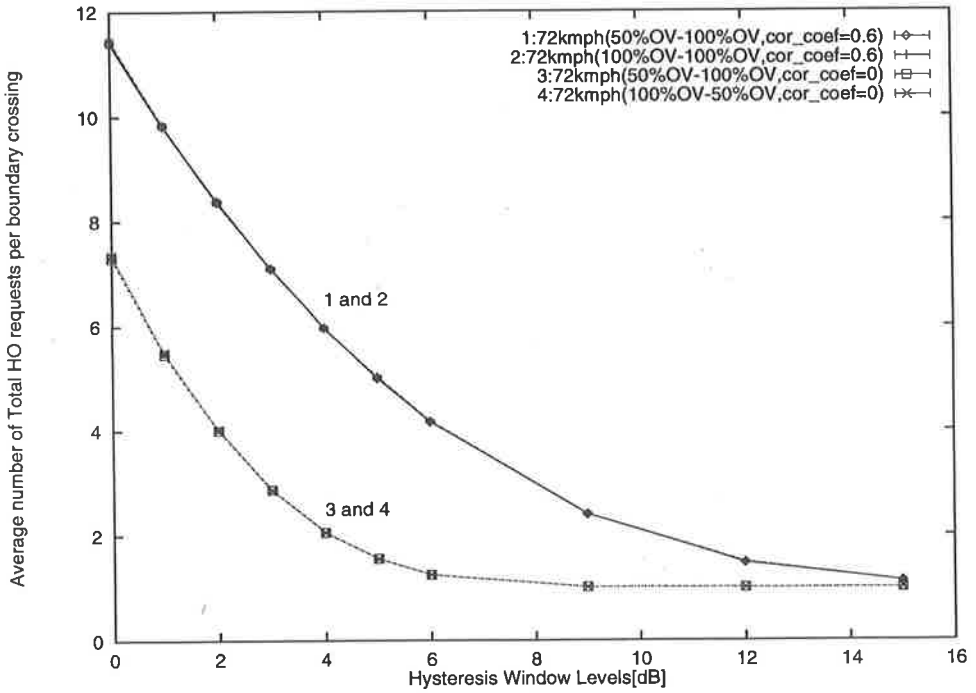

Figure 4.7: Average number of HO requests for the Basic HO Algorithm

4.2.4 Analytical Model

We use the same analytical model as that derived in Chapter 3, using the assumption that the received signal strength is a stationary Gaussian random variable. The averaged signal difference between the BSs is also assumed to be a stationary Gaussian random variable X having a mean and standard deviation as follows (See Appendix C):

given by equation 3.28.

The probability $P_{A/B}$ that the signal difference is greater than HYS, that is, the probability that the received signal strength of BS-A is less than that of BS-B plus HYS, is given by:

$$(P_t(A) - P_t(B)) + (-L_p(A) + L_p(B)) + (F(A) - F(B)) \geq HYS \tag{4.7}$$

The probability $P_{B/A}$ that the signal difference X is less than $-HYS$, that is, the probability that received signal strength of BS-B is less than that of BS-A plus HYS is given by:

$$(P_t(A) - P_t(B)) + (-L_p(A) + L_p(B)) + (F(A) - F(B)) \leq -HYS \tag{4.8}$$

We assumed in Chapter 3 that the first term in equations 4.8 and 4.7 was zero, because the equal BS transmit power model was used. However in this section we consider this term for the unequal BS transmit power model.

The probabilities given in equations 4.7 and 4.8 can be calculated using the signal coverage determination function of section 3.4.3. At the beginning of the interval k, $P_{A/B}$ and $P_{B/A}$ are given by:

$$\begin{aligned} P_{A/B}(k) &= 1 - P_{-HYS}(k) \\ &= \int_{-\infty}^{-HYS} \frac{1}{\sigma_X\sqrt{2\pi}} \exp(-\frac{(x-\mu_X)^2}{2\sigma_X^2})\, dx \qquad (4.9) \\ P_{B/A}(k) &= P_{HYS}(k) \\ &= \int_{HYS}^{\infty} \frac{1}{\sigma_X\sqrt{2\pi}} \exp(-\frac{(x-\mu_X)^2}{2\sigma_X^2})\, dx \qquad (4.10) \end{aligned}$$

where $\mu_X = ((K_2(\log(d_A) - \log(d_B))) - (P_t(A) - P_t(B)))$.

We rewrite the handover probability, equation 3.41, as follows:

$$P_{ho}(k) = P_A(k-1)P_{B/A}(k) + P_B(k-1)P_{A/B}(k) \tag{4.11}$$

4.2.5 Analysis Results

The average number of handover requests per boundary crossing and the number of total call degradations (sudden call degradation plus no-signal call degradation) are measured and compared with the simulation model for the case that the autocorrelation coefficient is zero, that is $\mu_{X_k} = \hat{\mu}$ and $\sigma_{X_k} = \frac{\hat{\sigma}}{\sqrt{n}}$ where n is the number of samples during a signal average interval.

- **The Average Number of Handover Requests**

As can be seen in figure 4.9, the analytical model shows that the mean number of handover requests per boundary crossing is not affected by the unequal BS transmit power model. The results for the analytical model (curves 2 and 4) are about half those from the simulation model (curve 1 and 3) at low HYS. However this difference reduces and the two results approach each other as HYS increases.

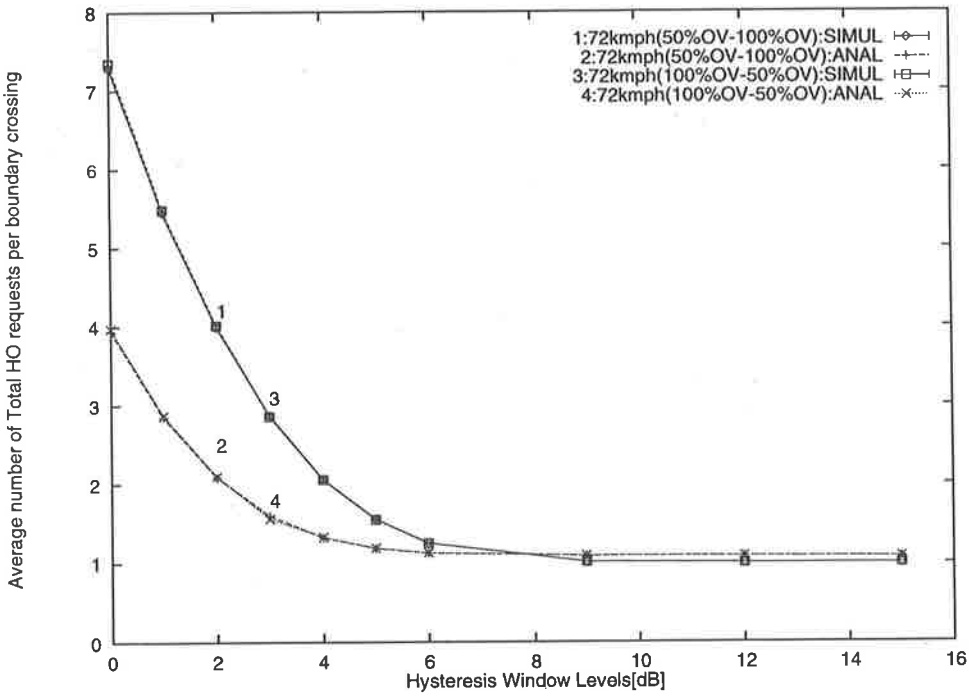

Figure 4.9: The Comparison of the mean number of Handover Request in unequal BS transmit power models for the Basic HO Algorithm

2. The area where both BSs provide similar transmit power. We call this the overlapping area,

3. The area where the BS-B provides the strongest transmit power to the MS

Based on our previous investigations in sections 3.3.3 and 4.2.2 the overlapping area is found to be highly related to the handover characteristics. Thus we will perform further investigations by creating a model in which the MS travels through the overlapping area, maintaining an equal distance between both BSs as shown in diagram (2) of figure 4.11. We call this the worst case model for the handover algorithm analysis in this thesis.

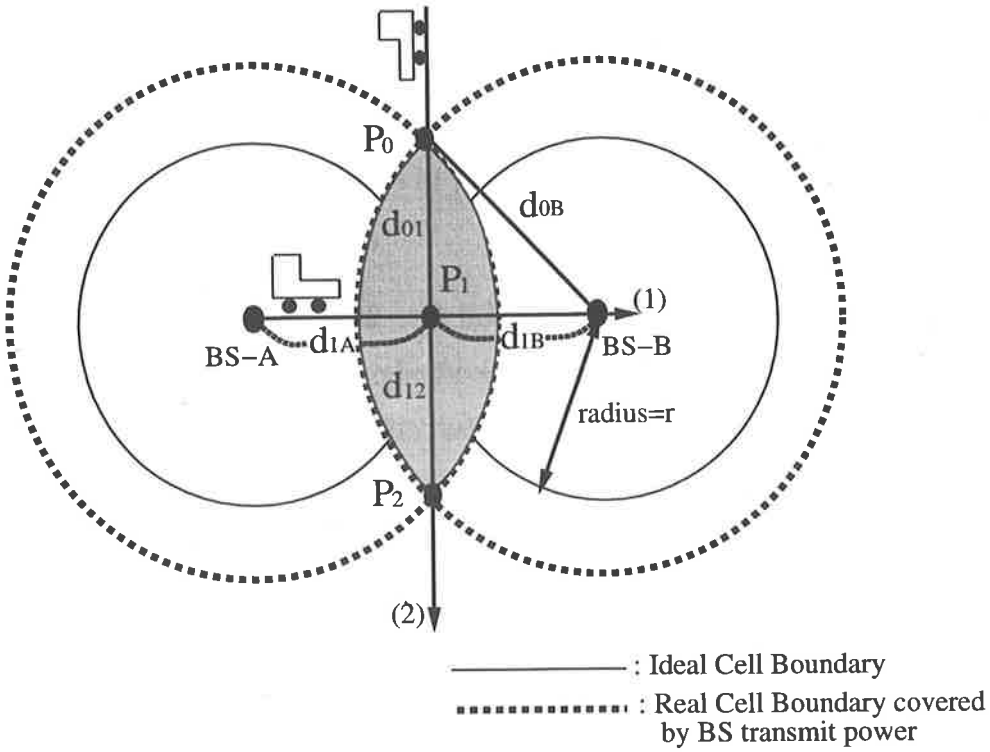

Figure 4.11: Layout of the Worst Case Model

In figure 4.11, we define the MS starting point P_0 which is d_{01} and d_{0B} km away from the point P_1 and BS-B respectively. The point P_1 is in the middle of a line connecting the two BSs and the distance to BS-B, d_{1B}, is equal to the distance to BS-A, d_{1A}. The distance d_{0B} is defined to endure that the signal level from BS-B is MIN_TH. Thus the d_{0B} is given from equation 4.1, as follows:

$$d_{0B} = r + r \times y \quad [\text{km}] \tag{4.16}$$

$$X = (F(A) - F(B)) \tag{4.19}$$

where $F(A)$ and $F(B)$ are the slow fading factors of the received signal from BS-A and BS-B respectively in dB. Thus the slow fading factors is the only parameter affecting the handover request characteristics, and is investigated in subsection 4.3.1.

If we consider an unequal BS transmit power model, where $P_t(A)$ and $P_t(B)$ are not equal, then the power difference between BSs will be a function of the slow fading factors and the BS transmit power as follows:

$$X = (P_t(A) - P_t(B)) + (F(A) - F(B)) \tag{4.20}$$

Thus the slow fading factors and BS transmit power difference are parameters which affect the handover request characteristics. These are investigated in subsection 4.3.2.

The same parameters used in Chapter 3 are also employed in this study except for the direction of motion of the MS.

4.3.1 Results for the Equal Transmit Power Model

The three equal BS transmit power models: 25%, 50% and 100% overlap are used to examine how the number of handover requests and call degradation are affected in this worst case environment.

- **Mean number of handover requests**

In figure 4.12, the average number of handover requests per boundary crossing is identical among the equal BS transmit power models. As HYS increases the number of handover requests reduces and becomes almost zero. The role of HYS in the handover algorithm is again shown to reduce the number handover requests as demostrated in sections 4.2.3 and 3.5.1. In particular it is shown that increasing HYS reduces the effect of slow fading which can otherwise result in a large number of handover requests.

the differences in call quality as does the call degradation measure. Secondly, HYS is a good technique for reducing the number of handover requests when the handover decision is made on the basis of slow fading (see equation 4.19). However it cannot guarantee that call degradation will be acceptable. Thirdly, the mean number of call degradations per boundary crossing becomes a useful measure for evaluating handover performance, because it shows clearly the differences among different environments having various overlapping conditions. In other words it shows how the call quality is affected by unequal BS transmit powers. Lastly, the BS transmit power level is one of the most important parameters affecting the call quality of users.

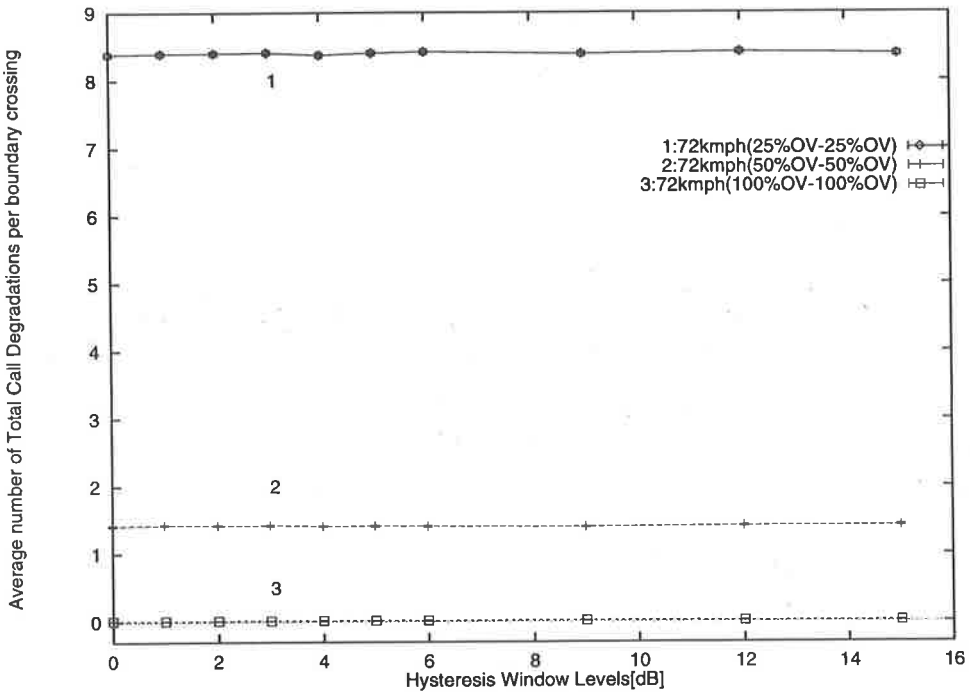

Figure 4.13: Average number of call degradations for the equal power model

4.3.2 Results for the Unequal Transmit Power Model

In this subsection, we use two types of unequal BS transmit power models as well as the equal BS transmit power model as follows:

1. 50% overlap and 100% overlap for BS-A and BS-B;
2. 100% overlap and 50% overlap for BS-A and BS-B;

call quality is related to the absolute level of received signal strength at the MS, in other words to the absolute level of the BS transmit power.

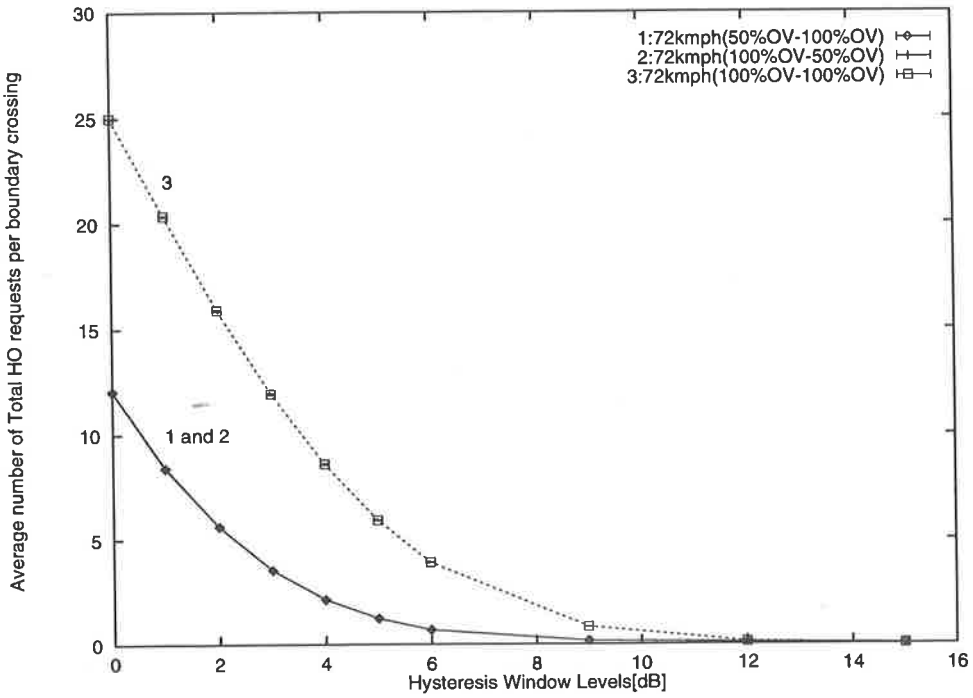

Figure 4.14: Average number of handover requests for the unequal power model

- **The mean number of call degradations**

In figure 4.15, both unequal BS transmit power models (curves 1 and 2) generate different numbers of total call degradations over all values of HYS. As HYS increases from 0 to 9dB the number of total call degradations decreases. However the call degradation increases rapidly above 9dB HYS. Increase of HYS, that is, HYS greater than X in equation 4.20, resulting in nearly no handover requests being generated, shows reduced call quality of 9 15dB HYS. This situation is considered to be a result of the delayed handover, that is, the handover decision being made too late. This is because high levels of HYS cause the handover occurrence to be postponed from the place where the handover should occur. This is what we call "delayed handover". Thus as HYS increases, the mean number of call degradations will become greater as the received signal strength of the current BS becomes smaller before handover occurs. The equal BS transmit power model (curve 3) maintains the same value for all HYS levels. This is because the MS is located an equal distance away from both BSs which are transmitting at the same power.

In unequal transmit power models, if the MS has the appropriate HYS levels, such as 6dB to 9dB as discussed above, then the MS will have the smallest number of call degradations (figure 4.15) and unnecessary handover requests (figure 4.14). However the power consumption (figure 4.16) at those HYS levels is greater than for the other levels. This indicates the importance of selection of HYS levels for both handover characteristics and power consumption. The simulations of unequal transmit power models, which are more realistic than the equal transmit power models, will demonstrate this.

In comparisons between the unequal and equal transmit power models, the unequal transmit power model has a smaller number of handover requests and a larger number of call degradations than the equal transmit power model, even though the latter has a greater power consumption. The lower call degradation in the equal transmit power model is obvious because both BSs transmit the same power levels for the 100% OV condition, and call degradation is dependent on the received power of the current BS. In the unequal transmit power model however, the handover algorithm should seek to connect to the stronger BS in order to minimize the number of call degradations.

The number of handover requests which can cause unnecessary signalling traffic processing loads to the mobile systems is not related to the BS transmit power in the basic handover algorithm used in this chapter. That is why the mean number of handover requests in the equal transmit power model is greater than that of the unequal transmit power model as shown in figure 4.15, even if the equal transmit power model provides the strongest transmit power to the MS at all times as shown in figure 4.16. Therefore the use of HYS in the basic handover algorithm will be one of the solutions which can provide better performance to the user and the system. From the point of view of the number of handover requests, the EN handover algorithm provides lighter processing loads to the system than the basic handover algorithm.

- **Importance of Cell Selection**

In practice the MS should measure the received signals of all adjacent BSs and decide the best BS to which a connection may be formed. This is called *Cell Selection* mode. However if the current BS is set to be a particular BS, then this is referred to as the *Default* mode.

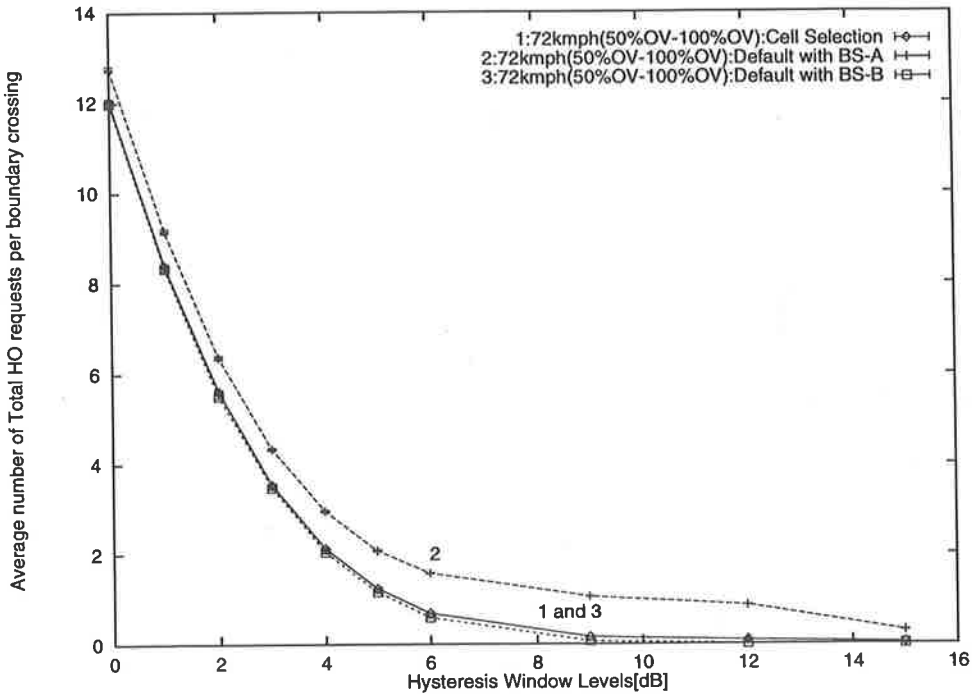

Figure 4.17: Average number of handover requests for equal and unequal power models

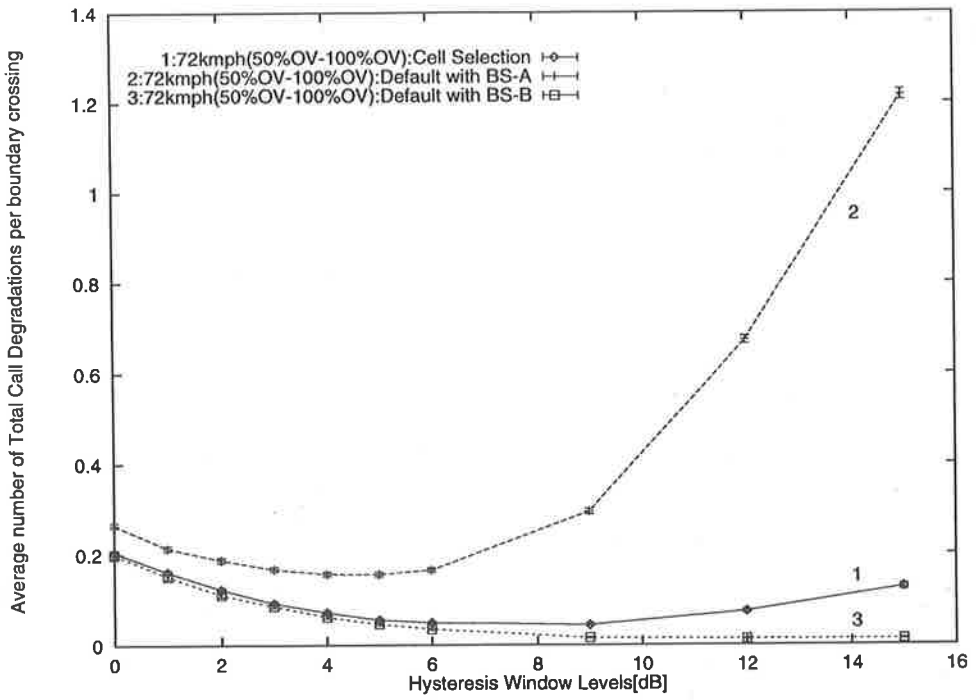

Figure 4.18: Average number of call degradations for equal and unequal power models

4.4 Call Quality for various Averaging Intervals

We have investigated handover request characteristics with three types of parameters:

1. environmental parameters - slow fading and its autocorrelation;
2. system parameters - BS transmit power (overlapping condition), HYS (Hysteresis window) and signal averaging interval (T_{av});
3. user parameters - movement direction and speed.

These three classes of parameters influence individually or collectively the handover request characteristics. However the environmental parameters and the user parameters are random and very difficult to predict. Thus we need to analyse and evaluate the system parameters effectively to provide better quality of services for users.

In our previous investigations we found that increasing the BS transmit power results in good call quality with small number of call degradations. HYS can be used to reduce the number of handover requests. We also found that when T_{av} is constant and the MS speed increases, the number of handover requests and call degradations decreases, but the handover area is reduced at low HYS and is delayed at medium and high HYS (See subsection 3.3.3 and 3.6.3). In general the first handover point is always delayed as the MS speed increases, that is, as the signal averaging distance increases. Miller *et al.* [43] also showed that for the large cell model (10km radius) with N tap block windows, longer signal averaging intervals with constant MS speed result in a smaller number of handover requests. However they did not consider the handover area (point) variation. Vijayan *et al.* [11] found that the mean number of handover requests reduces and the first handover area (point) delays as the signal averaging interval increases in the small cell model (1km radius) when exponential windows are used. Corazza *et al.* [25] also found that a long signal averaging interval reduces the number of handover requests but increases delay of the first handover point in the small cell model (1km radius) with rectangular and exponential windows.

In this section we present the results of our simulations in order to obtain comparisons of the handover request characteristics with those found from other studies. We allow the

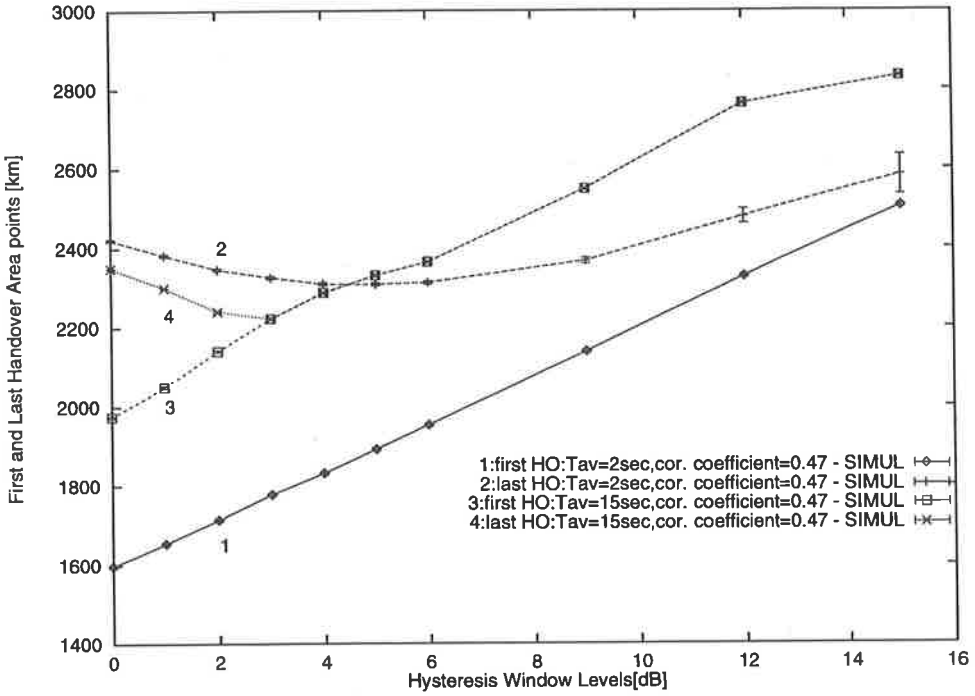

Figure 4.21: Average handover area for equal and unequal power models with 50% overlap and speed 30m/s

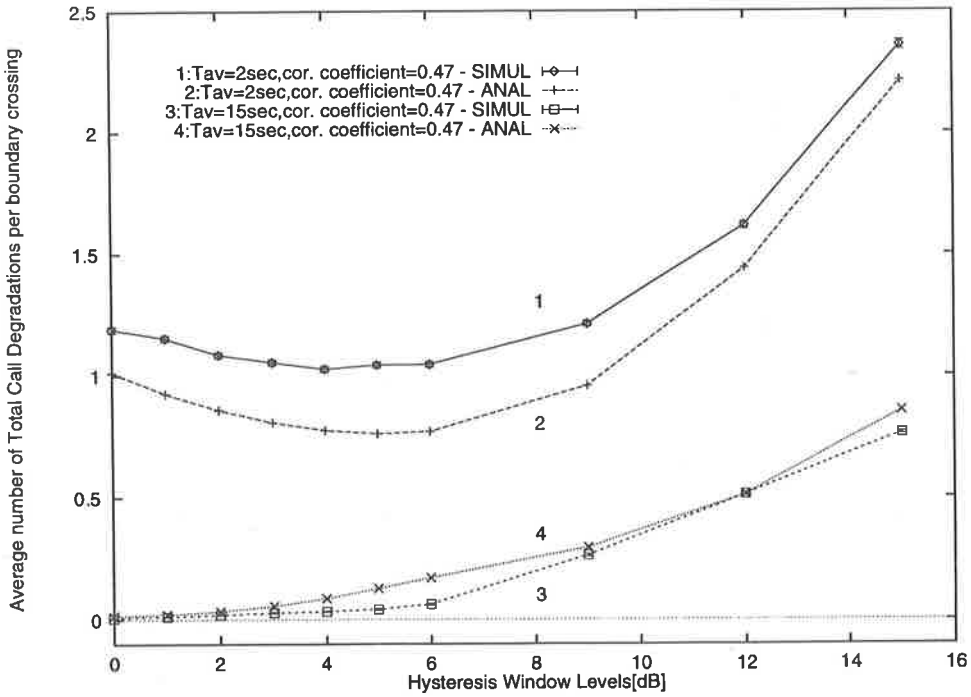

Figure 4.22: Average number of call degradations with 50% overlap and speed 30m/s

W.C.Y Lee [15, 27] suggested that the optimum signal averaging distance will range between 40λ and 200λ, where λ is the wavelength of the carrier frequency with an assumption that all random variables are stationary. In particular Lee showed that when the averaging distance is 40λ, which is long enough to smooth out the fast fading, the probability that a fluctuation among the random variables within 40λ is less than 1dB, is 86%. As the signal averaging interval reduces this probability also reduces. However as the signal averaging interval increases, the local mean may not be a stationary random variable. It is still not entirely clear whether a long signal interval is better than a short one in handover algorithm analyses.

Therefore in this subsection we will investigate the behavior of different signal averaging intervals by combining the probability that the MS is connected to the BS, with the average fade duration [15, 27, 26, 50] of the current BS. We call this new parameter the *modified average fade duration (mAFD)*. It is well known that the average duration of fade is primarily dependent on the speed of the mobile system [27]. Thus we can make comparisons using the mAFD by keeping the MS speed constant while the signal averaging interval is varied. Therefore the mAFD shows how much the MS experiences fading of the received signal during a trip from BS-A to BS-B.

We consider three different signal averaging intervals: 2, 5 and 15 seconds and 30 meters/sec of MS speed. The signal averaging distance is then 60 meters (180λ), 150 meters (450λ) and 450meters (1350λ) for 2, 5 and 15 seconds respectively.

The average fade duration is the average length of time interval during which the received signal X from the current BS, is below a given signal level threshold X_0. This is given by [28, 62]:

$$AFD = \frac{P(X \leq X_0)}{lcr} \tag{4.21}$$

where $P(X \leq X_0)$ is the expected total time where the received signal strength falls below X_0, and lcr is the expected number of crossings of the threshold level X_0, over a unit time interval of $t = 1$ seconds.

We assume that the average received signal strength is a stationary Gaussian random variable. Thus the numerator in equation 4.21 is a Gaussian distribution function with

$$P[X_u \leq X_0] = \int_{-\infty}^{X_0} \frac{1}{\sigma_B\sqrt{2\pi}} \exp(-\frac{(x-(P_t-(K_1+K_2\log(d_B)))^2}{2\sigma_B^2})dx \qquad (4.27)$$

• **Level Crossing Rate (lcr) - The mean number of crossings of the threshold level X_0**

The level crossing rate of the received signal strength is a second-order statistic because it is dependent on time and is affected by the MS speed [27, 63]. This level crossing rate, lcr, is derived using the assumptions that the received signal (level function) and the slope of the signal (phase function) are Gaussian distributed and statistically independent. In this section we only consider the level crossing rate for the electrical component received from an omnidirectional antenna, because the received signal strength is used for the handover criterion in this thesis.

By replacing the received signal level function with a path loss function and the slow fading function, the lcr during 1 second is given by [See equation B.19 in appendix B]:

$$lcr = \frac{\mu_2\sqrt{\pi}+\sqrt{2}\sigma_2}{2\sqrt{2}\pi\sigma_1} \exp(-\frac{(X_0-(P_t-(K_1+K_2\log(d)))^2}{2\sigma_X^2})\, dx \qquad (4.28)$$

where d is the distance between the MS and the BS [km]

As shown in figure B.21 of appendix B, the normalised level crossing rates $\acute{lcr}$ for BS-A and BS-B are given by:

$$\acute{lcr}_d(t) = \exp(-\frac{(X_d-(P_t-(K_1+K_2\log(d_A)))^2}{2\sigma_A^2})\, dX_d \qquad (4.29)$$

and

$$\acute{lcr}_u(t) = \exp(-\frac{(X_u-(P_t-(K_1+K_2\log(d_B)))^2}{2\sigma_B^2})\, dX_u \qquad (4.30)$$

We obtain the normalised fade duration during a signal averaging interval by summing the normalised fade duration during each sample interval. Thus the sum of the normalised AFD at the beginning of signal averaging interval k, $A\acute{F}D_d(k)$ when the current BS is BS-A, or $A\acute{F}D_u(k)$ when the current BS is BS-B, is as follows:

$$A\acute{F}D_d(k) = \sum_{i=1}^{n_j} A\acute{F}D_d(i) \quad (4.33)$$

where $A\acute{F}D_d(i)$ is given by equation 4.31.

$$A\acute{F}D_u(k) = \sum_{i=1}^{n_j} A\acute{F}D_u(i) \quad (4.34)$$

where $A\acute{F}D_u(i)$ is given by equation 4.32.

- **modified Average Fade Duration (mAFD)**

We can now determine how long the MS experiences a low quality of conversation service during a certain period of time such as the signal sampling interval or signal averaging interval. This is the period of time when the received signal strength of the current RSS falls below the threshold X_0. This is the minimum received signal strength $MIN_TH = -130$dBm of previous chapters.

There are two normalised average fade durations given in equations 4.33 and 4.34 during a signal averaging interval from the MS point of view. One is for the link from the MS to BS-A, and the other is for the link from the MS to BS-B. The MS does not know to which BS it will be linked in a fading environment. If the MS has an accurate handover algorithm, then the AFD will be short. This is because the MS is able to select the best BS at all times and unnecessary handover requests are minimized. Otherwise the AFD will be long because the possibility exists that the MS may become linked to the less desirable BS. Therefore we can say that the normalised AFD is dependent on the probability of linking to the best BS during a signal averaging interval. Thus by combining the probability of linking to a particular BS with the normalised average fade duration of that BS, we can produce a new measure which we call the *modified average fade duration mAFD*. This new measure can be used to provide fair comparisons of handover performance when the signal averaging interval is different, because it consists

$$E_{mAFD}(j) = \sum_{k=1}^{N_j}(\sum_{i=1}^{n_j} A\acute{F}D_d(k \times d_j + i \times d_u))P_A(k) + \sum_{i=1}^{n_j} A\acute{F}D_u(k \times d_j + i \times d_u))P_B(k)) \tag{4.40}$$

where $P_A(k)$ and $P_B(k)$ are given by equation 3.33 of Chapter 3. Other terms are explained in table 4.2.

4.4.1 Case Study

In this section we will determine the modified average fade duration for signal average intervals of 2, 5 and 15 seconds. We assume that the MS speed is 30 meters/sec and HYS varies between 0 to 15dB. The unit of time used is 1 second, thus the unit distance becomes 30 meters (90 λ). We assume no Rayleigh fading, and that the local mean of slow fading is obtainable because the unit distance is greater than the correlation distance of Rayleigh fading $\lambda/2$ and ranges between 40 to 200 λ [15, 27].

By substituting j into equation 4.39, we can obtain the total mAFD $E_{mAFD}(k)$ for the three different signal averaging intervals j =2, 5 and 15.

- **mAFD based on the normalised AFD**

The value of mAFD gives the duration during which the MS received signal strength is less than the minimum signal strength MIN_TH during a trip. As the value of mAFD increases the fade duration becomes large. Firstly we measure the mAFD derived on the basis of the normalised AFD as given by equations 4.31 and 4.32. Secondly we measure the mAFD derived on the basis of the signal slope having zero mean and two different variances as given by equations B.30 and B.31 in Appendix B.

The total mAFD using normalised AFD is shown in figure 4.23. In contrast to the results of the mean number of handover requests and call degradations shown in figures 4.20 and 4.22, the total mAFD shows that a short T_{av} generates quite stable values over the whole range of HYS, while a long T_{av} generates a relatively higher mAFD against HYS. Thus when the signal averaging interval ($T_{av} = j$) increases, the HYS level should be decreased to avoid unnecessary total mAFD increments. The investigation based on the total mAFD can help to optimise the level of HYS. We have shown that previous

time as shown in figure 4.25. The longest T_{av} shows the highest level of mAFD (curve 3) all the time. In figure 4.26 we show the cumulative mAFD of only two signal averaging intervals at 0 and 15dB HYS. This shows clearly that increasing HYS (curves 2 and 4) also raises the mAFD, that is, it decreases the call quality. Even though the total mAFD for the case where T_{av} is 15 seconds, is slightly lower than that for the case where T_{av} is 2 seconds, the latter gives a lower mAFD over the longest travelling time of the MS.

Based on these results, we believe that a relatively short signal average interval which can smooth out the short term fading, can provide a better mAFD and is able to be easily combined with an appropriate selection of a value for HYS to achieve a further reduction of mAFD.

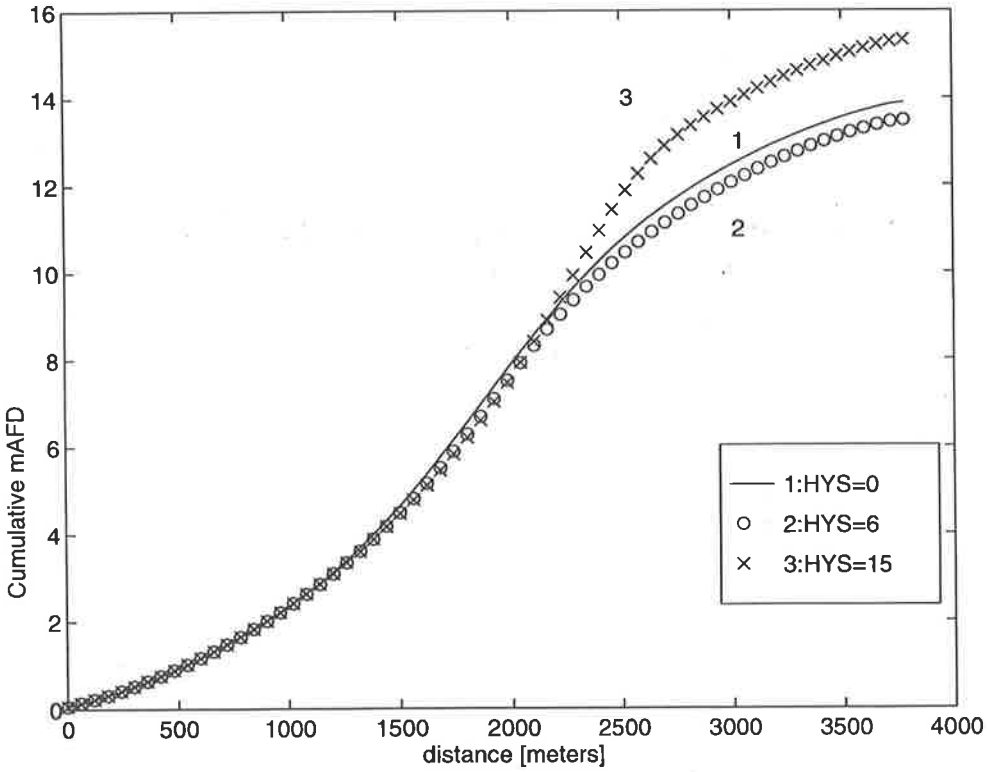

Figure 4.24: Accumulative mAFD when $T_{av} = 2$ seconds, speed=30m/sec, correlation=0.47

- **Comparisons of mAFD based on the signal slope**

The level crossing rate (lcr) is dependent on the mean and the variance of the signal slope as shown in equations B.30 and B.31 of appendix B. This means that the mAFD is also based on the signal slope. Thus we also investigate how the mAFD changes with

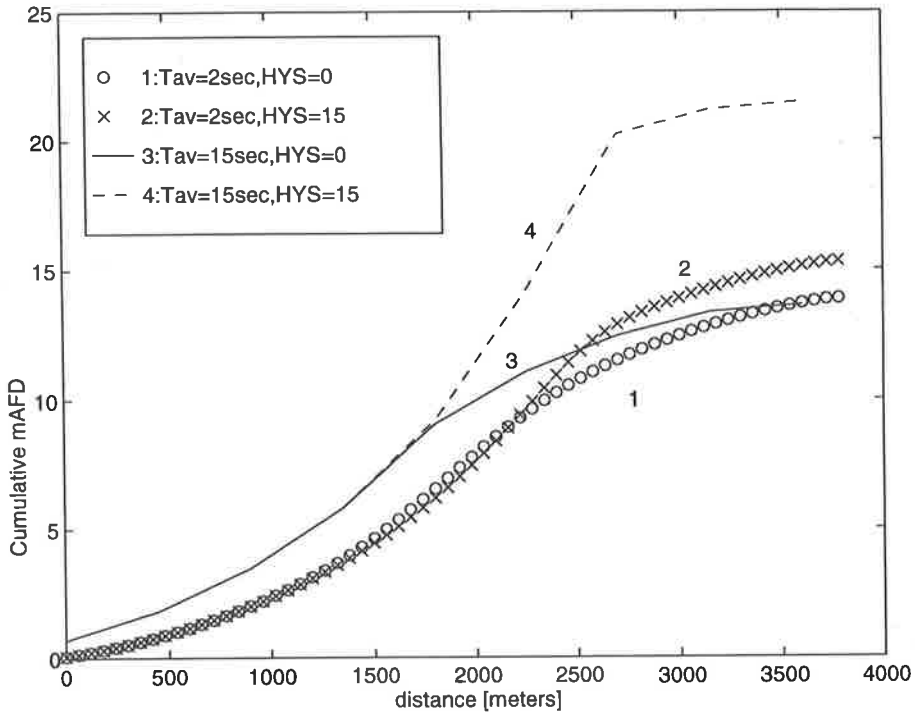

Figure 4.26: The accumulative mAFD comparison at 0 and 15dB HYS and 2 and 15 seconds T_{av}, speed=30m/sec, correlation=0.47

same mean and standard deviation. The use of normalised mAFD is reliable for measuring handover performance, and for comparisons between handover algorithms where the signal averaging interval is different.

We have not shown how mAFD varies with the mean of signal slope. However, as the mean μ_2 increases in equation 4.28, the lcr increases, and the AFD decreases. Therefore the mAFD is also reduced as the mean of signal slope increases.

4.5 Conclusions

In this chapter, we have carried out further investigations of the handover algorithm by varying other important parameters such as BS transmit power between BSs and the travelling direction of the MS. These are analysed in Chapter 3 to obtain various fundamental handover request characteristics and to obtain a greater understanding of handover algorithm analyses. The importance of cell selection in the handover algorithm

used in the basic handover algorithm analysis.

(d) HYS can be used to reduce the mean number of handover requests regardless of which BS transmit power models are used in the basic handover algorithm analysis.

(e) The proposed handover performance measure: the mean number of call degradations, shows very important characteristics which cannot be demonstrated by commonly used measures of handover performance such as the mean number of handover requests or handover area.

(f) A reduction of the mean number of handover requests by increasing HYS raises the mean number of call degradations. This means that unnecessarily high HYS provides excessively large numbers of call degradations.

(g) In particular when HYS is high, and the MS is connected to the BS which is transmitting the weaker power, the MS experiences much larger number of call degradations, because as HYS increases the probability that the MS remains connected to the weaker BS is increased. The mean power consumption comparisons for the equal BS transmit power model shows this clearly.

2. In the studies of worst case conditions the results obtained were as follows:

(a) If the handover decision is affected only by slow fading, that is, BS transmit power is equal and the distance between the MS and the two BSs is equal, then the mean number of call degradation will not change with HYS and the mean number of handover requests will be reduced as HYS increases.

(b) However if the handover decision is affected by both slow fading and power differences between the BSs, the size of HYS should be defined carefully to obtain the smallest number of call degradations rather than the smallest number of handover requests.

(c) The mean number of call degradations also provides useful data for evaluating the handover algorithm.

(d) The investigation of cell selection shows that the call quality based on the results of call degradation is particularly affected by a default decision for a current BS. This was demonstrated in the simulation study.

Chapter 5

Power Control in Handoff Algorithms

5.1 Introduction

The handover algorithm analysis studied in chapters 3 and 4 used an assumption that the handover decision and the handover processing intervals are very fast. Thus the call quality of users is not affected during the handover decision and the handover processing interval. This study is helpful to understand fundamental characteristics of the handover algorithm based on signal averaging interval lengths and HYS levels for handover algorithm parameters, the MS speed and the MS direction of motion as user parameters, and various BS transmit powers as system parameters in inherently uncertain mobile radio environments modelled with log-normal fading and its autocorrelation function. In our simulation and analyses, we obtained characteristics of the basic handover algorithm similar to those found in other studies [11, 43], which used the same assumptions mentioned above, in terms of the mean number of handover requests and the mean handover area versus HYS and the MS speed.

However, if the handover decision and the handover processing interval is relatively long (a few tens of meters), then we believe that the handover request characteristics will be affected by the slow fading within the length of handover decision and handover processing interval. Moreover the above assumption used in our previous studies in

algorithms as soft handoff algorithms, although there is no intention that the zero handover time should arise from connection to multiple base stations. We remain within the model of a TDMA system, and consider the ideal situation of a handover that takes no time.

Hard handoff and soft handoff have different system environments. One of them is the power control requirement. In a CDMA environment, power control is the only way to maintain an adequate level of a call quality by reducing the co-channel interference ratio (CIR) [65, 51]. However in a TDMA environment, power control is only an option for the system operator [28, 4]. Therefore we need more studies of the hard handoff algorithm with various handover processing intervals for the TDMA system environment and of the soft handoff algorithm combined with power control that would be used in the CDMA system environment.

Transmitter power control is one of the co-channel interference management methods available to the system designer. An efficient reverse link (from the MS to BS) and forward link (from BS to the MS) power control can also reduce the power consumption of the MS battery. In an early work on satellite systems, Aein [66] investigated CIR management with a concept that all users experience the same CIR levels. From the capacity comparisons with and without power control, previous studies [67, 68, 69] showed that power control provides high call carrying capacity of cellular systems. Since the CDMA technique has been introduced, the power control method becomes one of the core factors to manage the CIR in CDMA systems. System capacity comparisons between the TDMA and the CDMA systems have focused on the important role of power control in the CDMA. Many studies [70, 51, 55, 52] have been done from the system capacity point of view. Recently Viterbi [52] and others [68, 53] compared the outage probability between the hard and the soft handoff algorithms. They showed that a soft handoff algorithm provides better outage probability (see section 3.4.3) than a hard handoff algorithm because the MS can access two or more BSs during call conversation. CDMA also provides lower CIR than the hard handoff algorithm. These studies also compared system capacity based on outage probabilities, that is, the probability that the signal strength falls below a threshold.

However from the point of view of handover characteristics, the hard and soft hand-

Therefore in our power control algorithm we use the *guard* band as a handover request characteristic management parameter by increasing or decreasing transmitter power to provide a reasonable performance of the power control from the handover algorithm analysis point of view. This guard band is designed to minimize unnecessary power control reductions which possibly occur and which may cause poor handover request characteristics in a slow fading environment. As HYS in the handover algorithm reduces the number of handover request by ignoring handover occurrences, the guard band will reduce the number of power control change events. Note that the guard band is proposed by the author in this thesis to help to investigate the performance of the handover algorithm combined with adaptive power control.

In the next section we examine the hard handoff algorithm by varying the handover processing interval which was assumed to be zero in the previous chapters 3 and 4. In the third section we investigate the soft handoff algorithm combined with power control. First of all we introduce our power control algorithm and then investigate the handover request characteristics after combining with the soft handover algorithm. We also compare this with the handover request characteristics of the soft handoff algorithm without power control. In the last section, the handover request characteristics are compared for soft and hard handoff.

5.2 Hard Handoff

To explain the hard handoff algorithm, we shall review the handover procedures in TDMA systems [19, 4]. The system analyses the data reported from the MS through the mobile assist handover procedures (MAHO, See figure 2.2) each time interval in order to make a handover decision. These procedures are marked 1 and 2 in figure 5.1. The time spent during the procedure marked 2 is represented as t_{h_dec}. After the handover decision is made (marked 3), the system needs a new radio link setup procedure (marked 4) for maintaining the MS call conversation. The time spent during the procedure marked 4 is represented as t_{h_pro}. Therefore the sum of handover decision time t_{h_dec} and processing interval t_{h_pro} in the hard handoff algorithm is given by:

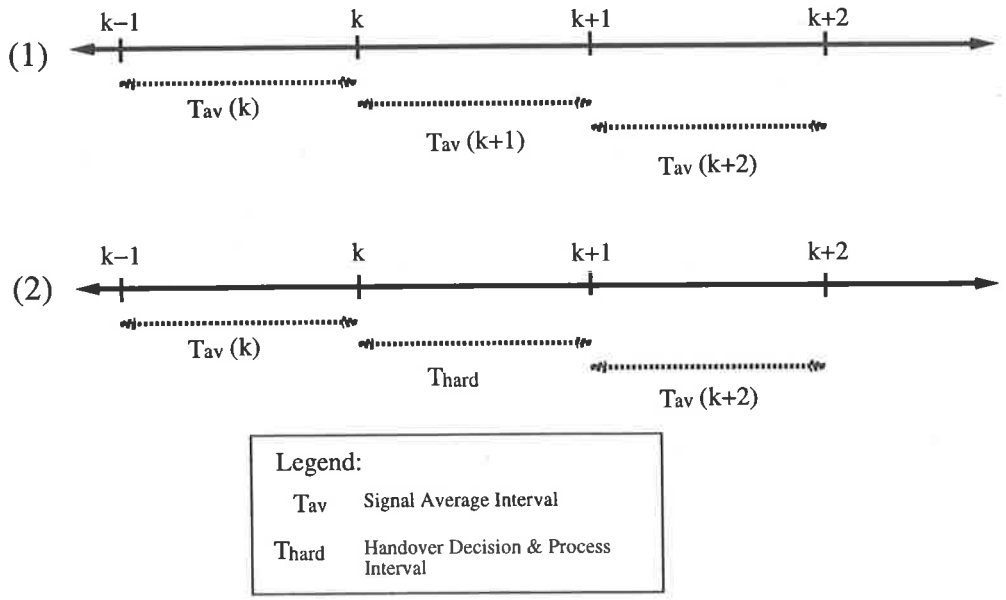

Figure 5.2: Time Comparison between (1) no handover and (2) handover in Hard Handoff Algorithms when $T_{av} = T_{hard}$

interval is the same. However, once a handover decision is made at the end of an interval $T_{av}(k)$, the next signal averaging interval for a new radio link only occurs after waiting an interval T_{hard} as shown in curve (2) of figure 5.2. That is, the MS still needs to remain connected to the old BS during T_{hard}. Thus, even if the system decides to change to a new BS for the MS, the MS needs to keep conversation through the radio link of the old BS during the interval T_{hard}.

If T_{hard} is very short, that is, the system provides very fast handover request processing, then we can assume that there is no effect on the call quality and other handover request characteristics during the handover processing interval T_{hard}. Thus the equation 5.1 becomes:

$$T_{av}(k) + T_{hard} \cong T_{av}(k) \tag{5.2}$$

This means that the MS connects to the new BS without any time delay and the MS starts averaging the received signal of the new link immediately as in the no handover case shown in curve (1) of figure 5.2.

Table 5.1: Parameter Values used in Simulation

parameter term	name	value
h_b	height of BS antenna	30[m]
h_m	height of MS antenna	1.5[m]
f_c	carrier frequency	900[MHz]
d	distance between transmitter and receiver	0 - 4[km]
r	cell radius	2[km]
$speed$	MS speed	72[km]
σ	standard deviation of slow fading	6[dB]
T_{av}	Signal average interval	2,4,6[sec]
T_s	Signal sampling interval	0.5[sec]
T_{hard}	Handover processing interval	0.5,1,3 [sec]

- **Handover Requests during T_{av}**

According to figure 5.3, the mean number of handover requests decreases as the handover processing interval T_{hard} increases in the hard handoff algorithm. However, as HYS increases, the mean number of handover requests approaches unity regardless of the length of T_{hard}.

We now use three different intervals of T_{av}: 2, 4 and 6 seconds, and 1 second for T_{hard} to obtain more general characteristics of the hard handoff algorithms. Similar to the results shown in figure 5.3, the figure 5.4 shows that non-zero T_{hard} produces a smaller number of handover requests than a T_{hard} of zero. As T_{av} increases and/or HYS increases the difference between zero and non-zero T_{hard} becomes small.

The number of handover requests is related to the length of T_{av} as we have already noted in subsection 4.4. The longer is T_{av}, the smaller is the number of handover requests. This is because the MS does not perform any handover decision during the interval of T_{hard}, assumed to be 1 second in hard handoff, after a handover occurrence. As more handovers occur at low HYS, the MS skips more handover decisions in T_{hard} intervals during a trip. Just one T_{hard} interval is skipped at high HYS because a single handover occurs as shown in figure 5.4. However, it is not necessarily true that a longer T_{hard} provides

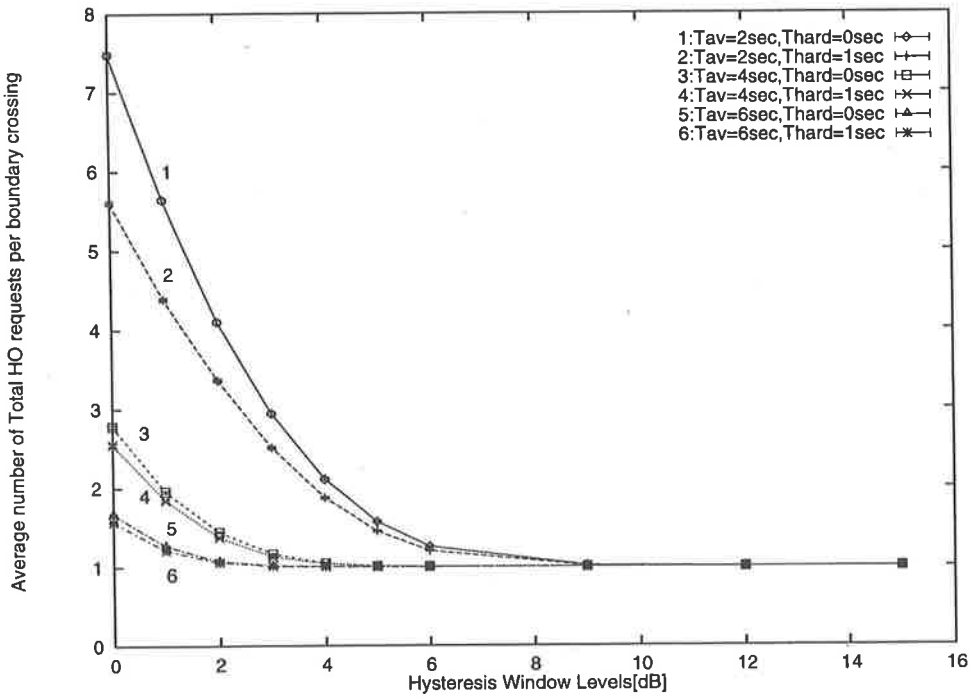

Figure 5.4: (Average number of handover requests/T_{av}) per boundary crossing, a variable T_{av} and a constant T_{hard} with 50% overlap and speed 72kmph

of the speed of the MS in a random radio environment. The comparisons using 'average fade duration (AFD)' will be discussed later.

- **Handover Area**

The comparisons of mean handover area for fixed T_{av} and various T_{hard} is shown in figure 5.7. The first handover points are the same for various T_{hard} because the first handover point is not affected by T_{hard} (which is only invoked *after* a handover request has been made). However this point drifts towards the cell boundary (2000 meters) and crosses over the boundary as HYS increases. The reason for this movement has been well explained in sections 3.3.3 and 3.6.3 in Chapter 3. The last handover request point is delayed from the cell boundary as T_{hard} increases in low and medium HYS. In particular we use 8 seconds for T_{hard}, which is four times greater than T_{av}. This causes further delays of the last handover point from the cell boundary at low and medium HYS. However since HYS is greater than or equal to 12dB, at which only one handover request occurs, there is no further delay caused by the different values of T_{hard}.

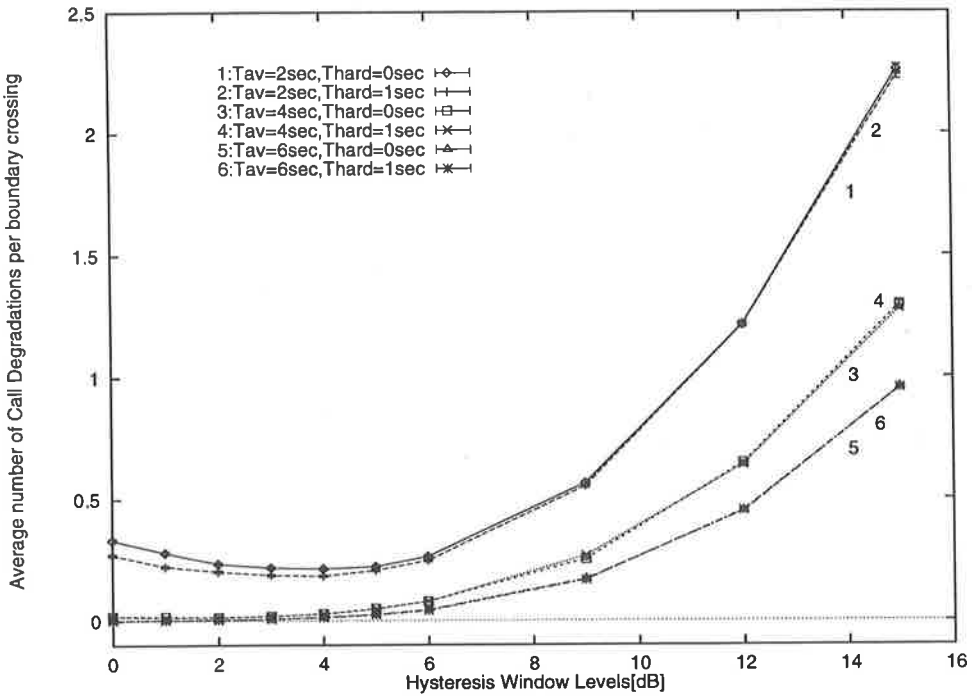

Figure 5.6: (Average number of total call degradations/T_{av}) per boundary crossing, a variable T_{av} and a constant T_{hard} with 50% overlap and MIN_TH=-130dBm and speed 72kph

because the call degradation is measured for the same time intervals. From this point of view, the comparisons shown in figure 5.8 are not valid because they are measured for different time intervals T_{hard}. We need to consider carefully how we should analyse the call degradation measured during two time intervals T_{av} and T_{hard}. We now consider this for two different conditions as follows:

1. If the two time intervals are taken separately, then the mean call degradation of the MS is obtained by adding two separate mean values of call degradation, each measured in the corresponding time interval.

2. If they are taken to form one time interval, then the mean call degradation of the MS should be measured with a new time interval, $T_{ho} = T_{av} + T_{hard}$.

Under the first condition, we measure the call degradation as follows:

- **Two Different Time Intervals T_{av} and T_{hard}**

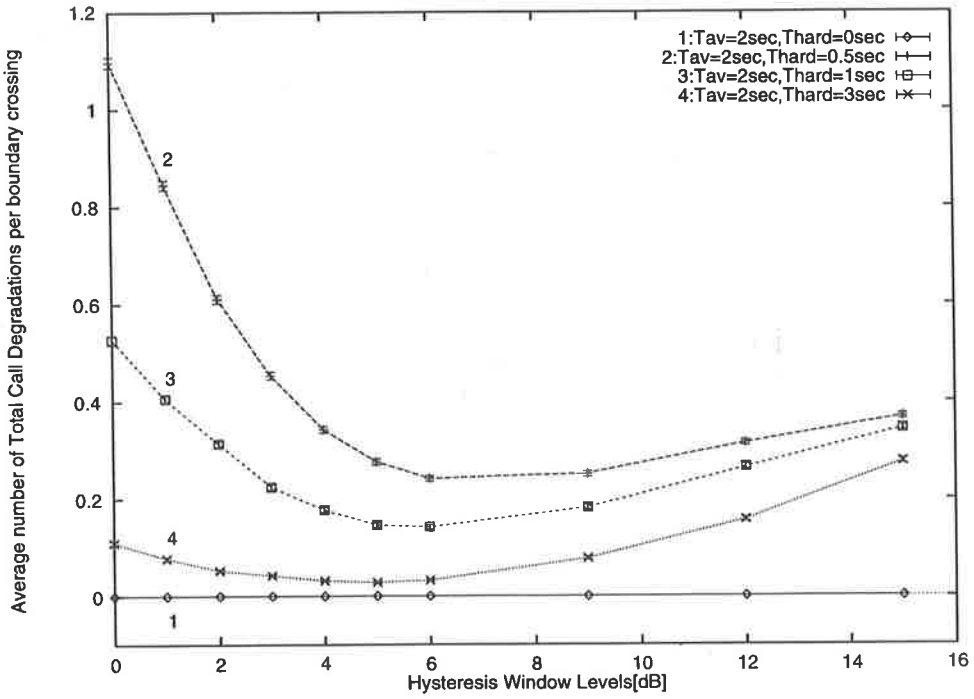

Figure 5.8: (Average number of total call degradation/T_{hard}) per boundary crossing, a constant T_{av} and a variable T_{hard} with 50% overlap and MIN_TH=-130dBm and speed 72kph

- **One Time Interval T_{ho}**

Under the second condition, we measure the call degradation as follows. According to figure 5.12, the mean number of call degradations/T_{ho} per boundary crossing varies dramatically. The hard handoff using the shortest T_{av} and a T_{hard} of 1 second (curve marked 2) has the lowest call degradation, but the soft handoff (zero T_{hard}) using the same T_{av} provides the greatest call degradation. Based on these results we see that the soft handoff algorithm provides worse performance than the hard handoff algorithm.

These comparisons cannot be valid because the time intervals T_{ho} and $T_{av} + T_{hard}$, are not the same among hard and soft handoff algorithms and among various hard handoff algorithms using different T_{av}.

The mean number of call degradation during T_{ho} is based on the length of T_{av} and/or T_{hard}. The call degradation analysis method we have used in this chapter cannot provide a good solution for fair comparisons among soft and hard handoff algorithms.

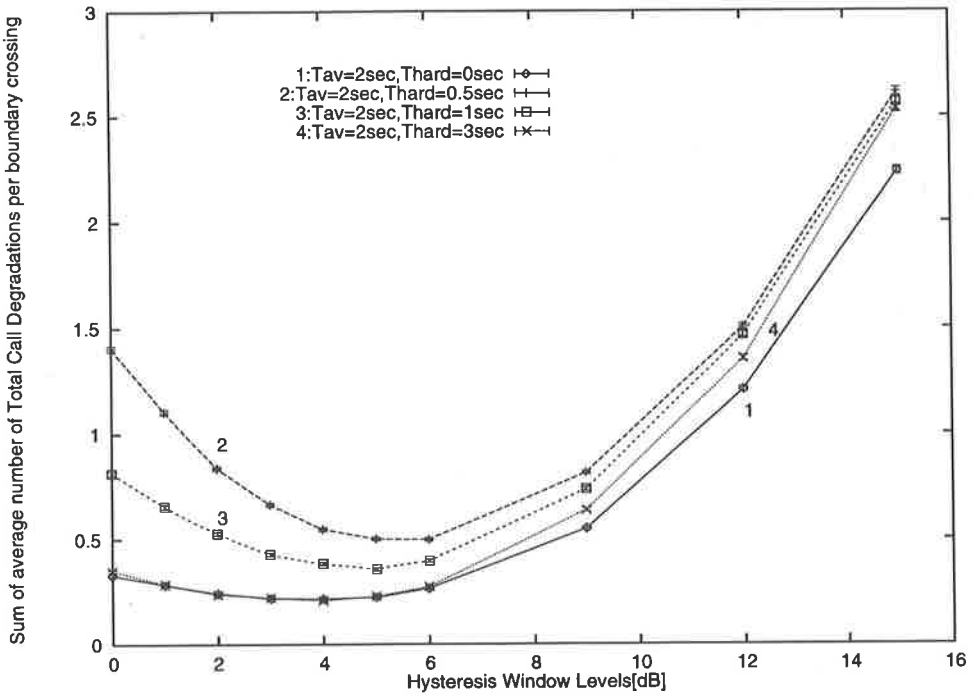

Figure 5.10: Sum of the average number of call degradations per boundary crossing measured during two intervals T_{av} and T_{hard}, a constant T_{av} and a variable T_{hard} with 50% overlap and MIN_TH=-130dBm and speed 72kph

intervals T_{ho} are comparable each other if $T_{ho} \geq T_u$ and $T_{ho} = n \times T_u$ where $n = 1, 2, 3, ...$

The mean number of $nAFD$ during T_{ho} is:

$$\frac{nAF}{Tu} = \frac{1}{n}\sigma_{i=1}^{n}(nAFD(T_u(i)) \tag{5.4}$$

The sum of the mean nAFD/T_u during a boundary crossing is measured to provide fair comparisons among hard and soft handoff algorithms having different signal averaging intervals and/or handover processing intervals as we have already discussed in section 4.4.

In this section we will use one second for T_u for the average fade duration and -130dBm for X_0 in equation 5.3.

The comparisons of normalised AFD among the soft and hard handoff algorithms are shown in figure 5.13. Low T_{av} of 2 seconds provides the lowest normalised AFD, while T_{av} of 6 seconds gives the highest value. In particular for a T_{av} of 6 seconds, the normalised AFD/T_u maintains the highest value over all HYS. We conclude that as T_{av} and/or T_{hard} become small, the normalised AFD/T_u becomes smaller. That is, the probability that

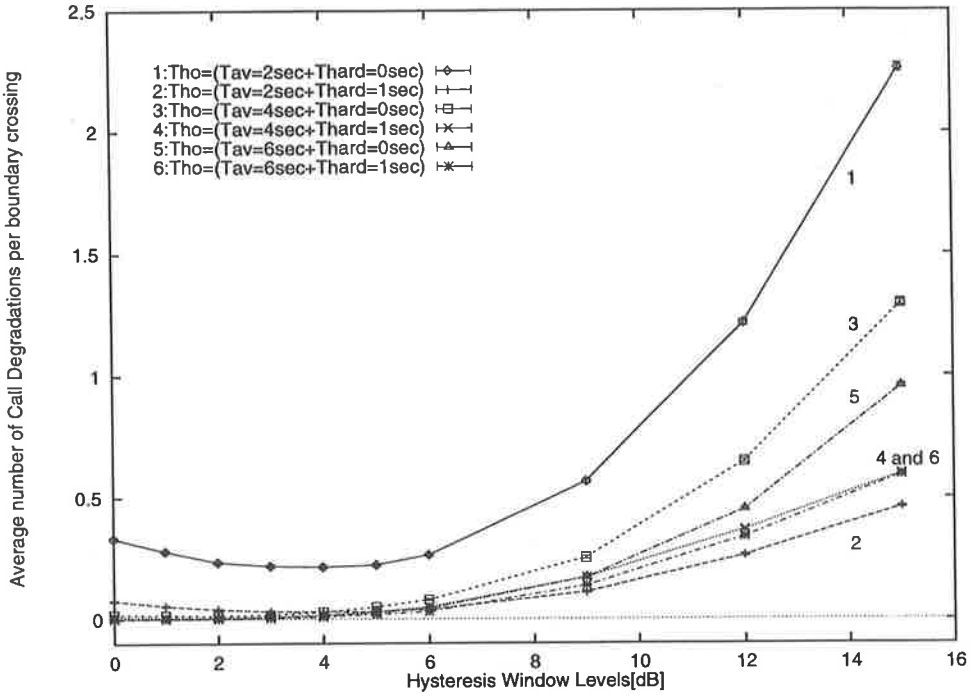

Figure 5.12: Sum of the Mean number of call degradation per boundary crossing measured during an interval $T_{av}+T_{hard}$, a variable T_{av} and a constant T_{hard} with 50% overlap and MIN_TH=-130dBm and speed 72kph

comparisons between zero T_{hard} and non-zero T_{hard} when T_{av} is constant.

Based on results in figures 5.13 and 5.14, with a fair handover characteristic measure (normalised AFD) the soft handover algorithm provides better call quality than the hard handover algorithm, even if the other two measures, the mean number of handover requests and the mean number of call degradations, do not agree with that result.

5.2.3 Conclusions

In the hard handoff algorithm analysis (T_{hard} is not zero), we found that the handover request processing interval would affect the handover characteristics such as the mean number of handover requests and call degradations. As this interval increases, the mean number of handover requests reduces. However the call degradation affected during T_{hard} (in the hard handoff algorithm) is always larger than that of the soft handoff algorithm where T_{hard} is zero. In particular comparisons of normalised AFD shows that

the hard handoff algorithm provides the same or worse performance than the soft handoff algorithm. This normalised AFD comparison is quite reliable because two parameters such as the speed of MS and unit time T_u, which depends on the normalised AFD, are constant in this investigation. That means that if the speed of MS is not constant, then fair comparisons with the normalised AFD among the handoff algorithms are difficult.

From this investigation we strongly recommend that the handover request processing interval should be included in the soft and hard handoff algorithm development and analysis to create more reliable algorithms and to achieve more accurate results. We also have quite important results from this investigation which show that providing a shorter handover request processing interval T_{hard} into the TDMA or CDMA systems can generate equal or better call quality from the handover algorithm analysis point of view. If the TDMA system uses HYS in its handover algorithm, then better call quality will be expected by providing a small T_{hard}.

Based on our results of the normalised AFD in this section, we see that the handover algorithm model proposed by Vijayan *et al.* [11] provides always the same or better call quality, because they consider a fast handover processing time (zero T_{hard}) in their model. This conclusion also agrees with the opinion of Viterbi [52] that "the handover algorithm of Vijayan *et al.* provides the best performance because they assume very fast handover request processing".

We now can conclude precisely that a short handover processing interval provides at least the same performance of in terms of call quality, but equal or worse performance in terms of the mean number of handover requests compared to other handover algorithms using relatively long handover processing.

5.3 Soft Handoff

The co-channel interference ratio (CIR) and transmit power levels are restraining factors on the capacity of cellular mobile systems [51, 70]. In particular, the CIR is very important in CDMA environments because the same carrier frequency with different codes among MSs is used. Thus power control is a basic requirement of the CDMA system

measure, and the probability that the MS is assigned to a BS for handoff analysis. In particular they show that as the drop timer increases, the number of Active Set updates decreases. They investigated more fundamental characteristics of the soft handoff algorithm rather than the performance of the system. However they did not show how power control affects the performance of the soft handoff algorithms.

For the hard handoff algorithm using various handover request processing intervals, the signal strength measurements for handover decision are dependent on many parameters such as signal sampling and averaging interval, signal averaging window types, slow fading and its auto-correlation function and so on. Moreover the soft handoff algorithm and the power control algorithm operate on the basis of the signal strength measurement. The analysis of the handover request characteristics for those two algorithms is necessary. The study in which the soft handoff algorithm is combined with a power control algorithm becomes very important to understand the more realistic soft handoff algorithm.

In this chapter, we use the hard handoff algorithm with a zero handover request processing interval for the soft handoff algorithm (because the MS can connect two or more links during conversation in CDMA systems). We assume that the add threshold and the drop threshold specified in IS-95 [17] are equal to $MIN_TH = -130$dBm and the drop timer is long enough to keep all BSs in the Active Set. Therefore our soft handoff model becomes equal to the hard handoff model used in the previous chapters 3 and 4. With this model we combine the power control algorithm and investigate handover characteristics.

Firstly the power control algorithm used in our study is discussed. The comparison with the handover request characteristics between soft handoff with and without power control is investigated. Secondly the modified power control algorithm to achieve the best handover performance is developed and explained.

5.3.1 Power Control Algorithms

Several power control models have been considered including:

1. fixed power transmit model (no power control model) - no variations in transmit power;
2. received signal based power control model - The aim of this model is to provide the minimum received signal level until the next power control decision. For example, *adaptive power control(APC)* [71] and *adaptive transmitter power control (ATPC)* [68];
3. SIR based tight power control model - The transmit power is adopted directly by the signal-to-interference ratio (SIR) variation and the MS selects the BS at which its SIR is maximised. For example, *local power control algorithm* [69, 73];
4. same as (3) except that the transmitter can select its power level after combining all interference sources. For example, *global power control algorithm* [69, 66, 73];
5. autonomous SIR based power control model - The transmit power can only vary by a fixed step when the received SIR is different from the target SIR threshold, for example *autonomous power control* [74].

The algorithms (2) and (5) are quite similar. The only difference is that algorithm (2) can provide a wide range of transmit power changes every power control interval, while algorithm (5) can only provide a single power increment per power control interval. Algorithms (3) and (4) can achieve substantial gain when combined with dynamic channel allocation (DCA). In particular algorithm (4) requires global management of channel and/or of power adjustment. This power control model is also required to avoid the *near-far* effect in CDMA mobile systems [75].

In this section, we assume that no co-channel or adjacent channel interference occurs, and no near-far effect, because we consider a model consisting only of two BSs and one MS. We adopt the adaptive power control model for our model with an assumption that the reverse link power level is equal to that of the forward link. We use 0dB HYS for the soft handoff algorithm model to provide an immediate handover to users. However we

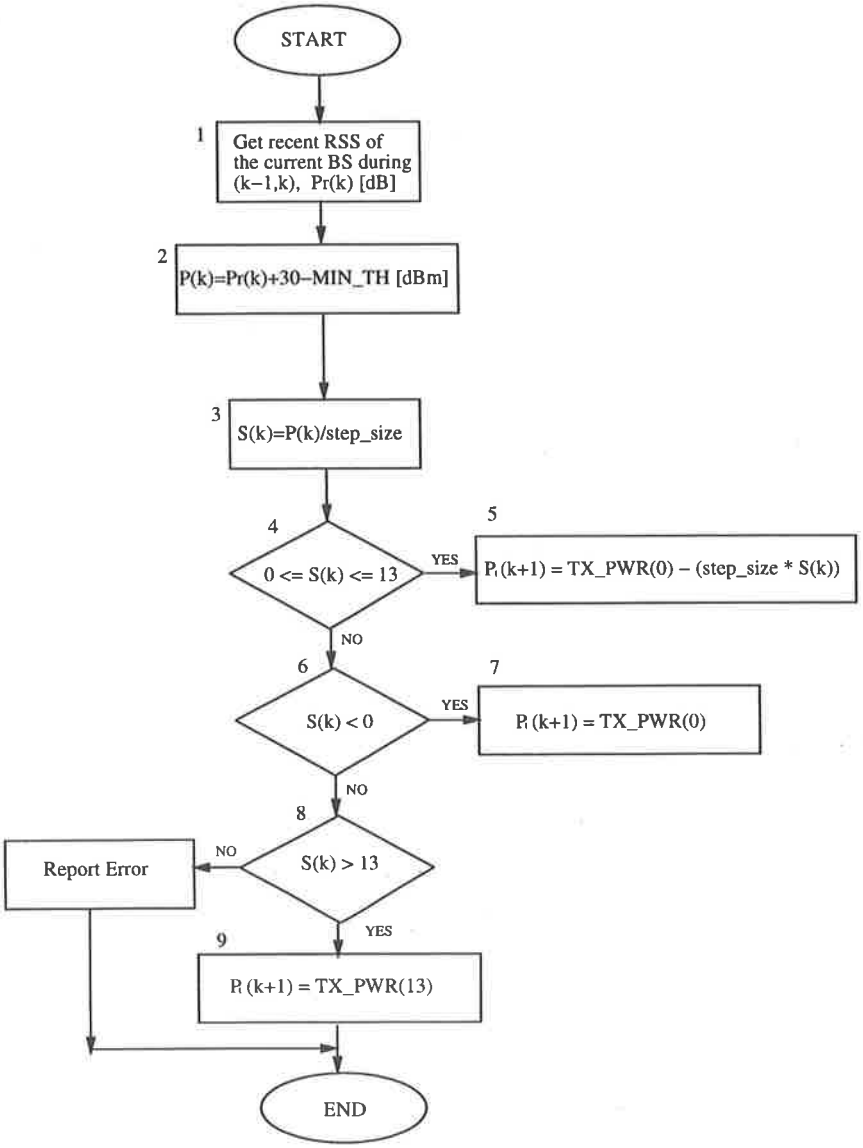

Figure 5.17: Power control algorithms

$$TX\_PWR(S(k)) = TX\_PWR(0) - (step\_size \times S(k)) \tag{5.7}$$

$$RX\_PWR(S(k)) = RX\_PWR(0) + (step\_size \times S(k)) \tag{5.8}$$

where $S(k)$ is the power step number, and k ranges between 0 and MIN_STEP.

At 100% overlap, the TX_PWR table is setup in the form as shown in figure 5.16. Thus $TX\_PWR(0)$ is set to 118.54 Watts (50.74 dBm). We assume that both TX_PWR and RX_PWR tables have 2dBm per power step, that is, $step\_size = 2$, and a total

Therefore the next transmit power level can be decided on the basis of the value of $S(k)$ obtained in equation 5.10 as follows:

1. If $0 <= S(k) <= 13$ (box 4), then the transmit power level shown in equation 5.7 is given by box 5:

$$P_t(k+1) = TX\_PWR(S(k)) = TX\_PWR(0) - (step\_size \times S(k)) \quad (5.11)$$

   where $TX\_PWR(0)$ is the strongest power level

2. If the power control step $S(k)$ is negative (box 6), that is, $P_r(k)$ is less than MIN_TH, then the next transmit power level becomes the strongest power control step by substituting 0 into $S(k)$ in equation 5.11 as follows (box 7).

$$P_t(k+1) = TX\_PWR(0) = TX\_PWR(0) - (step\_size \times 0) \quad (5.12)$$

3. If the power control step $S(k)$ is greater than $MIN\_STEP = 13$ (box 8), that is, $P_r(k)$ is greater than the maximum power, then the next transmit power level becomes the weakest power control step by substituting 13 into $S(k)$ in equation 5.11 as follows (box 9 in figure 5.17):

$$P_t(k+1) = TX\_PWR(13) = TX\_PWR(0) - (step\_size \times MIN\_STEP) \quad (5.13)$$

We understand that the next transmit power level decision is based on the received signal strength by following the procedures mentioned above. We determine the handover characteristics by combining this power control algorithm with the basic handover algorithm using $T_{hard} = 0$. Then we compare handover request characteristics between the soft handoff algorithms with and without the power control algorithm.

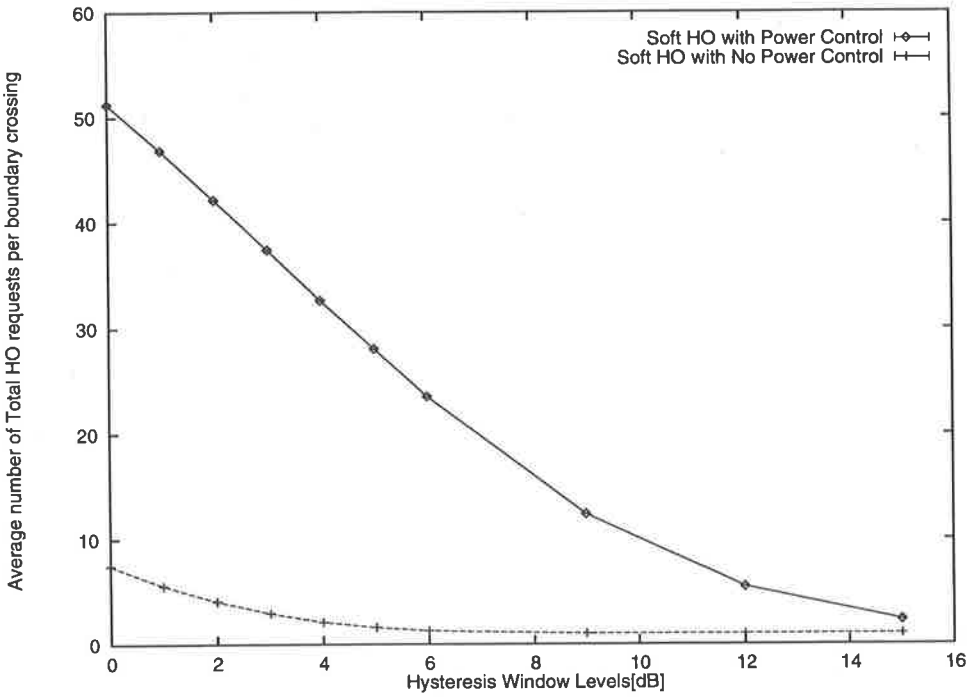

Figure 5.18: Average number of handover requests with 100% overlap and MIN_TH=-130dBm and speed 72kph

- **The mean number of total call degradations**

We now look at the comparisons of the mean number of call degradations shown in figure 5.19. Because 100% overlap is considered to represent a very strong BS transmit power, the SWPC algorithm generates almost zero call degradation over the whole range of HYS. However the SOPC algorithm gives a large number of call degradations against all HYS levels. It is shown that the power control algorithm also affects the mean number of call degradations. Even if high HYS reduces dramatically the mean number of call degradations, this reduction is still unacceptable compare to the SWPC algorithm.

Based on the call degradation condition described in section 4.2.1, we can say that the poor results of the SOPC algorithm are caused by slow fading in the radio environment. In other words, if an inadequate power control algorithms is used in the MS, the transmit power decision should be carefully re-evaluated in terms of the slow fading.

In spite of the poor handover request characteristics of the SOPC algorithm, the mean power consumption shows very interesting results in figure 5.21. The SOPC algorithm gives about 14dB less power consumption to up/down links (we assumed that transmit powers for up/down links are the same). Clearly it shows that the power control helps to reduce the power consumption, that is, it extends the battery life of the MS.

Now we can have a closer comparison between the SOPC and the SWPC algorithm. From the power consumption point of view, the SOPC algorithm shows much better performance than the SWPC algorithm. However from the handover request characteristic point of view (from the user service point of view), the SOPC algorithm should be reconsidered to provide more acceptable handover request characteristics compared to those of the SWPC algorithm. Based on our previous studies regarding the call degradation analysis done in Chapters 1, 3 and 4, call degradation is highly affected by the transmit power level. With this relation between the call degradation and the transmit power level, we believe that the transmit power decision in the SOPC algorithm is too sensitive to the signal variations caused by slow fading. Therefore the reduction of this sensitivity will play a key role in providing better handover request characteristics by sacrificing power consumption. One particular power control algorithm called the *autonomous SIR power control algorithm* [74] was developed to overcome this sensitivity to slow fading. In this chapter, we introduce a parameter called *guard* to increase (or decrease) the transmit power decision level in the power control algorithm. In the next section we will explain the power control model using the guard parameter, and investigate how this guard in the power control model changes the handover request characteristics.

5.3.3 Power Control Algorithms with *guard*

By following the transmit power level decision procedures shown in figure 5.17, we derive the transmit power level of the new power control algorithms with *guard*. We add the guard parameter into equation 5.9. Thus a new signal difference $\hat{P}(k)$ is given by:

$$\hat{P}(k) = P_r(k) + 30 + guard - MIN\_TH \quad \text{dBm} \tag{5.14}$$

$$= P(k) + guard \qquad \text{dBm} \tag{5.15}$$

where $P(k)$ is the difference between $P_r(k)$ and MIN_TH.

The next transmit power control step $\hat{S}(k)$ is obtained by dividing the signal difference $\hat{P}(k)$ by $step\_size$ as follows:

$$\hat{S}(k) = \hat{P}(k)/step\_size \tag{5.16}$$

By replacing $\hat{P}(k)$ with $P(k) + guard$ the equation 5.16 becomes:

$$\begin{aligned} \hat{S}(k) &= \frac{P(k) + guard}{step\_size} \\ &= \frac{P(k)}{step\_size} + \frac{guard}{step\_size} \end{aligned} \tag{5.17}$$

The transmit power control step is written more generally as:

$$\hat{S}(k) = S(k) + S(guard) \tag{5.18}$$

where $S(k)$ is the transmit power control step based on the received signal strength and shown in equation 5.10 and $S(guard)$ is the additional power control step based on the guard parameter.

Finally the next transmit power level is decided by following the procedures shown in figure 5.17 with boxes 5 to 9. Details are also shown in equations 5.11, 5.12 and 5.13. Thus by replacing $S(k)$ with $\hat{S}(k)$ we can obtain the next transmit power level as follows:

$$P_t^{\hat{S}}(k+1) = TX\_PWR(\hat{S}(k)) \tag{5.19}$$

The role of the guard parameter is to increase or decrease the next transmit power level by reducing or increasing the recently received signal strength without any change in the power control conversion table shown in figure 5.15. That means the variation

5.3.4 Characteristics of the Power Control Algorithm with *guard*

The handover request characteristics of soft handoff combined with power control and using the guard parameter are measured and discussed. First of all we vary guard with negative values down to -15dB from 0dB, that is, the transmit power level is increased according to *Definition 2*, to provide more transmit power to users. All other parameters used in this study are the same as that used in the previous section 5.3.1.

- **The mean number of handover requests**

In figure 5.22, the mean number of handover requests per boundary crossing decreases dramatically as the guard decreases, that is, as the transmit power increases. In addition high HYS decreases the mean number of handover requests. Thus when guard is less than or equal to -11dB and above 9dB HYS, the mean number of handover requests becomes unity.

We can easily show that the effects of slow fading in the radio environment should be considered carefully for not only the power level decisions but also the handover decisions.

- **The mean number of call degradations**

In figure 5.23 the mean number of call degradations is also decreased dramatically, as the guard parameter decreases. When the guard is less than or equal to -11dB, it approaches zero over the whole range of HYS.

- **The mean handover area**

The mean handover area is shown in figure 5.24. The distance between the first and the last handover request decreases as the guard parameter decreases. Thus we believe that the reduction of guard, that is, increase of the transmit power, helps to avoid the unnecessary handover requests occurring too early or too late from the cell boundary as shown in figure 5.20 curves 1 and 2. When the guard parameter is less than or equal to -11dB, the mean handover area becomes narrow and reduces to a point above 12dB HYS.

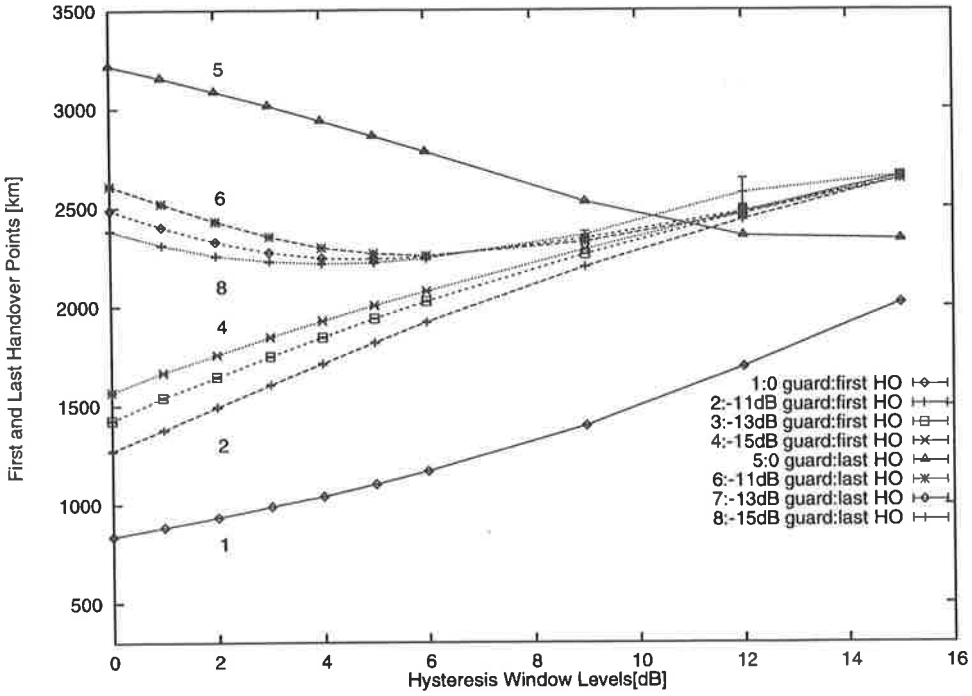

Figure 5.24: Average handover area per boundary crossing with 100% overlap and MIN_TH=-130dBm and speed 72kph

- **The mean power consumption**

The mean power consumption increases dramatically as the guard parameter decreases as shown in figure 5.25. This shows clearly that the guard parameter in the power control algorithm plays a role in managing the transmit power level.

In our adaptive power control algorithm analysis, we realise that there is a trade-off between the power consumption and the performance of the handover algorithm. We demonstrate this trade-off with the guard parameter in our power control algorithm. One of important factors causing this trade-off is the slow fading radio environment. That means that the transmit power decision based on the recently received power level will not be accurate from the user service (handover performance) point of view (see figures 5.18, 5.19 and 5.20), while it gives greater savings in the power consumption (see figure 5.21). Therefore our results of this investigation strongly recommend that the power control algorithm development should be combined with the handover algorithm and then tested from the user service (handover performance) point of view as well as system capacity and power consumption point of view.

for the hard and soft handoff algorithms is equally weighted over the intervals T_{hard} and T_{av}.

For consistent comparisons between the algorithms with and without power control, we define the value of the guard to be -20dB in the power control algorithm to achieve the same level of call degradation of the no power control algorithm for soft handoff. Thus the SOPC-G algorithm gives very similar handover request characteristics to the SWPC algorithm. We use 100% overlap which is assumed to cover almost 100% of a cell in this study. Other system parameters used for those three handoff algorithms are exactly the same in this section.

- **Mean number of handover requests**

In figure 5.26, three handover algorithms show that the mean number of handover requests per boundary crossing decreases and becomes unity as HYS increases. As we set the guard parameter to -20dB in the SOPC-G algorithm, both soft handoff algorithms (curves 1 and 2) provide the same number of handover requests against all values of HYS. However the HWPC algorithm generates a smaller number of handover requests (curve 3) at low and medium HYS than the other soft handoff algorithms because the HWPC algorithm has a handover request processing interval T_{hard} during which no handover request occurs and only the call degradation is measured. The difference between the mean number of handover requests in the HWPC, SOPC-G and SWPC algorithms reduces as HYS increases, because the number of handover processing interval T_{hard} reduces and does not affect the mean number of handover requests.

- **Mean number of call degradations**

As we have discussed in the previous chapters, the comparison of the call degradation, one of the call quality measurements in this thesis, is noteworthy, because the call degradation is highly related to the call quality and call drop from the user service and system performance point of view.

In figure 5.27 both soft handoff algorithms provide the same number of call degradations (curve 1 and 2) over the whole range of HYS. However the HWPC generates more call degradations (curve 3) against all HYS levels compared to the two soft handoff algorithms. As we have mentioned in section 5.2, the HWPC algorithm gives additional

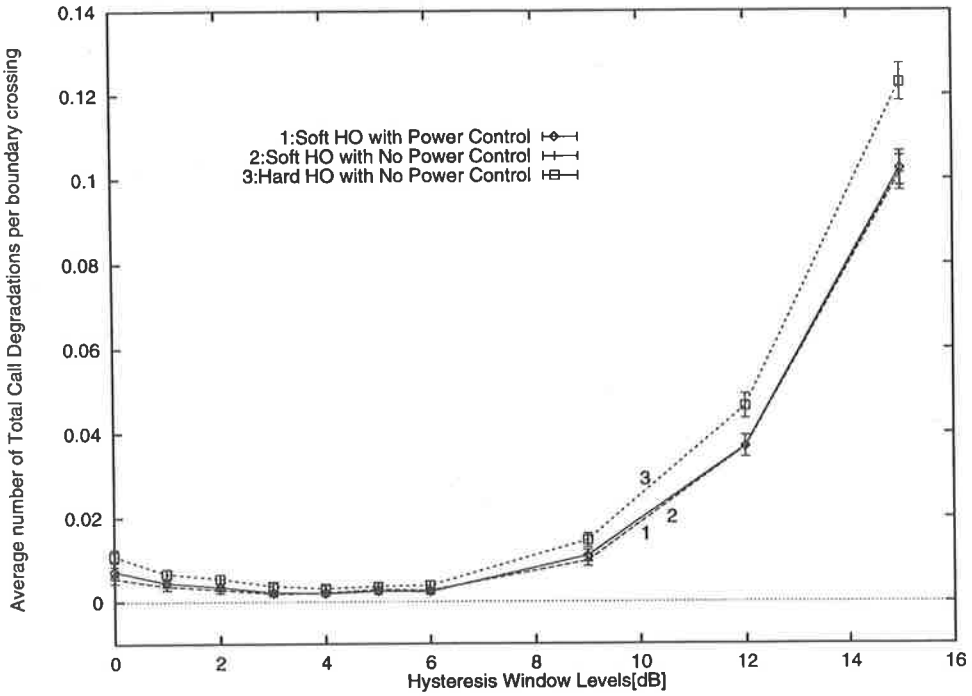

Figure 5.27: Average call degradation per boundary crossing, with 100% overlap and MIN_TH=-130dBm and speed 72kph

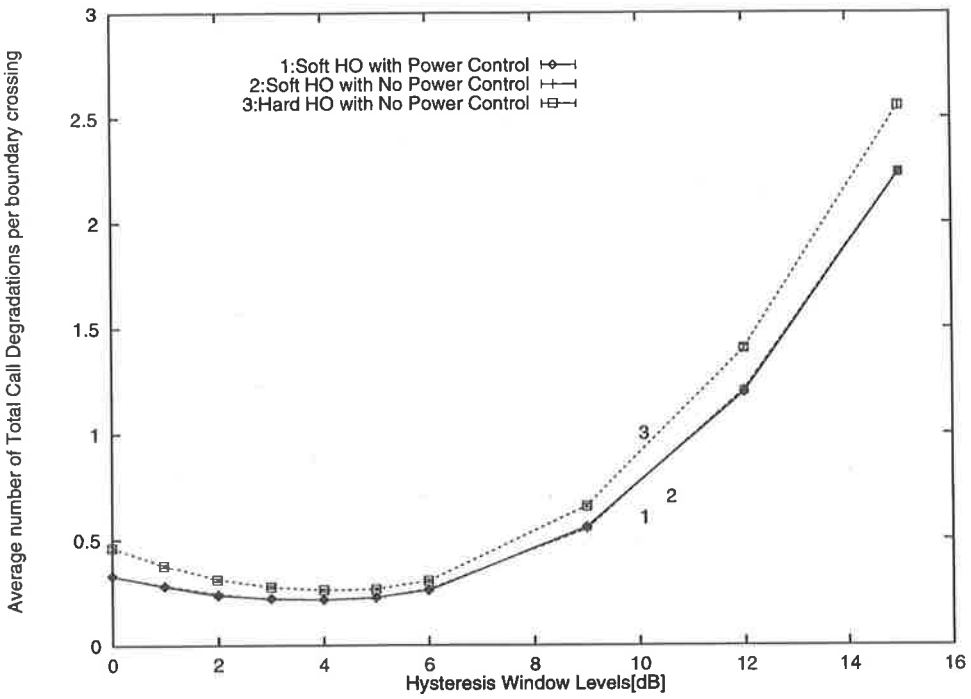

Figure 5.28: Average call degradation per boundary crossing, with 50% overlap and MIN_TH=-130dBm and speed 72kph

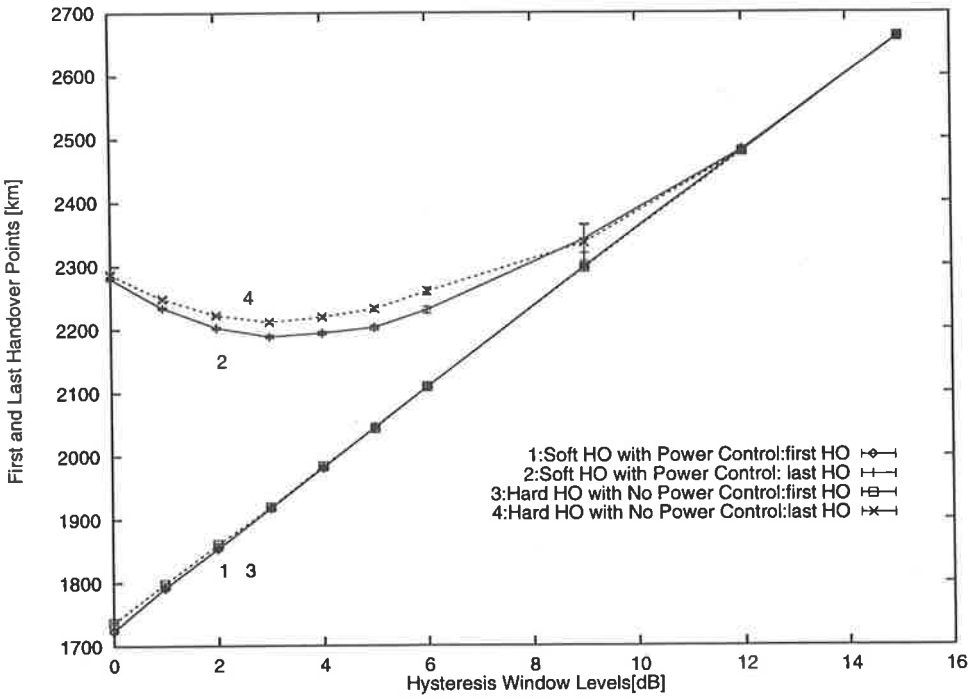

Figure 5.31: Average handover area per boundary crossing, with 100% overlap and MIN_TH=-130dBm and speed 72kph

- **Mean handover area**

In figure 5.31, the SOPC-G algorithm gives quite similar handover area results against all HYS levels compared to the HWPC algorithm. Both algorithms show that the mean handover area is wide at low HYS and as HYS increases the handover area becomes narrow and is delayed from the cell boundary (2000meters).

As was discussed in section 5.4, the SOPC-G algorithm provides smaller call degradation (figures 5.27 and 5.28) and lower power consumption (figures 5.29 and 5.30). This is what we expected to achieve in the handover algorithm analysis using a power control algorithm. We concluded in the previous chapters that without a power control algorithm, a strong transmit power of a BS (providing high RSS to MS) always gives a lower call degradation regardless of the number of handover requests. However, the power control algorithm shows the way to obtain an efficient transmit power level decision without increasing the call degradation which we have used for a call quality measure in handover algorithm analysis.

of call degradations and the mean normalised AFD per handover procedure, shows that a short handover processing interval gives better service quality but more handover requests than those of a long handover processing interval.

2. In the SOPC algorithm analysis, we obtained valuable results as follows:

   (a) The SOPC algorithm can reduce significantly the mean power consumptions compared to the SWPC algorithm.

   (b) However the SOPC algorithm gives much worse handover request characteristics than those of the SWPC algorithm, because an accurate transmit power decision, which is a sort of a next signal prediction, in randomly fading radio propagation environment is very difficult.

   (c) Based on 2(a) and 2(b), we understand that there is a trade off between the mean power consumption and the handover request characteristics in the SOPC algorithm.

   (d) To improve the poor handover request characteristics mentioned in 2(c), we developed the SOPC-G algorithm which combines the SOPC algorithm with a guard band. This SOPC-G algorithm is very useful for measuring efficiently the trade off between the mean power consumption and the handover request characteristics, because the guard band eliminates the unnecessary next transmit power level decision in SOPC algorithm, which is caused by signal fading.

   (e) Based on 2(c) and 2(d), even if one of the important goals of the power control algorithm is to reduce the co-channel interfence by decreasing the transmit power of the MS and BS, the handover request characteristics should be investigated carefully to develop a more efficient and reliable power control algorithm.

   (f) Fast handover decision and its fast processing are important. However because we cannot optimize the length of the signal averaging time in a faded radio environment, a short handover processing interval will give better call quality. A good choice of HYS can minimize the number of handover requests, improve the call quality.

Chapter 6

Handover Performance Enhancement Schemes

6.1 Introduction

In the previous chapter, a new handoff algorithm which takes into account nonzero handover processing intervals, has been developed and analysed. Handover request characteristics relevant to call quality have also been investigated. We found that the call degradation caused by the handover request processing interval cannot be overlooked and it is very difficult to minimise or reduce, unless the handover decision is very accurate and intelligent to predict the signal strength during the handover processing interval. This is very difficult in reality. Further investigation of the call degradation experienced during the handover processing interval is valuable. For system performance analysis we need to investigate the causes of call drop. From the system point of view, there is another parameter related to the handover request processing interval, caused by signalling traffic delays resulting from congestion and queueing in the processing system hardware. We call this the *handover waiting interval.* These handover processing and waiting intervals will increase the call degradation, that is, increase the call drop, thus reducing the system performance. In this chapter, using the knowledge which we have gained from chapters 3, 4 and 5 in relation to handover algorithm analysis, the new handoff algorithm is evaluated at the mobile system level to determine the effects of this

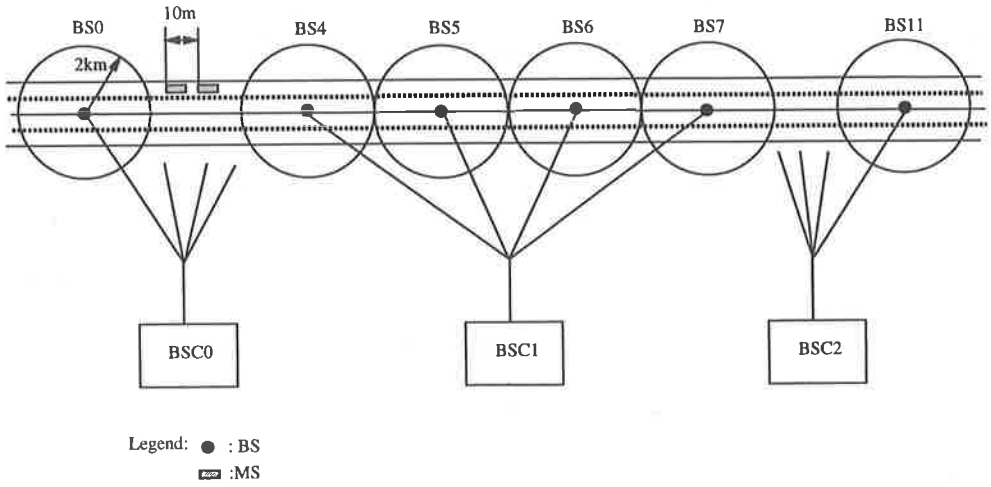

Figure 6.1: Cell Layout

particularly the handover rejection schemes and channel reservation scheme will be introduced and discussed.

6.2 System Model

6.2.1 Cell Layout

In the scenario that we have chosen for this study, 12 BSs having 2km radius are linearly located on the highway as shown in figure 6.1. Four BSs are controlled by a base station center (BSC) and 3 BSCs are controlled by a mobile switching center (MSC). Four lanes on the highway pass through the center of each cell where the BS is located. The MS moves along the highway with a constant speed: 72kmph for the high speed model. Inter MS distance is 10 meters and MSs moving out of the cell located at the end of the cell layout (BS0 or BS11) enter into the opposite end cell. Thus 800 MSs per cell are travelling all the time.

Table 6.1: CIR Variation Versus propagation path loss slope γ

γ	$\frac{I}{C}$ at the center of cell	$\frac{I}{C}$ at the cell boundary
2.0	15.05 dB	12.55 dB
2.5	19.57 dB	16.46 dB
3.0	24.08 dB	20.34 dB
4.0	33.11 dB	28.12 dB

6.2.4 Co-channel Interference Ratio (CIR)

In this study we mainly consider the channel reuse distance to be 16 km (four BSs). Thus there are a maximum of two interferers in one tier. CIR is measured when the carrier is 2 km away and the two interferers are 12 and 16 km away as follows:

$$\begin{aligned} \frac{C}{I} &= \frac{P_r(2)}{P_r(12)+P_r(16)} \quad \text{[watts]} \\ &= 27.01 \quad \text{dB} \end{aligned} \tag{6.3}$$

If we measure CIR based on the path loss slope, γ ranges from 2 to 4 [50]. γ depends on the topography of terrain and cannot be less than 2, which is the free-space condition.

$$\frac{C}{I} = \frac{r^{-\gamma}}{\sum_{i=1}^{K_I} D_i^{-\gamma}} \tag{6.4}$$

where r is the cell radius in km, γ is the propagation path loss slope ranges 2 to 4, K_I is the number of co-channel interferers, D_i is the distance between a receiver and an interferer in km.

CIR is measured and shown in table 6.1 for the cases where r is 2, K_I is 2 and D_i is 16 and 12 and γ varies 2 to 4 dB.

Based on the CIR of 27.01 dB shown in equation 6.3, γ reaches 4. This is the value used for the general propagation attenuation model [80]. We now understand that a BS channel reuse distance of 4 represents a good choice because the CIR is greater than the 18 dB needed to provide acceptable voice quality such that slow fading and CIR do

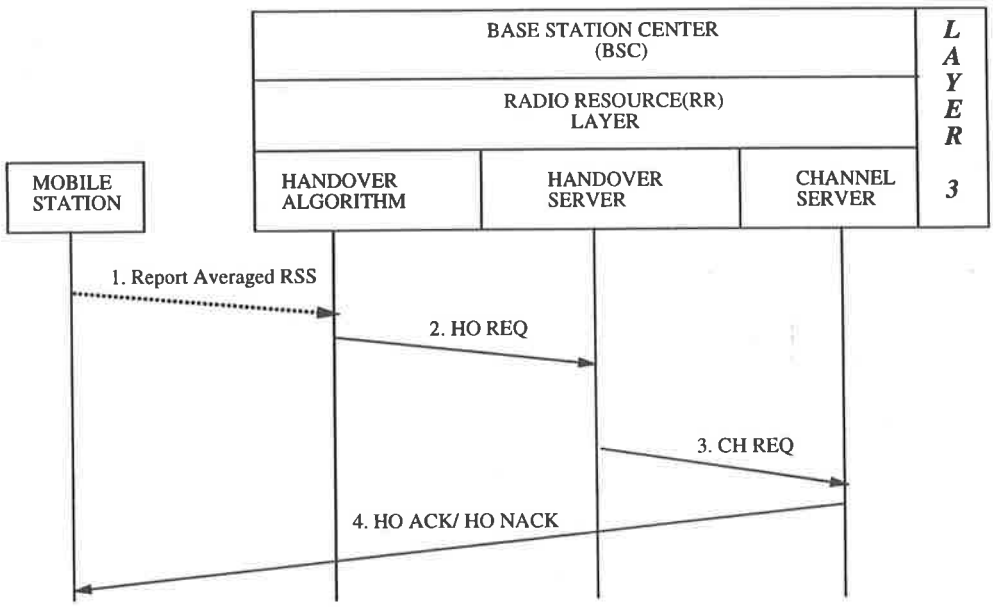

Figure 6.2: Handover Process Modules and Procedures

(channel request) message to the channel server to occupy a new radio channel as shown in scenario 3. Based on the radio resource status of the new-BS, the MS receives the handover success message, HO ACK (handover acknowledge) or the handover failure message, HO NACK (handover not acknowledge) from the BSC.

- **Handover Algorithm**

We use the basic handover algorithm classified into normal and enforced handover requests on the basis of the EN handover algorthm concept, as follows:

1. The Normal Condition in the Basic Handover algorithm (NCBH):

$$RSS(m) + HYS \leq RSS(n) \quad \text{and} \quad RSS(m), RSS(n) \geq MIN\_TH \tag{6.5}$$

2. The Enforced Condition in the Basic Handover algorithm (ECBH):

$$RSS(m) < MIN\_TH \quad \text{and} \quad RSS(n) \geq MIN\_TH \tag{6.6}$$

where m is the current BS Id, n is a neighbouring BS Id, HYS is the hysteresis window in dB and MIN_TH is a minimum RSS threshold, which is normally taken to be -130dB.

6.4 Performance Analysis

An accurate and efficient system performance analysis will be useful in attempts to improve the system performance. To obtain accurate data, appropriate system performance measurements are chosen by system designers and system operators. In a mobile environment, obtaining accurate data is a much harder task than for fixed systems such as the public switch trunk network (PSTN), because of the randomnesses of various system parameters which are difficult to predict in the system operation environment. One of the system performance measurements which differs most significantly between mobile (wireless) networks and the PSTN, is call drop rate. In the wireless environment this is considered to be more important than new call blocking from user service point of view.

Based on the handover request characteristics studied in the previous Chapters 3, 4 and 5, call drop occurs by disconnection of a user or a system when the received signal strength from the current BS falls below a receive threshold level for a certain period of time. There are many factors which cause this call drop in the mobile environment. We explain this in more detail with regard to the handover server mentioned above.

The handover arrival rate is dependent on five categories: 1) user behavior, 2) cell layout, 3) radio propagation model, 4) handover model and 5) system resource management. More details of each category are shown in table 6.2.

In the early stages of mobile system performance studies, many such studies involved system performance measurement and enhancement with the assumption that the blocking of handover requests is equivalent to the call drop rates. Posner *et al.* [22] and Guérin [23] used this assumption and created an analytical model with the further assumptions that the following call drop elements of table 6.2: (1.3) is Poisson distributed, (1.4) is negative exponentially distributed, (4.8) is Poisson distributed, (5.3) is FCA. They adjusted (5.4) to decrease call drop rates but it showed clearly that the reduction of call drop rates results in a dramatic increase of the new call blocking probability. To minimise the call blocking probability they also adjusted element (5.6).

Hong *et al.* [21] also used this assumption. They focussed more on the call drop elements (1.1) and (1.2) of user behavior in table 6.2 and (2.1) in cell layout. They derived teletraffic models of user behavior such as (1.3) and (1.4). They discovered that (5.4)

These studies [22, 23, 21, 77] all contributed to creating more reliable teletraffic models of mobile systems and showed that the handover arrivals were more important than the new call arrivals from the system and user quality point of view. However they did not consider the categories 2 and 3 in table 6.2 in their model. That means that the performance analyses based on their models may not be accurate and reliable.

Many studies have been done with concentration on the radio propagation model (category 3) in table 6.2. Chu *at al.* [79, 35] developed an analytical highway model using *generalised fixed channel assignment* (GFCA). They included path loss (3.1), slow fading (3.2) and CIR (3.4) but not autocorrelation of slow fading (3.3). They defined the call drop as occurring in two ways: the signal strength fallen below the minimum receive threshold, and the handover request call does not find any free channel at a target BS. They showed that the BS selection for new call attempts (GFCA) provides better performance than for FCA.

Luo *et al.* [78] investigate city microcell system performance with considerations of the major elements in categories 1), 2), 3) and 5), with the exception of (3.3). They also assumed that the handover blocking probability is not equal to the call drop rate, that is, the call drop rate is based on the signal strength from current BS. They used the handover queueing scheme (5.5) for improving system performance, in particular call drop rates.

Senarath *et al.* [7] also investigated system performance in the Manhattan microcellular model (2.2) with various BS transmit power (2.3) and most elements in category 3) such as the path loss model (3.1) of Hata [8] and Harly [81], lognormal fading (3.2), exponential correlation function of slow fading (3.3) [9, 49] and CIR (3.4). They included the handover algorithm (4.1) and HYS (4.2) into their model as well, with the exception of the handover request processing time (4.7 and 4.8 in table 6.2). In their ongoing research [59], they improved call drop rates by using handover priority (5.4) and handover queueing (5.5) schemes. They also made an assumption that the call drop rate is not based on the handover blocking probability but rather on the signal strength and the channel availability at the target BS.

Kuek *et al.* [24] also investigated a bidirectional highway microcell model. They considered most elements in categories 1), 2), 3) and 5) with the exception of (3.4). They used

measure.

- **New Call Blocking Probability**

The New Call Blocking Probability:

$$P_{call} = \frac{\text{total number of calls blocked}}{\text{total number of new calls}} \tag{6.7}$$

is one of the important measures related to the grade of service (GOS) in mobile communication systems because one of the main functions of the wireless terminals is to make or receive a call anytime and anywhere. In the highway mobile system model, new calls can only be blocked when all radio channels at the channel server located in the current BS are busy.

- **Handover Blocking Probability**

Handover Blocking Probability:

$$P_{ho} = \frac{\text{total number of handovers blocked}}{\text{total number of handovers}} \tag{6.8}$$

is used to show how many handover requests are blocked in the middle of a call conversation. A handover request is considered to be blocked when all channels at the channel server are busy, just as when a new call is blocked. In addition we consider that the handover request can be blocked in the handover server due to delay of the handover reponse. We have an interesting aspect of the analysis of P_{ho}, in that unless the blocked handover request causes the call conversation to disconnect, handover blocking does not directly cause call drop. That is, the handover blocking probability is not equal to the call drop rate. The call drop rates and the call drop decisions are discussed next.

- **Call Drop Rates**

The call drop rates are given by:

$$P_{drop} = \frac{\text{total number of calls dropped}}{\text{(total number of new calls - total number of calls blocked)}} \tag{6.9}$$

With the purpose of examining how the handover request response time (handover queueing time plus handover processing time) affects the system performance, the average queueing time at the handover server shown in figure 6.2 is measured. In particular, this queueing time is used to gain further understanding of the features of the call drop rates caused by handover process delay.

6.4.2 Call Drop Analysis

In this chapter, the call drop decision is defined on the basis of the call degradation conditions studied in subsection 3.2.5 and 3.4.6 in Chapter 4 and subsection 4.2.1 in Chapter 4. First of all we will review the call degradation conditions as follows:

1. No-Signal Call Degradation condition (NDEG):

$$RSS(\text{all BSs}) \leq MIN\_TH \tag{6.13}$$

2. Sudden Call Degradation condition (SDEG):

$$RSS(\text{current BS}) \leq MIN\_TH \quad \text{and} \quad RSS(\text{neighbour BS}) \geq MIN\_TH \tag{6.14}$$

where RSS is the received signal strength and MIN_TH is the minimum signal strength.

We have used the mean number of call degradations as a call quality measure in the previous chapters, because call degradation conditions can reveal the different characteristics of the handover algorithm for various BS transmit power levels and HYS levels, which is not clearly revealed by other measures such as the number of handover requests. Therefore we use call degradation for the call drop condition in system performance analysis.

The *call drop condition* is that if the received signal strength from the current BS falls below MIN_TH during a call conversation, then we will consider the call to be dropped. A question arises why the MS experiences this call drop condition. There are two conventional reasons:

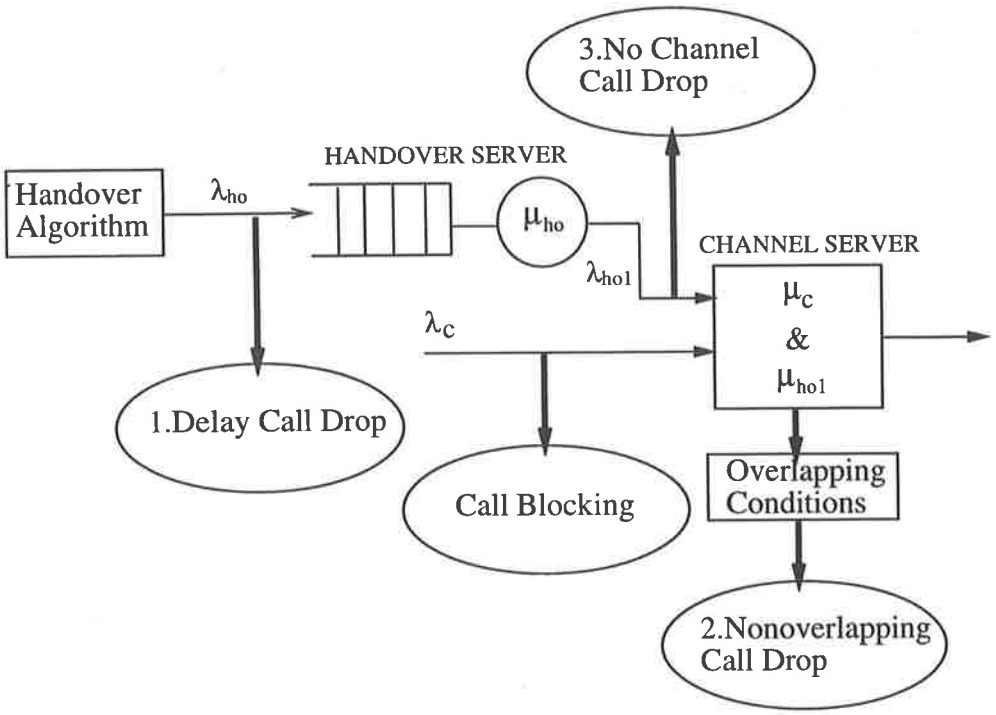

Figure 6.3: Call Drop Model

6.4.3 Results

For simulation analysis, each BS has 50 channels and the offered traffic per channel is assumed to be 0.95 for the heavy traffic model. Thus the new call arrival rate is 0.451 calls/sec/BS for heavy traffic. The call holding time is negative exponentially distributed with mean 105.6 seconds as used by COX [83], but the channel holding time is based on the handover conditions. Two different BS transmit power conditions: 25% and 50% overlapping, are used. All MSs move 72kph constant speed and the signal average distance is 40 meters (about 120λ).

The service time at the handover server, $\frac{1}{\mu_{ho}}$, is 50ms and 500ms for the fast handover processing model (FHPM) and the slow handover processing model (SHPM) respectively. The handover server has 60 waiting queues. The call will be dropped regardless of queue size, when the received signal strength of each MS monitoring individually every signal averaging interval by the system, falls below the $MIN_TH = -130$dB.

To get rid of edge effects [24, 82] in this linear highway simulation model, the results are only measured at the center BS (BS6 in figure 6.1).

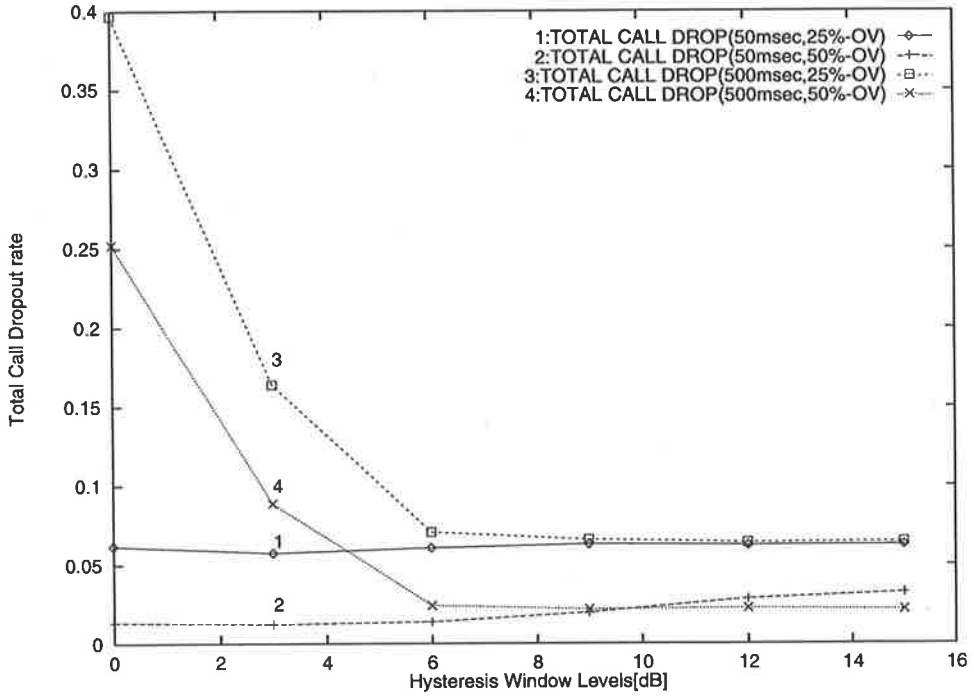

Figure 6.5: Total Call drop Rate, offered traffic per channel = 0.95

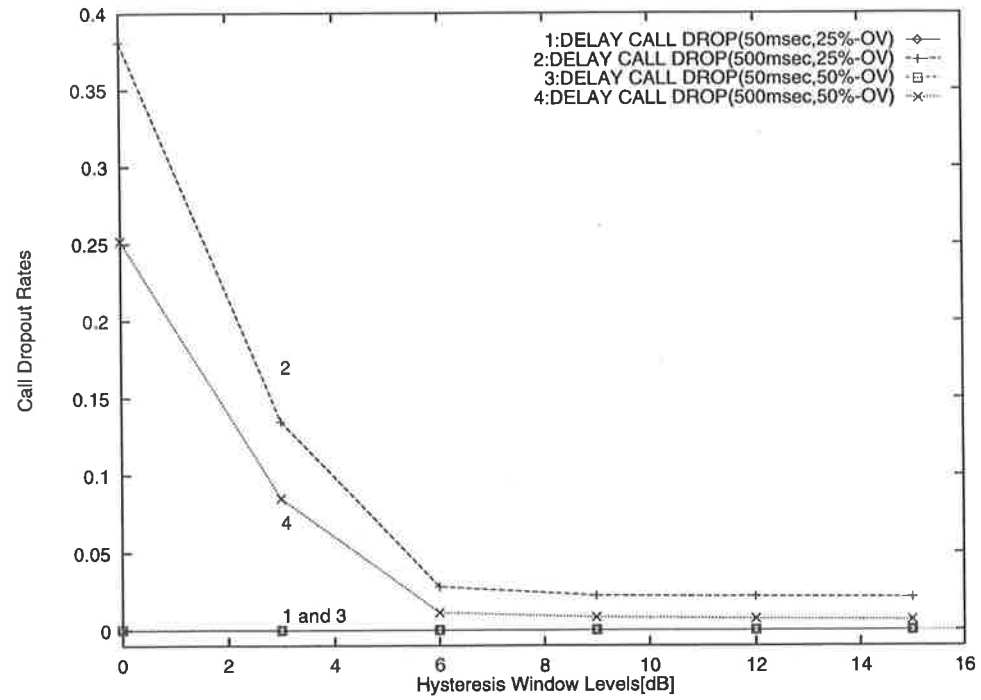

Figure 6.6: Delayed Call drop Rate, offered traffic per channel = 0.95

This means that even if a high speed of handover request processing reduces the delayed call drop rates, two other call drop effects: no-channel and nonoverlapping call drop, contribute to this total call drop rate (curves 1 and 3 in figure 6.5). Those two call drop effects will be discused next.

- **Nonoverlapping Call Drop**

We now focus on the call drop caused by weak BS transmit power. In general, as the BS transmit power increases, the overlapped area between BSs increases and the MS can obtain stronger power from the current BS throughout a call conversation. To avoid any confusion caused by the three call drop effects in the nonoverlapping call drop analysis, we use FHPM to keep the delayed call drop rate to almost zero. In figure 6.7, when the overlapping condition is 25%, the nonoverlapping call drop rate (graph 3) is about a half of the total call drop rates (graph 1) over the whole range of HYS, while the nonoverlapping call drop rate (graph 4) is almost zero over all HYS when the overlapping condition is 50%. However, the total call drop rate (graph 2 in figure 6.7) is maintained at more than 1% over the whole range of HYS levels. We have seen the importance of the overlapping conditions, in other words the BS transmit power level, in system performance analysis and improvement. This is the same as we discovered during the call degradation analysis in chapters 3, 4 and 5.

When the overlapping condition is 50% and the handover request processing time is 50ms, we obtained almost zero nonoverlapping call drop rate in figure 6.7 and almost zero delayed call drop rate in figure 6.6. Thus the difference between curves 2 and 4 in figure 6.7 is considered to be caused by no-channel call drop. This no-channel call drop will be discussed next.

- **No-Channel Call Drop**

In figure 6.8, we show the total call drop rates and the no-channel call drop rates, when the overlapping conditions is 25% and 50%. FHPM is used for the handover request processing model. Therefore the portion of the delayed call drop rate out of the total call drop rate is negligible. When the overlapping condition is 25%, the no-channel call drop rate (graph 3) takes about half of the total call drop rate (graph 1) over all values of HYS, while the no-channel call drop rate (graph 4) is the same as the total call drop

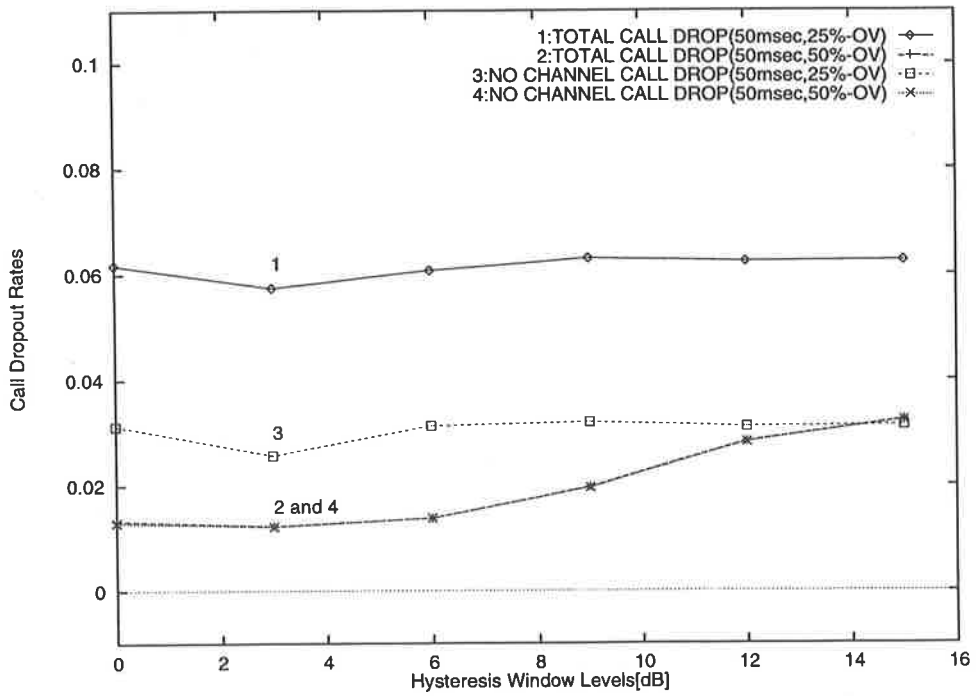

Figure 6.8: No-Channel Call drop Rate, offered traffic per channel = 0.95

6.4.4 Proposed Grade of Service (PGOS and PGOS1) and Total Call drop rates

The curves 2 and 4 in figure 6.9 show that the call degradation contribution to PGOS1 at 0dB HYS is almost 100% of PGOS1, and that this portion reduces as HYS increases. This is because very high call drop rates at low HYS provide more opportunities for new call arrivals to occupy free channels. In contrast when HYS is high, the portion of the new call blocking probability (difference between graph 4 and graph 2) in PGOS1 increases, and that difference is less than the total call drop rate (graph 2). Similar characteristics are achieved over the whole range of HYS levels when the handover request processing interval is 50ms (curves 1 and 3). Thus we see that the system performance, from the call drop (user service) point of view, is poor. However, as the BS transmit power increases from 25% to 50% and the handover request processing time decreases from 500ms to 50ms, the portion of total call degradation in PGOS1 (graph 1 in figure 6.10) is much less than the new call blocking probability (difference between graph 3 and graph 1 in figure 6.10). As HYS increases, that is, as the handover request queueing time decreases,

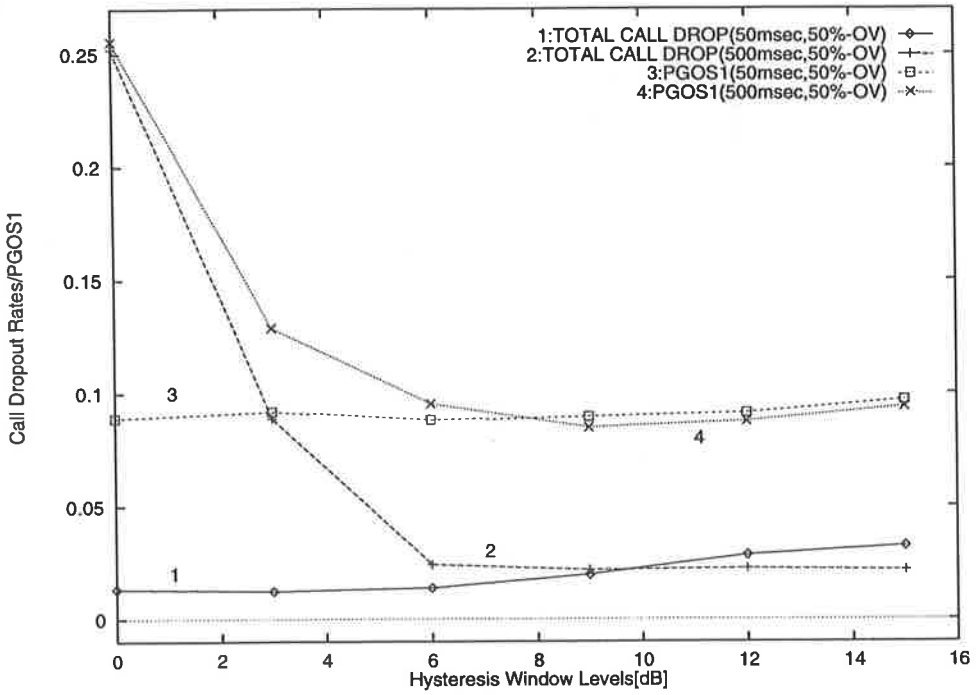

Figure 6.10: PGOS1 and Total Call drop rate (50% OV), offered traffic per channel = 0.95

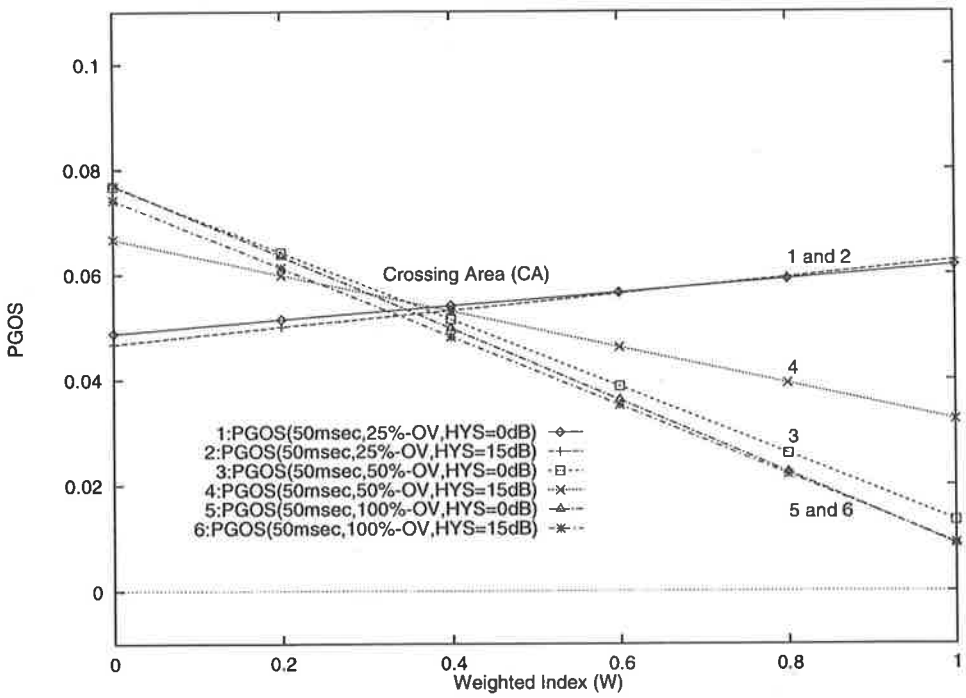

Figure 6.11: PGOS Comparisons on Weighted Index (W), offered traffic per channel = 0.95

becomes 0.25. Thus a reduction of P_{call} from 5% to 0 can cause call drop rate to increase by about four times. On the other hand a big reduction in P_{drop} can only cause P_{call} to increase by a factor of $\frac{1}{4}$.

If the CA is placed at 0.5 W_{CA}, that is, P_{call} and P_{drop} have equal variation, then ΔY_1 will be 0.05 and ΔY_2 will be 0.05. Thus Y_2 is 0.1.

The PGOS analysis will help us to understand better how to evaluate and improve system performance in terms of call drop rates and the new call blocking probability.

In summary we have investigated a linear highway model using various parameters, in particular hysteresis windows and handover processing intervals in the handover model. The effect of the handover processing time and its queueing time at the handover server has been investigated as one of the reasons for call drop. This investigation which is an extended study of our previous 'hard handoff algorithm analysis' in Chapter 5 provided valuable results from the system performance analysis point of view. The effect called delayed call drop showed that the handover request processing delay at the system level will affect the system performance. Two conventional reasons for call drop: no-channel call drop and nonoverlapping call drop, have also been examined in this section.

The next section focuses on the improvement of call drop rate, because P_{drop} is normally considered to be more important than P_{call} in a wireless environment. We consider the system performance enhancement based on the results of analyses of those three call drop effects. We hope that some system performance enhancement will be gained naturally if our call drop effects are classified and correctly analysed.

6.5 Performance Enhancement

One of the more popular methods for improving the call drop rate is to use a handover request priority scheme (we refer to this scheme as the channel reservation scheme in this thesis) [21, 84]. The main concept for this scheme is to give more opportunity to the handover requests to access free channels, rather than the call requests, by reserving some portions of the free channels exclusively for the handover requests. The rest of channels are shared with the call requests and the handover requests. This channel

(Ch_TH), the enforced handover requests (equation 6.6) only are permitted to access free channels. That means the normal handover requests (equation 6.5) are rejected. But if the number of busy channels is less than (Ch_TH), both types of handover requests are accepted at the destination BS. If this load sharing scheme operates at each BS, then it is called the *BS rejection scheme.* If the load sharing scheme operates at each BSC, then it is called the *BSC rejection scheme.* Both schemes will be investigated when the user demands are heavy, ρ (offered traffic/ch) = 0.95.

- **BS Rejection Scheme**

In figure 6.13, the handover rejection scheme is shown. The handover algorithm invokes a handover request (block 1). The system then checks the handover rejection type flag (block 2). If the flag is set by the BS Rejection Scheme, then the system will extract the destination BS ID of the handover request from the data base (block 3) and then examine the channel usage status at the destination BS (block 4). If the number of busy channels, the channel usage, is less than a threshold (Ch_TH) (block 4), then the handover request is transferred to the channel server of the destination BS. But if the number of busy channels is greater than the threshold, then the invoked handover request will be checked for its handover request type (block 5). If it is a normal handover request, then it will be rejected, otherwise the enforced handover request will be passed over to the destination BS. If there is a free channel (block 12) at the channel server, this handover request will access a free channel (block 13), otherwise the handover request will be blocked (block 14).

- **BSC Rejection Scheme**

In general a BSC controls a set of BSs to maintain the call procedures in the mobile system. The BSC rejection scheme ensures that if any BS in a set satisfies the condition for BS rejection as discussed in the previous subsection, then every BS in the set will initiate the BS rejection scheme. We explain details of the BSC rejection scheme as follows. After a handover request is invoked, the system gets its destination BS ID and the IDs of other BSs controlled by the same BSC (block 6). If at least one BS has its channel usage greater than a threshold (block 7), only enforced handover requests will be passed over to the destination BS (block 5), and normal handover requests will be rejected. After that the flows are exactly the same as the BS rejection scheme.

6.5.2 Results

As we have seen in figures 6.4 and 6.6, an overloaded handover processor causes call drop rate to be high. Thus we control the normal handover request arrival rate based on the channel usage to reduce the handover process delay as well as the delayed call drop rate by using the handover request rejection scheme.

To investigate the performance of the handover rejection schemes, we choose the model in which the call drop is delayed call drop, that is, handover request processing time is 500ms (SHPM), as we have already seen in figures 6.4 and 6.6. This model uses the FCA scheme. To identify this model with the handover rejection scheme, we refer to it as the FCA scheme. Then we combine the BS and BSC handover rejection schemes with this model. The (Ch_TH) is set to 80%.

In figures 6.14 and 6.15, we compare the mean queueing time of handovers between the BS and BSC rejection schemes and the FCA scheme when the overlapping conditions are 25 and 50%. Both BS and BSC rejection schemes reduce the mean queueing time dramatically at low and medium HYS but maintain a similar queueing time at high HYS of the FCA scheme regardless of overlapping conditions.

The delayed call drop rate shown in figures 6.16 and 6.17 also decreases significantly. Again it maintains similar levels at high HYS for the FCA scheme regardless of the overlapping conditions. The delayed call drop rate remains at about 2% and 1% for 25 and 50% overlapping conditions respectively over the whole range of HYS levels. Therefore it is demonstrated that the handover rejection schemes can be useful for improving the call drop rate caused by handover processing delay.

To examine the overall system performance of handover rejection schemes, we measure the total call drop rate as shown in figures 6.18 and 6.19. The total call drop rate is about 6% and 2.3% for 25% and 50% of overlapping conditions respectively for all HYS levels. The handover rejection scheme demonstrates similar total call drop rates for the FCA scheme at high HYS. We believe in the main that the handover rejection schemes reduce the delayed call drop rates because the difference between delayed and total call drop rates maintains the same level, about 4% and 1.3% for 25% and 50% overlapping conditions respectively over the whole range of HYS levels.

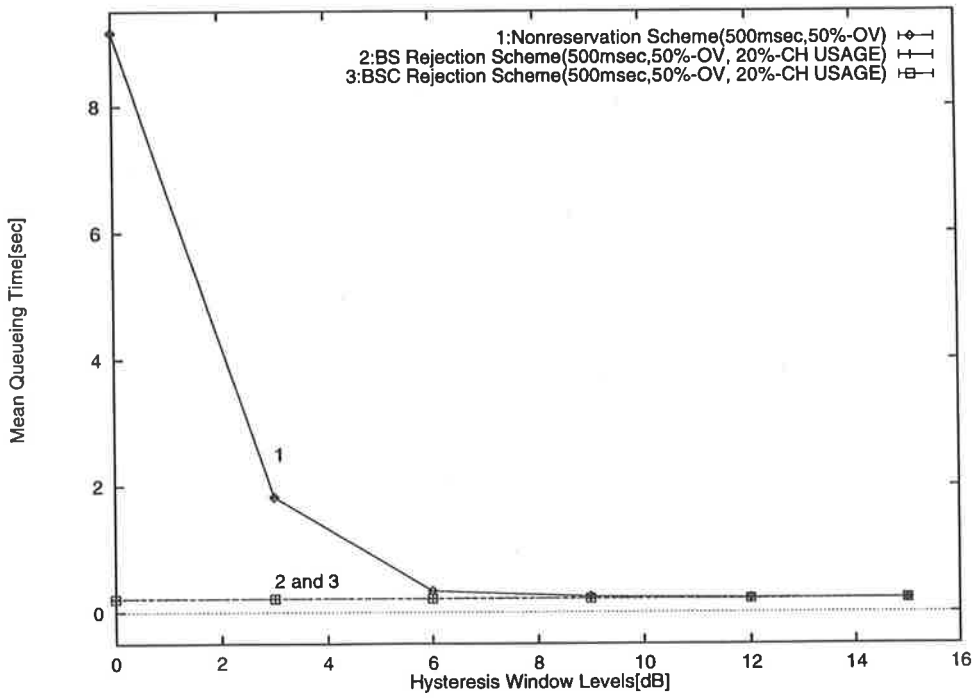

Figure 6.15: Mean Handover Process Queueing Time of Handover Rejection Scheme (50% overlapping condition and 500ms handover processing time), offered traffic per channel = 0.95

Now we consider one of the popular system performance enhancement schemes, the channel reservation scheme, to reduce the no-channel call drop rates.

6.5.3 Channel Reservation Schemes

The channel reservation scheme is shown in figure 6.20. The idea is that handover arrivals and new call arrivals will access free channels in CH_1, but if all channels in CH_1 are busy, then the new call arrivals will be blocked but the handover requests will access free channels in CH_2. The handover and the new call blocking probability is varied based on the ratio between CH_1 and CH_2. In general, if the proportion of CH_1 increases, the new call blocking probability increases but the handover blocking probability decreases. However the proportion of CH_1 should be carefully selected to reduce the handover blocking probability by maintaining a reasonable new call blocking probability.

To demonstrate the effects on the total and no-channel call drop rates of the channel

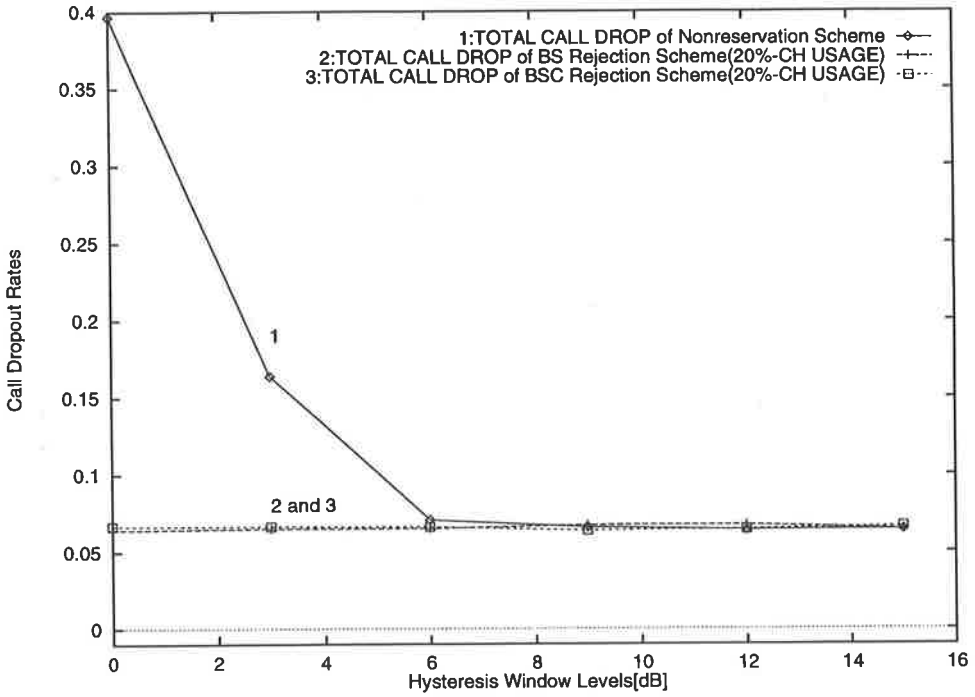

Figure 6.18: Total Call drop Rates of Handover Rejection Scheme (25% overlapping condition and 500ms handover processing time), offered traffic per channel = 0.95

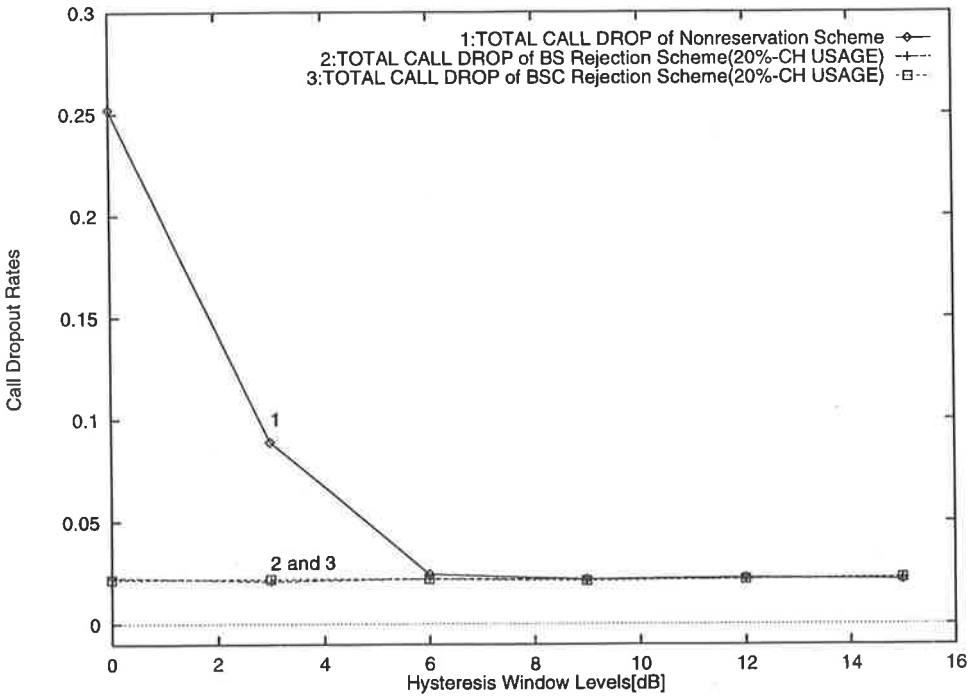

Figure 6.19: Total Call drop Rates of Handover Rejection Scheme (50% overlapping condition and 500ms handover processing time), offered traffic per channel = 0.95

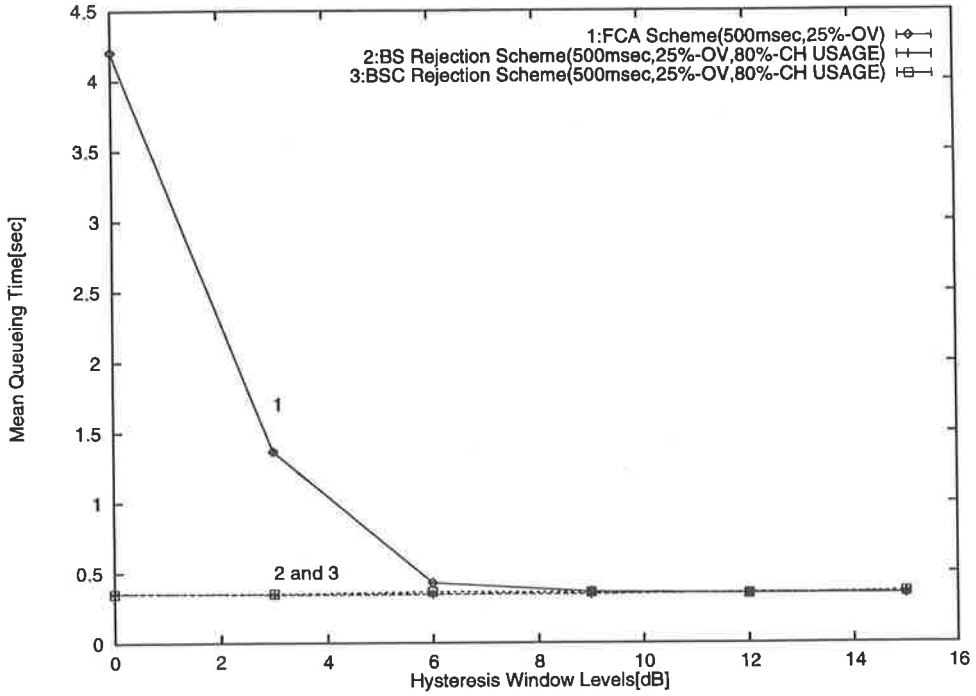

Figure 6.21: Call drop Rates of Channel Reservation Scheme, offered traffic per channel = 0.95

6.5.4 Combination Handover Rejection Scheme with Channel Reservation Scheme (HR-CR)

We believe that the rates of each of the three types of call drop can be reduced effectively when an appropriate individual enhancement scheme is operated. This is quite reasonable based on the analyses of BS and BSC handover rejection schemes and the channel reservation scheme. Moreover if those individual performance enhancement schemes are combined, then we can expect further call drop rate reduction than for individual enhancement schemes. In this study we consider the handover rejection scheme with an 80% channel usage at each channel server and 40% of channels reserved for the handover requests. The mean queueing time for handover request processing is shown in figure 6.22. The combination scheme (HR-CR) provides the shortest queueing time at low and medium HYS out of the three schemes: FCA, BSC rejection scheme and HR-CR scheme. When HYS is greater than 9dB, the mean queueing time is the same among those schemes. In figure 6.23, the HR-CR scheme shows the lowest total call drop rate.

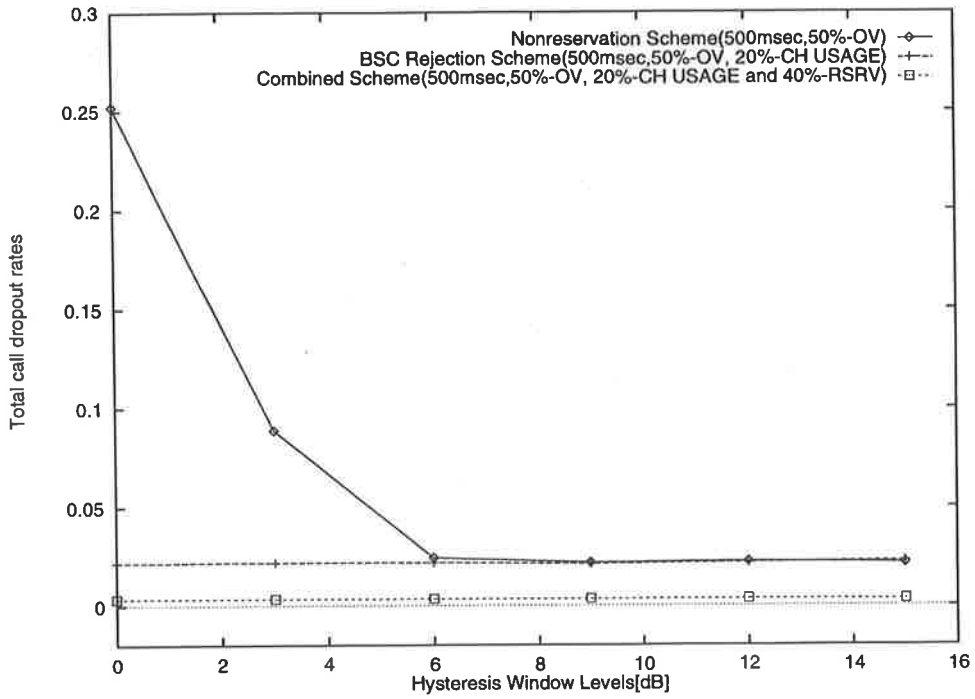

Figure 6.23: Call drop Rates of Combination scheme, offered traffic per channel = 0.95

performance enhancement schemes from the call drop point of view. We propose PGOS and PGOS1 as new performance measure.

1. Firstly, in handover performance measurement we found results as follows:

   (a) A long handover request response (service time plus queueing time) time can cause call drop to increase.

   (b) Thus a new call drop category, delayed call drop, should be considered with other two conventional call drop categories: no-channel call drop and nonoverlapping call drop.

   (c) The BS transmit power level affects all three call drop categories but the BS transmit level increment cannot entirely get rid of delayed and no-channel call drop, while nonoverlapping call drop is reduced to almost zero.

2. Secondly, in handover performance enhancement, we found very important results as follows.

Chapter 7

Conclusions and Future Work

7.1 Conclusions

In this thesis a number of handover algorithms in cellular mobile systems have been analysed and simulated to provide a more complete picture of the handover algorithm design and system performance enhancement, and to investigate the reasons for call drop. In particular the handover algorithm in this thesis uses the rectangular (block) window, which has not been investigated to any extent, rather than one of the more popular methods such as the rectangular sliding window, for averaging the received signal strength. The rectangular window method has the advantage of generating a smaller number of handover requests compared to the rectangular sliding windows, as we have discussed in subsection 2.4.3.

Previously published research on the handover algorithm analyses and the call drop analyses has assumed that the handover request decision and process time is negligibly small. This assumption is hardly acceptable in current digital mobile systems. Moreover those analyses have been done individually, even though the system performance is strongly related to the characteristics of the handover algorithms. The work presented in this thesis has attempted to reveal, firstly the handover request characteristics of the handover algorithms using various handover decision and process intervals from the handover algorithm analysis point of view in chapters 3, 4 and 5, and secondly the system performance based on the various handover decision and process intervals from

relative measurements of received signal strength, while the EN handover algorithm uses both relative and absolute measurement of received signal strength. Lastly, the zero time handoff and hard handoff algorithms are classified based on the length of handover processing interval in chapter 5. We assume that the handover request processing interval of the zero time handoff algorithm is too short to result in significant call degradation or call disconnection during the interval. In addition, the handover processing wait interval which may be caused by heavy signalling traffic at the mobile system level, is introduced and studied in chapter 6.

Chapter 3 commences the investigation of handover request characteristics with simulation and analytical models. First of all, we review the radio simulator model. Then we introduce autocorrelation effects in slow fading as an important parameter which changes the handover request characteristics. As done in many other studies [9, 7, 11, 24, 58], we also consider the exponentional autocorrelation function of Gudmundson [49] for a correlation model. A simple model consisting of two base stations and one mobile station is considered to investigate the performance of handover algorithm. The call degradation conditions for a new handover algorithm performance measurement is displayed. This investigation has certain important goals:

1. Conventional handover request characteristic measurements such as the mean number of handover requests and the mean handover area are valuable to analyse the performance in various handover algorithms.

2. How the MS speed, the overlapping condition and autocorrelation function affect the handover characteristics.

3. Development an analytical model to verify the simulation results.

Based on the simulation results described in section 3.3, we saw that as the signal averaging interval becomes short (slow movement of MS and/or short signal averaging interval), the mean number of handover requests increases regardless of the form of the handover algorithms. However, as HYS increases the mean number of handover requests reduces dramatically. In the basic handover algorithm analysis, we found that high HYS produces the same number of handover requests regardless of the length of signal averaging

quests can only reduce the call degradations caused by unnecessarily high HYS. However the EN handover algorithm becomes useful when it becomes difficult to make a correct decision for the HYS level, because this algorithm demonstrates only small variations in the number of call degradations and handover requests, and in the the mean handover area and call degradation points over the whole range of HYS levels.

The results of call degradation analysis shows that an excessively high HYS will increase the call degradation for users. However a correct decision for the HYS level will help to minimise the mean number of handover requests and the mean number of call degradations. These conclusions are very important for an efficient analysis of the handover algorithm and for developing an accurate handover algorithm.

In section 3.4, analytical models for the basic and the EN handover algorithms are derived to verify the results obtained in the simulation study. These models assume that the sampled and averaged signals are stationary Gaussian random variables. A two-state Markov model is used for the analytical models of the basic and the EN handover algorithm. The analytical model of the call degradation conditions is also derived based on two-state Markov models. The correlation among the samples within the rectangular window is considered to be an exponential autocorrelation function proposed by Gudmundson [9]. The handover request characteristics are compared between analytical and simulation models in two models: uncorrelated and correlated.

For the uncorrelated model, the mean number of handover requests of the analytical model in the basic handover algorithm agrees well with that of the simulation model at medium and high HYS, while it is does not agree well at low HYS. The analytical model shows quite similar results for the number of total call degradations and no-signal call degradations versus HYS. The mean number of normal and enforced handover requests of the analytical model also agrees well with that of simulation model at medium and high HYS. In the EN handover algorithm analysis, the analytical model also shows quite similar behaviour for the total call degradations and no-signal call degradations versus HYS.

The comparisons for the correlated model give some important results:

1. Correlation function is an additional factor affecting the handover request charac-

power model investigated in Chapter 4. This is an extension of the research which has been published in [12, 13].

The MS experiences quite different handover request characteristics in the unequal transmit power model as follows:

1. The mean number of handover requests does not change between the equal and unequal transmit power models.

2. The mean number of call degradations shows clearly the difference between the equal and unequal transmit power models. When the transmit power of the source BS is greater than that of the destination BS, the MS experiences the smallest number of call degradations over the whole range of HYS, while when the transmit power of source BS is less than that of the destination BS, the MS has the largest number of call degradations.

3. Unnecessarily high HYS causes the mean number of call degradations to become worse.

4. The variation of the mean power consumption of the MS shows similar characteristics to the variation of call degradations versus HYS. This is because the call degradation conditions are related to the absolute measurement of the received signal strength.

5. The mean handover area and the mean call degradation points are also shifted as the overlapping area varies in equal power model.

6. The correlation function affects the mean number of handover requests and call degradations.

7. The verification of simulation results using two-state Markov models showed quite good comparisons (the uncorrelated model is used).

Discussions with Professor David Everitt at the University of Melbourne identified further research on handover characteristics when the MS has equal path loss from both BSs during a trip, that is, slow fading is the only factor in the handover algorithm analysis. This question, which provided some useful additional information, had not been

The importance of cell selection is emphasized to show that different handover request characteristics will be achieved with and without cell selection in the worst case. This becomes more important from the teletraffic analysis of mobile systems, because when the MS attempts a new call within the overlapping area, the MS can only be selected by a BS which provides the strongest transmit power. Our investigation has been done from the handover algorithm analysis point of view, while Chu *et al.* [79, 35] and Senarath *et al.* [7] discussed the importance of cell selection in from a mobile system performance analysis point of view.

The call degradation conditions rather than the conventional measurements have been used to obtain efficient handover algorithm analysis data: the mean number of handover requests and the mean handover area. However, the call degradation conditions are not suitable for revealing the change in call quality as the signal averaging interval varies. To make fair comparisons, we introduced the modified average fade duration (mAFD) which is a function of the average fade duration and the probability that the MS is connected to the current BS during a trip. The normalised level crossing rate, which is a second-order statistic [15, 27, 50] in signal strength measurement in mobile systems, is used as a basic element of mAFD. W.C.Y. Lee [27] recommended that the performance measurements combined with the level crossing rate and average fade duration will provide valuable data. In this way, the new measure mAFD gave important results in section 4.4 as follows:

1. The comparisons using mAFD are quite reasonable, because they show similar behavior of the call degradations versus HYS when T_{av} is fixed.

2. When T_{av} varies, a long T_{av} (T_s being fixed) generates similar call quality in terms of mAFD compared to a short T_{av}. However, during most of the travelling time a short T_{av} provides a lower mAFD (better call quality) to the MS than that for a long T_{av} as we have shown in accumulative mAFD comparisons.

The introduction of mAFD and the comparisons of handover request characteristics based on the mAFD is quite useful when the signal averaging interval is different. Moreover the mAFD becomes a valuable call quality measure when the received signal strength is a handover decision criterion like the call degradation condition. In addition the signal

algorithm of Vijayan *et al.* provides the best performance because they assume very fast handover request processing time.

These results also suggest further possible investigations of the different handover request processing intervals as well as handover request processing delays which can possibly occur at the mobile system level.

Chapter 5 also examines the zero time handover algorithm combined with power control based on the discussions with Professor David Everitt and Gamini Senarath at the 2nd Bi-Annual International Conference on Mobile and Personal Communications Systems in Adelaide and at the University of Melbourne, and the results of the worst case study in section 4.3. This study is identified to be valuable because the performance of the power control algorithm can be analysed from the handover algorithm point of view, while previously published studies [70, 51, 55, 52] mainly focus on the system capacity analysis of the power control algorithm using outage probability. We combine the adaptive power control algorithm (in which the next transmit power level is decided based on the signal strength received recently) with the zero time handoff algorithm (which is the same as the hard handoff algorithm but using almost zero handover request processing interval). First of all, we measure the handover request characteristics when the power control algorithm achieves the best (lowest) power consumptions as follows:

1. A power control algorithm based on previously measured received signal strength can provide lower power consumption but rather poor handover request characteristics to users. A power control algorithm analysis combined with the handover algorithm can provide more accurate data for designing a power control algorithm. However, as Zander [69] has stated, transmitter power reduction using power control in a link will cause the link to be more vulnerable to interference. Thus to develop an perfect power control algorithm may be very difficult.

2. A faster handover decision in zero time handoff algorithms using 0dB HYS may not be useful, even making the handover request characteristics worse, unless the power decision in the power control algorithm is accurate. This is because when the power decision is not correct, and HYS is high causing the power decision to be delayed (slow handover decision) the handover request characteristics will

In Chapter 5, investigations of the zero time handoff algorithm combined with power control have been done in a simple model in which the co-channel interference ratio is negligible, MS movement is restricted from one BS to the other, uplink power is equal to the downlink power, and call holding time is equal to the travelling time of MS. Thus the performance of power control and handoff algorithms will be different as the models have different environments, for example when the uplink power is not equal to the downlink power, or the MS direction and speed of travel is random. However the basic properties of the handover performance revealed in Chapter 5 are valuable for further investigations of different models in which the handover request processing intervals are not negligibly small and/or the handoff algorithm is combined with power control.

Chapter 6, investigates the effects on the system performance of various handover request processing intervals in the hard handoff algorithm, and classifies the reasons for call drop based on the research of the early chapters. Moreover to minimise the call drop phenomenon called 'delay call drop', handover rejection schemes are introduced and analysed. The call drop reasons are classified into three: Delay Call Drop in which a call is dropped because of relatively long delay of handover request process caused by heavy signalling traffic (in that chapter we only considered the signalling traffic of handover requests when the system is heavy loaded); No-channel Call Drop in which a call is dropped because of channel shortage; and Nonoverlapping Call Drop where a call is dropped because of insufficient BS transmit power.

The delay call drop analysis provides useful results as follows:

1. As we have found that the handover request processing interval influences the call degradations in the hard handoff analysis, the delay in the handover request processing can affect the system performance.

2. This delay call drop can be minimised by providing fast handover request processing procedures. However this solution is not simple to implement. Thus we use handover rejection schemes using two types of handover requests and load sharing schemes.

3. The handover rejection schemes are efficient for reducing the call dropout rates caused by the handover request processing delay.

2. One solution for signal prediction, the adaptive averaging methodology [16], needs more attention.

3. Call drop analyses based on the signal quality as well as signal strength for an accurate system performance analysis and an efficient and effective system performance enhancement, would be valuable.

Appendix A

Mathematical Analysis for Radio Simulator

A.1 Rayleigh Fading

The mathematical backgrounds for the radio simulator used for radio channel model in the simulation study are presented here. The fields of the N arriving waves are assumed to be a random baseband signal superimposed on a carrier. By following Rice [86]'s representation of a random noise signal, equation 2.21 becomes:

$$E(t) = Re[E_x] = Re[T(t)e^{j\omega_c t}] \tag{A.1}$$

where $T(t) = E_0 \sum_{n=1}^{N} c_n e^{j(\omega_m t cos(\alpha_n)+\phi_n)}$

ω_c is the carrier frequency, ω_m is the maximum Doppler frequency, α_n are the arrival waves's angles, c_n is a set of normalised constants such that $< \sum_{n=1}^{N} c_n^2 >= 1$, and $\omega_n = \omega_m \cos(\alpha_n)$.

If we assume that $N/2$ is an odd integer, then $T(t)$ becomes:

$$T(t) = \frac{E_0}{\sqrt{N}}\Big(\sum_{n=1}^{N/2-1} [e^{j(\omega_n t+\phi_n)} + e^{-j(\omega_n t+\phi_{-n})}] + e^{j(\omega_n t+\phi_N)} + e^{-j(\omega_m t+\phi_{-N})}\Big) \tag{A.2}$$

$$X_c(t) = 2\sum_{n=1}^{N_0} \cos(\beta_n)\cos(\omega_n t) + \sqrt{2}\cos(\alpha)\cos(\omega_m t) \tag{A.6}$$

$$X_s(t) = 2\sum_{n=1}^{N_0} \sin(\beta_n)\cos(\omega_n t) + \sqrt{2}\sin(\alpha)\cos(\omega_m t) \tag{A.7}$$

where α is an arrival angle, β_n is the phase, N_0 is the number of offset oscillators, and ω_n is the doppler frequency shift.

The first terms in equations A.6 and A.7 represent oscillators having Doppler shifted frequencies $+\omega_m \cos(2\pi/N)$ to $-\omega_m \cos(2\pi/N)$. The second term in the equation represents the maximum Doppler frequency $+\omega_m$ and $-\omega_m$.

The output of the simulator is:

$$Y(t) = X_c(t)\cos(\omega_c t) + X_s(t)\sin(\omega_c t) \tag{A.8}$$

Each component of the received field is approximately zero mean Gaussian distributed, but the envelope of $Y(t)$ is approximately Rayleigh distributed.

Jake uses $< X_c^2 > \approx < X_s^2 >$ and $< X_c X_s > \approx 0$ to make the phase of the simulator output random and uniformly distributed for 0 to 2π. He chooses $\alpha = 0$ and $\beta = \pi n/(N_0 + 1)$, thus $< X_c X_s > \equiv 0$ and the mean-square of both components are defined as follows:

$$X_c^2(t) = N_0 \tag{A.9}$$

$$X_s^2(t) = N_0 + 1 \tag{A.10}$$

Because we assumed that $\alpha = 0$ and $\beta = \pi n/(N_0 + 1)$, the inphase and quadrature components shown in equations A.6 and A.7 are given by:

$$X_c(t) = 2\sum_{n=1}^{N_0} \cos(\beta_n)\cos(\omega_n t) + \sqrt{2}\cos(\omega_m t) \tag{A.11}$$

$$X_s(t) = 2\sum_{n=1}^{N_0} \sin(\beta_n)\cos(\omega_n t) \tag{A.12}$$

Appendix B

Level Crossing Rate

Since we assume that the slow fading signal y is lognormally distributed with a mean μ and variance σ^2, the measured signal strength $x = \ln(y)$, after passing the logarithm circuit, is normally distributed with mean μ_1 of path loss function and variance σ_1^2 of the slow fading and the time derivative of the slow fading signal $\dot{x}$ is also normally distributed with a mean μ_2 and variance σ_2^2.

The probability that the random variable x crosses a constant level C of the received signal during unit time, called the *level crossing rate* (lcr), is given by:

$$lcr(x = C) = \int_0^\infty \dot{x} p(x, \dot{x})\, d\dot{x} \tag{B.1}$$

As Jakes [26] proved that x and $\dot{x}$ are uncorrelated and independent. If we assume that $x = x_1$ and $\dot{x} = x_2$, then the joint density function between x_1 and x_2 is given by:

$$p(x_1, x_2) = \frac{1}{2\pi\sigma_1\sigma_2} \exp[-\frac{(x_1 - \mu_1)^2}{2\sigma_1^2} - \frac{(x_2 - \mu_2)^2}{2\sigma_2^2}] \tag{B.2}$$

Therefore lcr in equation B.1 is written as:

$$lcr(x1) = \int_0^\infty x_2 p(x_1, x_2)\, dx_2 \tag{B.3}$$

Equation B.10 is manipulated as follows:

$$\begin{aligned} lcr(x_1) &= \frac{1}{2\pi\sigma_1}[\mu_2 \int_0^\infty \exp(-\frac{1}{2}(M^2+Z^2))\,dZ \\ &\quad +\sigma_2 \int_0^\infty \exp(Z-\frac{1}{2}(M^2+Z^2))\,dZ] \qquad \text{(B.11)} \\ &= \frac{1}{2\pi\sigma_1}[\mu_2 \exp(-\frac{M^2}{2}) \int_0^\infty \exp(-\frac{Z^2}{2})\,dZ \\ &\quad +\sigma_2 \exp(-\frac{M^2}{2}) \int_0^\infty \exp(-\frac{Z^2}{2})\,dZ] \qquad \text{(B.12)} \end{aligned}$$

If $\frac{Z^2}{2} = k$, then $Z = \sqrt{2k}$ and by differentiating Z with respect to k, we obtain:

$$dZ = \frac{1}{\sqrt{2k}} dk \qquad \text{(B.13)}$$

By substituting equation B.13 into equation B.12 the $lcr(x_1)$ is obtained as follows:

$$\begin{aligned} lcr(x_1) &= \frac{1}{2\pi\sigma_1}[\mu_2 \exp(-\frac{M^2}{2}) \int_0^\infty \exp(-k) \frac{1}{\sqrt{2}} k^{-\frac{1}{2}}\,dk \\ &\quad +\sigma_2 \exp(-\frac{M^2}{2}) \int_0^\infty \exp(-k)\,dk] \qquad \text{(B.14)} \\ &= \frac{1}{2\pi\sigma_1}[\mu_2 \frac{1}{\sqrt{2}} \exp(-\frac{M^2}{2}) \int_0^\infty \exp(-k) k^{\frac{1}{2}-1}\,dk \\ &\quad +\sigma_2 \exp(-\frac{M^2}{2}) \int_0^\infty \exp(-k)\,dk] \qquad \text{(B.15)} \end{aligned}$$

We know that $\int_0^\infty \exp(-k) k^{\frac{1}{2}-1}\,dk = \Gamma(\frac{1}{2}) = \sqrt{\pi}$ and $\int_0^\infty \exp(-k)\,dk = \Gamma(1) = 1$.

Therefore the equation B.15 results in:

$$\begin{aligned} lcr(x_1) &= \frac{1}{2\pi\sigma_1}[\frac{\mu_2 \exp(-\frac{M^2}{2})\sqrt{\pi}}{\sqrt{2}} + \sigma_2 \exp(-\frac{M^2}{2})] \qquad \text{(B.16)} \\ &= \frac{1}{2\pi\sigma_1} \exp(-\frac{M^2}{2})[\frac{\mu_2\sqrt{\pi}}{\sqrt{2}} + \sigma_2] \qquad \text{(B.17)} \\ &= [\frac{\mu_2\sqrt{\pi} + \sqrt{2}\sigma_2}{2\sqrt{2}\pi\sigma_{x_1}}] \exp(-\frac{M^2}{2}) \qquad \text{(B.18)} \end{aligned}$$

By replacing M with $(\frac{x_1-\mu_1}{\sigma_1})$ in equation B.18, $lcr(x_1)$ is:

1. When the signal level is equal to the mean of the signal, $x_1 = \mu_1$,

$$lcr(\mu_1) = \frac{\sigma_2}{2\pi\sigma_1} \tag{B.26}$$

2. When the signal level is equal to zero, $x_1 = 0$,

$$lcr(0) = \frac{\sigma_2}{2\pi\sigma_1} \exp(-\frac{1}{2}(\frac{-\mu_1}{\sigma_1})^2) \tag{B.27}$$

But if the slope of signal x_2 has zero mean and its variance σ^{x_2} equals to that of received signal strength σ^{x_1} then lcr is given by:

$$lcr(x_1) = \frac{1}{2\pi} \exp(-\frac{1}{2}(\frac{x_1 - \mu_1}{\sigma_1})^2) \tag{B.28}$$

By substituting the path loss formula of equation 2.7 for the mean μ_1 and equation B.25 for the variance σ_1^2 into equation B.21, the normalised level crossing rate of the received signal random variable x is given by:

$$\acute{lcr}(x) = \exp(-\frac{(x - (P_t - (K_1 + K_2 \log(d))))^2}{2\sigma_x^2})\, dx \tag{B.29}$$

Following the same procedures, the equation B.25, that is, $\mu_2 = 0$ and $\sigma^{x_2} = 1$, is given by:

$$lcr(x_1) = \frac{\sqrt{2}\sigma_2}{2\pi\sigma_1} \exp(-\frac{(x - (P_t - (K_1 + K_2 \log(d))))^2}{2\sigma_x^2})\, dx \tag{B.30}$$

and equation B.28 becomes:

$$lcr(x_1) = \frac{1}{2\pi} \exp(-\frac{(x - (P_t - (K_1 + K_2 \log(d))))^2}{2\sigma_x^2})\, dx \tag{B.31}$$

Appendix C

Variance of Samples for Rectangular Window

As shown in equation 2.24, the received signal strength transmitted from a BS to the MS, $X(d)$, becomes a function of path loss for the mean and slow fading for the variance as follows:

$$X(d) = P_t - L_p(d) + F(d) \tag{C.1}$$

where P_t is the transmitting power of the BS [dBm], d is the distance between the MS and the BS [km], $L_p(d)$ is the path loss between the MS and the BS [dB], $F(d)$ is the standard deviation of slow fading [dB].

The $L_p(d)$ is considered to be a constant because we assume that the $X(d)$ is a stationary gaussian random variable. The slow fading $F(d)$ is also assumed to be a gaussian random variable F having zero mean and the same variance of $X(d)$.

The mean of the weighted sum of slow fading samples during a signal averaging interval (n samples) is given by:

$$\bar{F}(k) = \alpha_i \sum_{i=1}^{n} F_{k-1+i} \tag{C.2}$$

Appendix D

Lower Bound for Mean Number of Handovers

We derive the lower bound of the mean number of handover requests for the basic and the EN handover algorithms to prove that the mean number of handover requests is equal to the sum of the probability that the MS handovers, as shown by Miller *et al.* [43].

D.1 Lower Bound on E_{ho} for Basic Handover Algorithm

Theorem: When the MS links to BS-A at the beginning of journey and moves toward BS-B, if $P_{B/A} = 1$ then $E_{ho} \geq 1$.

Proof: The probability that the MS connects to BS-A at the beginning of interval k is

$$P_A(k) = P_A(k-1)(1 - P_{B/A}(k)) + P_B(k-1)P_{B/A}(k) \quad \text{(D.1)}$$

Each component in each term is non-negative. Thus if $\hat{P}_A(k) = P_A(k-1)(1 - P_{B/A}(k))$, then $\hat{P}_A(k) \leq P_A(k)$. Initially the MS is connected to BS-A at the beginning of the interval 1, we assume that 0, $\hat{P}_A(k) = P_A(0) = 1$ Because $\hat{P}_A$ is recursive in $(1 - P_{B/A}(k))$,

$$\begin{aligned} \hat{E}_{ho}(k) &= P_{B/A}(1) \\ &= 1 \end{aligned} \tag{D.7}$$

Because $P_{ho}(k) \geq \hat{P}_{ho}(k)$, E_{ho} is always greater than or equal to $\hat{E}_{ho}$. Thus we can show that:

$$\begin{aligned} E_{ho} &\geq \hat{E}_{ho} \\ &\geq 1 \end{aligned} \tag{D.8}$$

D.2 Lower Bound on E_{tho} for EN Handover Algorithm

Theorem: When the MS links to BS-A at the beginning of journey and moves toward BS-B, if $P^N_{N1/A} = 1$ then $E_{tho} \geq 1$.

Proof: The probability that the MS is being connected to BS-A at the beginning of interval k is:

$$P^T_A(k) = P^T_A(k-1)(1 - P^T_{B/A}(k)) + P^T_B(k-1)P^T_{B/A}(k) \tag{D.9}$$

As we did in section D.1, we note that each component in each term is non-negative. Thus if $\hat{P}^T_A(k) = P^T_A(k-1)(1 - P^T_{B/A}(k))$, then $\hat{P}^T_A(k) \leq P^T_A(k)$. Initially the MS is connected to BS-A at the beginning of the interval 1, we assume that at an interval $k = 0$ $\hat{P}^T_A(k) = P^T_A(0) = 1$. Because the $\hat{P}^T_A$ is recursive in $(1 - P^T_{B/A}(k))$, the $\hat{P}^T_A(k)$ is given by:

$$\begin{aligned} \hat{P}^T_A(k) &= 1 \quad \text{for} \quad k = 1 \\ &= \prod_{i=1}^{k}(1 - P^T_{B/A}(i)) \quad \text{for} \quad k > 1 \end{aligned} \tag{D.10}$$

$$\begin{aligned} E_{thr} &\geq \hat{E}_{thr} \\ &\geq 1 \end{aligned} \tag{D.16}$$

The state transition can occur independently in two ways: by normal handover condition; and by enforced handover condition. Thus $P^T_{B/A} = 1$ indicates that one of these conditions occur during the MS trip. This leads to the result:

$$P^T_{B/A}(k) = P^N_{N_1/A}(k) + P^E_{E_1/A}(k) = 1 \tag{D.17}$$

Appendix E

Publications

1. Dohun Kwon, "Handover Request Rejection Scheme in Overloaded Mobile Systems", 2nd Bi-Annual International Conference on Mobile and Personal Communications Systems, pp.193-202, Adelaide, Australia, April, 1995.

2. Dohun Kwon, "Handover Request Rejection Scheme in Overloaded Mobile Systems", IEEE Fourth Interl. Conf. on Universal Personal Communications (ICUPC'95), pp.662-666, Tokyo, Japan, Nov. 1995.

3. Dohun Kwon and Kenneth. W. Sarkies, "System Performance Enhancement Combining Handover Rejection Scheme with Channel Reservation Scheme", Australian Telecommunication Networks and Applications Conference 1995 (ATNAC'95), pp.497-502, Sydney, Australia, Dec. 1995.

4. Dohun Kwon and Kenneth W. Sarkies, "Handover Algorithm Analysis Combined with Overlapping Conditions", Proceedings of the 46th IEEE Vehicular Technology Conference, Atlanta, USA, Apr. 1996, pp.1331-1335.

Appendix F

Glossary and Notation used in this thesis

F.1 Glossary

The following terms are used throughout the thesis:

ANAL analytical model

APC adaptive power control

ATPC adaptive transmitter power control

BCC blocked call clear

BS base station

BS-A base station A

BS-B base station B

BSC base station center

BS ID base station identification

CDMA code division multiple access

CH REQ the channel request message

CIR co-channel interference ratio or carrier to interference ratio

DCA dynamic channle assignment

DS-CDMA direct sequency code division multiple access

PSTN public switched telephone network

QOS quality of service

RSS received signal strength

SACCH slow associated control channel

SDEG sudden call degradation condition

SHPM slow handover processing model

SIMUL simulation model

SOPC soft handoff **with** power control

SOPC-G soft handoff **with** power control using *guard*

SWPC soft handoff **without** power control

TDMA time division multiple access

F.2 List of Common Symbols

Where possible, the following notation has been used for quantities that are referred to in various parts of the thesis, in order to preserve continuity.

v the speed of the MS

h_b height of BS the antenna

h_m height of MS the antenna

f_c carrier frequency

P_t transmitting power

P_r receiving power

$\acute{P}_t$ transmit power of the dipole antenna

d distance between transmitter and receiver

r cell radius

y overlapping condition

T_{av} signal average interval

d_{av} signal average distance

T_s signal sampling interval

the beginning of interval k in the basic handover algorithm

E_{ho} total number of the handover requests during the MS travelling time in the basic handover algorithm

$P_{ho}(k)$ probability that a handover occurs at the beginning of the kth interval in the basic handover algorithm

P_A^T probility that the MS is being connected to the BS-A at the beginning of the kth interval in the EN handover algorithm

P_B^T probility that the MS is being connected to the BS-B at the beginning of the kth interval in the EN handover algorithm

$P_{B/A}^T(k)$ probability that the MS changes its current BS from the BS-A to the BS-B at the beginning of interval k in the EN handover algorithm

$P_{A/B}^T(k)$ probability that the MS changes its current BS from the BS-B to the BS-A at the beginning of interval k in the EN handover algorithm

E_{thr} total number of the handover requests during the MS travelling time in the EN handover algorithm

$P_{thr}(k)$ probability that a handover occurs at the beginning of the kth interval in the EN handover algorithm

lcr expected number of crossing level x_0 during unit interval

$\acute{lcr}$ the normalised level crossing rate

AFD average fade duration during unit interval

$\acute{AFD}$ normalised average duration of fade

$TX\_PWR(.)$ transmit power control conversion table

$RX\_PWR(.)$ receiver power control conversion table

$S(k)$ power control step

$step\_size$ size of one power control step

MAX_STEP total number of power steps

$guard$ guard band in power control algorithm

Bibliography

[1] Carrington, "From mobile to personal communications," in *IERE Land Mobile Radio Conference*, 1987.

[2] J. Dasilva and B. Fernandes, "The European research program for advanced mobile systems," *IEEE Personal Communications*, pp. 14–19, Feb. 1995.

[3] V. MacDonald, "The cellular concept," *The Bell System Technical Journal*, vol. 58, pp. 15–42, Jan. 1979.

[4] *Handover Procedures*, GSM recommendation 02.01 ed., Oct. 1991.

[5] M. Mouly and M. B. Pautet, *The GSM System for Mobile Communications*. European Media Duplication S.A., 1992.

[6] T. Kanai and Y. Furuya, "A handoff control process for microcellular systems," in *Proceedings of the 38th IEEE Vehicular Technology Conference*, pp. 170–175, 1988.

[7] G. Senarath and D. Everitt, "Combined analysis of transmission and traffic characteristics in micro-cellular mobile communication systems (emphasis: Propagation modelling)," in *1st Bi-Annual International Conference on Mobile and Personal Communications Systems*, pp. 319–333, Nov. 1992.

[8] M. Hata, "Empirical formula for propagation loss in land mobile radio services," *IEEE Transactions on Vehicular Technology*, vol. 29, pp. 317–325, Aug. 1980.

[9] M. Gudmundson, "Analysis of handover algorithms," in *Proceedings of the 41st IEEE Vehicular Technology Conference*, pp. 537–542, Dec. 1991.

[21] D. Hong and S. Rappaport, "Traffic model and performance analysis for cellular mobile radiotelephone systems with prioritized and non-prioritized hand-off procedures," *IEEE Transactions on Vehicular Technology*, vol. 35, pp. 77–92, Aug. 1986.

[22] E. Posner and R. Guérin, "Traffic policies in cellular radio that minimize blocking of handoff calls," *Proceedings 11th International Teletraffic Congress*, vol. 1, p. 2.4B2, 1985.

[23] R. Guérin, "Queueing-blocking system with two arrival streams and guard channels," *IEEE Transactions on Communications*, vol. 36, pp. 153–163, Feb. 1988.

[24] S. Kuek, W. Wong, R. Vijayan, and D. Goodman, "A predictive load-sharing scheme in a microcellular radio environment," *IEEE Transactions on Vehicular Technology*, vol. 42, pp. 519–525, Nov. 1993.

[25] G. Corazza, D. Giancristofaro, and F. Santucci, "Characterization of handover initialisation in cellular mobile radio networks," in *Proceedings of the 44th IEEE Vehicular Technology Conference*, pp. 1869–1872, June 1994.

[26] W. Jakes, *Microwave Mobile Communications.* New-York: John Wiley & Sons, 1974.

[27] W. Lee, *Mobile Communications Engineering.* New York: McGraw-Hill Book Company, 1982.

[28] J. Parsons and J. Gardiner, *Mobile Communication Systems.* USA: Halsted Press: Blackies, 1989.

[29] R. Macario, *Personal and Mobile Radio Systems*, vol. 25 of *IEE Telecommunications Series.* Hertfordshire: Peter Peregrinus Ltd., 1988.

[30] I. V. S. C. on Radio Propagation, "Coverage prediction for mobile radio systems operating in the 800/900 MHz frequency range," *IEEE Transactions on Vehicular Technology*, vol. 37, no. 1, p. Special Issue on Mobile Radio Propagation., 1988.

[42] E. Gilbert, "Energy reception for mobile radio," *The Bell System Technical Journal*, vol. 44, pp. 1779–1803, Oct. 1965.

[43] C. Miller and R. Wyrwas, "Probabilistic analysis of handover algorithms," in *IEEE International Conference on UWA*, pp. 77–81, 1994.

[44] W. Jakes and D. Reudink, "Comparison of mobile radio transmission at UHF and X band," *IEEE Transactions on Vehicular Technology*, vol. 16, pp. 10–14, Oct. 1967.

[45] W. Aranguren and R. Langseth, "Baseband performance of a pilot diversity system with simulated Rayleigh fading signals and co-channel interference," *Joint IEEE Communications Society-Vehicular Technology Group Special Transactions on Mobile Radio Communications*, pp. 1248–1257, Nov. 1973.

[46] P. Carter and A. Turkmani, "Performance evaluation of Rayleigh and log-normal GMSK signals in the presence of co-channel interference," *IEE Proceedings*, vol. 139, pp. 156–164, Apr. 1992.

[47] M. Hodges, "The GSM radio interface," *British Telecommunications Technology Journal*, vol. 8, pp. 31–43, Jan. 1990.

[48] N. Zhang and J. Holtzman, "Analysis of handoff algorithms," in *Proceedings of the 44th IEEE Vehicular Technology Conference*, pp. 82–86, June 1994.

[49] M. Gudmundson, "Correlation model for shadow fading in mobile radio systems," *Electronics Letters*, vol. 27, pp. 2145–2146, Nov. 1991.

[50] M. Yacoub, *Foundations of Mobile Radio Engineering.* CRC Press, 1993.

[51] K. G. et al., "On the capacity of a cellular CDMA system," *IEEE Transactions on Vehicular Technology*, vol. 30, pp. 303–312, May 1991.

[52] A. Viterbi, A. Viterbi, and E. Zahavi, "Soft handoff extends CDMA cell coverage and increases reverse link capacity," *IEEE Journal on Selected Areas in Communications*, vol. 12, pp. 1281–1288, Oct. 1994.

[63] W. Lee, "Finding the statistical properties of the median values of a fading signal directly from its decibel values," *Proceedings of the IEEE*, vol. 58, pp. 287–188, Feb. 1970.

[64] J. Ku, "Strategies on the immediate assignment procedure within the GSM call setup scenario," in *Proceedings of the 42nd IEEE Vehicular Technology Conference*, pp. 786–789, 1992.

[65] M. Soroushnejad and E. Geraniotis, "Performance comparison of different spread-spectrum signaling schemes," *IEEE Transactions on Communications*, vol. 40, pp. 947–956, May 1992.

[66] J. Aein, "Power balancing in systems employing frequency reuse," *COMSAT Technical Review*, vol. 3, no. 2, 1973.

[67] T. Nagatsu, T. Tsuruhara, and M. Sakamoto, "Transmitter power control for cellular land mobile radio," in *Global Telecommunications Conference Globecom 83*, pp. 1430–1434, 1983.

[68] T. Fujii and M. Sakamoto, "Reduction of co-channel interference in cellular systems by intra-zone channel reassignment and adaptive transmitter power control," in *Proceedings of the 38th IEEE Vehicular Technology Conference*, pp. 668–672, 1988.

[69] J. Zander, "Performance of optimum transmitter power control in cellular radio systems," *VT*, vol. 41, pp. 57–62, Feb. 1992.

[70] W. Lee, "Power control in CDMA," in *Proceedings of the 41st IEEE Vehicular Technology Conference*, 1992.

[71] H. Panzer and R. Beck, "Adaptive resource allocation in metropolitan area cellular mobile radio systems," in *Proceedings of the 40th IEEE Vehicular Technology Conference*, pp. 638–645, 1990.

[72] C. Chuah and R. Yates, "Evaluation of a minimum power handoff algorithm," in *The Sixth IEEE International Symposium on Personal, Indoor and Mobile Radio Communications*, pp. 814–818, Sept. 1995.

[83] D. Cox, "Empirical formula for propagation loss in land mobile radio services," *IEEE Transactions on Vehicular Technology*, vol. 29, pp. 317–325, Aug. 1980.

[84] G. Senarath and D. Everitt, "Performance of handover priority and queueing systems under different handover strategies for micro-cellular mobile communication systems," in *Proceedings of the 45th IEEE Vehicular Technology Conference*, pp. 319–333, July 1995.

[85] J. Karlsson and B. Eklundh, "A cellular mobile telephone system with load sharing and enhancement of directed retry," *IEEE Transactions on Communications*, vol. 37, pp. 530–535, May 1989.

[86] S. O. Rice, "Mathematical analysis of random noise," *The Bell System Technical Journal*, vol. 23, pp. 282–332, 1944.